

WETTING OF CURVED SURFACES

T. Bieker and S. Dietrich

*Fachbereich Physik, Bergische Universität Wuppertal, D-42097 Wuppertal,
Federal Republic of Germany*

As a first step towards a microscopic understanding of the effective interaction between colloidal particles suspended in a solvent we study the wetting behavior of one-component fluids at spheres and fibers. We describe these phenomena within density functional theory which keeps track of the microscopic interaction potentials governing these systems. In particular we properly take into account the power-law decay of both the fluid-fluid interaction potentials and the substrate potentials. The thicknesses of the wetting films as a function of temperature and chemical potential as well as the wetting phase diagrams are determined by minimizing an effective interface potential which we obtain by applying a sharp-kink approximation to the density functional. We compare our results with previous approaches to this problem.

PACS numbers: 68.45.Gd, 68.10.Cr, 68.15.+e

arXiv:cond-mat/9711033v2 10 Nov 1997

I. Introduction

If colloidal particles are dissolved in a solvent consisting of a binary liquid mixture, necessarily one of these two components is preferentially adsorbed on the spherical surfaces of the colloidal particles. Near a first-order phase separation of the bulk solvent this adsorption may lead to the coating of the colloids by wetting films which snap into a bridgelike structure if two colloids come close to each other. This coagulation can become so pronounced that it results in flocculation [1–5]. Such experiments have inspired several theoretical investigations [6–16] which have shed light on various features of these complex phenomena.

Although there are indications that for higher concentrations of colloidal particles their effective mutual interactions are beyond a superposition of effective pair potentials [11], for low concentrations the knowledge of the effective interaction between two isolated colloidal particles at a fixed distance immersed into the solvent is important. Moreover, this latter configuration is interesting in its own, because the bridge formation between individual pairs is not solely accessible indirectly via flocculation but can be studied also directly with atomic or surface force apparatuses [17]. Besides colloidal systems these problems are in addition relevant for technical applications such as the contact between lubricant films on the disk surfaces in magnetic recording with the recording head [18], sintering [19], latex film formation [20], catalyst wetting efficiency in trickle-bed reactors [21], or for the bonding mechanism of emulsified adhesives in granular and fibrous substrates [22].

As a prerequisite for understanding the effective interaction between such spherical particles immersed into a solvent one must know the structural and thermal properties of these systems in the case that the distance between two colloidal particles is macroscopically large. Near a first-order phase transition of the solvent this amounts to studying the wetting behavior of the solvent at the surface of a spherical substrate. The paradigmatic case is the formation of a liquidlike film at the curved substrate-vapor interface upon approaching the liquid-vapor coexistence curve in the bulk of a one-component fluid from the vapor side. This problem has been studied theoretically by several authors [23–29] based on various versions of phenomenological models. They confirm the general expectation (see Subsect. X.B in Ref. [30]) that the positive curvature of the surface of a substrate prevents the build-up of macroscopically thick wetting films because, in contrast to a planar geometry, the area of the emerging liquid-vapor interface increases with the thickness of the wetting film. This increasing cost of the free energy of the film has effectively the same consequence as if the bulk fluid is kept off liquid-vapor coexistence. Therefore continuous wetting transitions are eliminated and first-order wetting transitions are reduced to quasi-first-order transitions between small and large, but finite, film thicknesses, smeared out due to the finite size of the substrate area.

However, beyond these general aspects it is important to know to which extent the film thicknesses of these wetting films are limited and how these limitations depend on the radius of the colloidal particles, on the character and the form of the substrate potential

and the interaction potential between the solvent molecules, and on the size of the solvent molecules. The aforementioned phenomenological models do not allow one to answer these questions because they do not keep track of the microscopic details of the system. In particular the experience with wetting phenomena on flat substrates tells that it is essential to take into account equally the power-law decay of the substrate potential and of the interaction potential between the fluid particles [30,31]. Inter alia, the long range of the forces between the fluid particles causes the breakdown of a gradient expansion for treating the deviations of the emerging liquid-vapor interface from its flat configuration and leads to a *nonlocal* Hamiltonian [32]. For simple geometric shapes of the interfaces involved this long-ranged character of the dispersion forces acting in and on fluids is taken into account by the Dzyaloshinskii-Lifshitz-Pitaevskii (DLP) theory [33] which has been applied to spheres and cylinders [34]. For a given system this allows one to compute the cost in free energy $\Omega_s(l)$ to maintain a thick liquid film of prescribed thickness l adsorbed on the substrate in terms of the frequency dependences of the permittivities of the substrate, the bulk liquid, and the bulk vapor. Although this approach has the advantage to take into account many-body forces and retardation, it suffers also from some shortcomings. (i) The DLP theory gives access only to the leading asymptotic behavior of $\Omega_s(l \rightarrow \infty)$ and thus does not allow one to describe critical wetting transitions which result from the competition between the leading and next-to-leading order term in $\Omega_s(l)$ for large l [30,31]. (ii) Details of the substrate potential, which are important for first- and second-order wetting transitions [30,31], are not captured by the DLP theory. (iii) $\Omega_s^{(DLP)}(l)$ exhibits an unphysical divergence for $l \rightarrow 0$ because this approach ignores the repulsive part of both the substrate potential and the fluid-fluid interaction potential and thus the structure of the emerging substrate-liquid interface. (iv) The broadening of the emerging liquid-vapor interface upon raising the temperature cannot be accounted for. (v) The dependence of $\Omega_s^{(DLP)}(l)$ on temperature and chemical pressure, in particular close to phase transitions in the bulk fluid, is not transparent. (vi) In the present context, as expounded above, the most severe drawback of the DLP approach is, that the DLP results for wetting of a single sphere or cylinder [34] cannot be used as a building block for investigating later on the effective interactions between two such objects because the shape of the bridging wetting film between them is not known in advance which precludes the practical application of the DLP theory to the problem described in the beginning.

Therefore in this paper we compute (Sect. II) and discuss (Sect. III) the effective interface potential $\Omega_s(l)$ for the wetting of a single sphere and of a single cylinder on the basis of density functional theory [35]. This microscopic approach allows one to address the aforementioned points (i)-(vi) and overcomes the shortcomings of the phenomenological theories. The price to be paid is that the results do not account for the effects of many-body forces.

In the beginning of this introduction we have focused on the physical interest in spheres exposed to a fluid. It turns out that there is also substantial interest in the cylindrical geometry. In view of its importance for technical processes such as the lubrication of textile fibers, optical fiber processing, and the formation of fiber-reinforced resins [36]

there are many studies of the statics and dynamics of adsorption on cylinders [9,26,37–47]. In addition the adsorption on cylinders is important for the vibrating-wire microbalance as a standard technique to study wetting phenomena [48]. However, one has to keep in mind that the convoluted surface of graphite fibers impedes the interpretation of these experiments on the basis of theoretical models which assume a smooth cylindrical surface [49]. (Such surface inhomogeneities may even play a role for spherical colloidal particles [50].) For the same reasons given above for the spherical geometry we apply a microscopic density functional theory also to the problem of wetting of wires in order to obtain a detailed picture of their behavior in systems with long-ranged interactions.

We conclude the introduction with two remarks. First, the present study is dealing with volatile liquids, i. e., it is important that the liquid phase and the surrounding vapor are in thermal equilibrium. Second, we do not address the problem of *interfacial* wetting at curved surfaces, i. e., the substrate is passive. Therefore our results do not apply directly to such phenomena as surface melting of small particles and wires.

II. Effective interface potential from density functional theory

A. Density functional

As for the description of wetting phenomena in planar geometries we describe the one-component fluid by a simple grand canonical density functional [30,35]:

$$\begin{aligned} \Omega[\{\rho(\mathbf{r})\}; T, \mu] &= \int_V d^3r f_h[\{\rho(\mathbf{r})\}, T] \\ &+ \frac{1}{2} \int_V d^3r \int_V d^3r' \tilde{w}(|\mathbf{r} - \mathbf{r}'|) \rho(\mathbf{r}) \rho(\mathbf{r}') + \int_V d^3r \rho(\mathbf{r}) (\rho_w v(\mathbf{r}) - \mu). \end{aligned} \tag{2.1}$$

V is a macroscopic but finite volume into which the substrate \mathcal{S} is embedded but is not a part of it. $\Omega[\{\rho(\mathbf{r})\}; T, \mu]$ is the grand canonical free energy for a given density configuration $\rho(\mathbf{r})$ as a function of the temperature T and the chemical potential μ . We assume a spherically symmetric pair interaction potential $w(r)$ for the fluid particles which according to standard procedures [35] is divided into a short-ranged repulsive and a long-ranged attractive part $\tilde{w}(r)$ with $\tilde{w}(r \rightarrow \infty) \sim r^{-6}$. Here we do not consider retardation effects which would lead to $\tilde{w}(r \rightarrow \infty) \sim r^{-7}$. The divergent repulsive part of the interaction potential gives rise to a reference free energy which is mapped onto $f_h(\rho, T)$ as the free energy density of a homogeneous system of hard spheres with an effective diameter $d(T)$ [51] and number density ρ . An appropriate expression for f_h is given by the Carnahan-Starling formula [52]

$$f_h(\rho, T) = k_B T \rho \left(\ln(\eta) - 1 + \frac{4\eta - 3\eta^2}{(1 - \eta)^2} \right) \quad (2.2)$$

where $\eta = \frac{\pi}{6} \rho d(T)^3$ is the dimensionless packing fraction. The second term in Eq. (2.1) accounts for the long-ranged attractive interaction which we treat according to the Barker-Henderson scheme [51],

$$\tilde{w}(r) = \Theta(r - \sigma)w(r), \quad (2.3)$$

where Θ denotes the Heaviside function. For many purposes it may be useful to adopt the Lennard-Jones potential $\phi_{LJ}(r)$ as the actual full interaction potential $w(r)$:

$$w(r) = \phi_{LJ}(r) = 4\epsilon \left(\left(\frac{\sigma}{r} \right)^{12} - \left(\frac{\sigma}{r} \right)^6 \right) \quad (2.4)$$

with depth ϵ and diameter σ of the fluid particles so that $d(T) = \int_0^\sigma dr (1 - e^{-\beta\phi_{LJ}(r)})$. For this interaction potential Eq. (2.1) leads to a phase diagram of the bulk fluid with a critical point at $k_B T_c / \epsilon = 1.09858$, $\rho_c \sigma^3 = 0.27201$, and $\mu_c / \epsilon = -3.77713$ [53]. The fluid is exposed to a substrate which in a first approximation one may consider to follow from a superposition of Lennard-Jones interaction potentials ϕ_{LJ}^{wf} between wall and fluid particles,

$$\phi_{LJ}^{wf} = 4\epsilon_{wf} \left(\left(\frac{\sigma_{wf}}{r} \right)^{12} - \left(\frac{\sigma_{wf}}{r} \right)^6 \right), \quad (2.5)$$

i. e., $v(\mathbf{r}) = \int_S d^3r' \phi_{LJ}^{wf}(|\mathbf{r} - \mathbf{r}'|)$ where S is the substrate volume. Ignoring the exponentially decaying corrugation effects of an atomically structured substrate, $v(\mathbf{r})$ depends only on the radial distance to the substrate surface, $v(\mathbf{r}) = v(r)$. In general, however, $v(r)$ is more complicated than a linear superposition of Eq. (2.5) and enters the problem as a free parameter function. The equilibrium number density, which minimizes Eq. (2.1), depends also only on r and yields the corresponding grand canonical potential of the system.

For the above interaction potentials this minimum can only be determined numerically. Here, however, we construct an effective interface potential $\Omega_s(l)$ which is the cost in free energy to maintain a liquidlike film of a prescribed thickness l near the substrate although the bulk fluid is in the vapor phase. The equilibrium thickness l_0 minimizes this effective interface potential. This approach yields a transparent insight into the various wetting transitions which can occur [54]. It has turned out that the so-called sharp-kink approximation, in which the trial-functions $\rho(\mathbf{r})$ compatible with the thickness l are approximated by piecewise constant density profiles, yields a surprisingly accurate expression for the actual effective interface potential $\Omega_s(l)$ [55]. (In the present context there are also approaches beyond the sharp-kink approximation [56]. These numerical studies yield valuable information about specific systems but no overall picture for the

wetting phenomena near curved surfaces.) For spherical and cylindrical substrates the sharp-kink approximation amounts to using the following trial function (see Fig. 1(a)):

$$\hat{\rho}(r) = [\rho_l \Theta(h - r) + \rho_g \Theta(r - h)] \Theta(r - r_1). \quad (2.6)$$

h and r_0 denote the radius of the emerging gas-liquid interface and of the substrate, respectively, so that $l = h - r_0 \geq d_w$. The repulsive part of the substrate potential leads to an excluded volume close to the substrate. This is taken into account by the radius $r_1 = r_0 + d_w$; approximately $d_w = \frac{1}{2}(\sigma + \sigma_{wf})$. Actually d_w is given by the zeroth moment of the wall-liquid interface profile $\rho_{wl}(z)$, $d_w = \int_0^\infty dz(1 - \rho_{wl}(z)/\rho_l)$, at gas-liquid coexistence $\mu = \mu_0(T)$ [55(c)]. $\rho_l = \rho_l(T, \mu = \mu_0(T))$ denotes the equilibrium liquid density at two-phase coexistence, whereas $\rho_g = \rho_g(T, \mu)$ is the actual vapor density. From Eq. (2.6) one obtains the sharp-kink profile for the flat geometry if one sets $r_0 = 0$ and replaces r by the distance z perpendicular to a half-space filled with substrate atoms (see Fig. 1(b)).

If Eq. (2.6) is inserted into Eq. (2.1) Ω can be decomposed into a bulk contribution proportional to $V^{(i)}$, $i = s, c$, and into subdominant terms. The superscripts s and c correspond to a sphere and a cylinder, respectively, so that $V^{(s)} = \frac{4\pi}{3}(L^3 - r_0^3)$ and $V^{(c)} = \pi M(L^2 - r_0^2)$; M is the length of the cylinder. In the cylindrical case we consider the thermodynamic limit $M \rightarrow \infty$ which leaves one with a wire. In the planar geometry, $i = p$, $V^{(p)} = AL$ where A is the substrate area. In all cases L denotes a macroscopic system size (see Fig. 1). The systematic application of the sharp-kink approximation to Eq. (2.1) leads for all geometries $i = s, c, p$ and independent of the form of $w(r)$ and $v(\mathbf{r})$ to (sometimes we omit the superscripts)

$$\Omega[\hat{\rho}(r); T, \mu] = V\Omega_b(\rho_g, T, \mu) + \Sigma_{g,vac} + \bar{\Omega}_s(l). \quad (2.7)$$

Ω_b is the bulk free energy density of the vapor phase. The finite volume $V^{(i)}$ introduces an artificial gas-vacuum interface which gives rise to the surface contribution $\Sigma_{g,vac}$. This and other surface contributions $\Sigma_{\alpha,\beta}(r)$ are proportional to the surface area $A(r)$ of the corresponding interface with radius r so that $\lim_{r \rightarrow \infty} \Sigma_{\alpha,\beta}(r)/A(r) = \sigma_{\alpha,\beta}$ is finite and is the surface tension between phases (substrate, liquid, or vapor) α and β in planar geometry:

$$\Sigma_{\alpha,\beta}(r) = A(r)\sigma_{\alpha,\beta}(r). \quad (2.8)$$

We denote the r -dependent surface tension as $\sigma_{\alpha,\beta}(r)$. The third contribution in Eq. (2.7) is the effective interface potential $\bar{\Omega}_s(l)$ which contains the dependence on the film thickness l :

$$\bar{\Omega}_s(l) = V_{liq}\Delta\Omega_b + \Sigma_{l,g} + \Sigma_{l,s} + \bar{\omega}(l) \quad (2.9)$$

In Eq. (2.9) $V_{liq}\Delta\Omega_b = V_{liq}(\rho_l - \rho_g)(\mu_0 - \mu) \equiv V_{liq}\Delta\rho\Delta\mu$ is the cost in free energy to fill the volume $V_{liq}^{(s)} = \frac{4\pi}{3}(h^3 - r_0^3)$ and $V_{liq}^{(c)} = \pi M(h^2 - r_0^2)$, respectively, with liquid although

μ and T favor the vapor phase. Upon approaching liquid-vapor coexistence $\mu_0(T)$ from below, i. e. $\mu < \mu_0$, $\Delta\Omega_b$ is positive, so that $V_{liq}\Delta\Omega_b$ increases with the radius of the liquid volume. Thus for all geometries the formation of an macroscopically thick layer is prohibited as long as one is off coexistence.

If the equilibrium value $l_0(T, \mu)$, which minimizes $\bar{\Omega}_s(l)$, diverges for $\mu \rightarrow \mu_0(T)$ one has a so-called complete wetting transition [30,31]. However, for curved geometries a macroscopically thick film cannot emerge even when coexistence is reached because the free energy contribution due to the liquid-gas interface, $\Sigma_{l,g} = A(h)\sigma_{l,g}(h)$, increases with the area $A(h)$ of the interface, i. e. with the film thickness l . Therefore the equilibrium film thickness l_0 on spherical and cylindrical substrates will *always* be limited to a finite value [30]. The free energy of the liquid-solid interface does, by contrast, not depend on l , so that $\Sigma_{l,s} = A(r_0)\sigma_{l,s}(r_0)$ is a constant with respect to the minimization of $\bar{\Omega}_s(l)$.

As long as the liquid-gas and the solid-liquid interface are not macroscopically far apart from each other, there will be a nonzero interaction between them. This is taken into account by the last term in the effective interface potential, $\bar{\omega}(l)$, which by construction vanishes for $l \rightarrow \infty$. In the case of a planar substrate, interfacial phase transitions along the coexistence curve $\mu_0(T)$ are determined by $\bar{\omega}(l)$ only [30,31,54]. For spheres and cylinders, however, the wetting behavior at $\Delta\mu \equiv \mu_0 - \mu = 0$ is governed by $\bar{\omega}(l)$ as well as Σ_{lg} .

It is convenient to normalize the effective interface potential $\bar{\Omega}_s(l)$ by the area of the substrate surface, $A(r_0)$, so that (see Fig. 1)

$$\begin{aligned}\Omega_s(l) &= \frac{1}{A(r_0)}\bar{\Omega}_s(l) \\ &= \frac{V_{liq}}{A(r_0)}\Delta\Omega_b + \frac{A(r_0+l)}{A(r_0)}\sigma_{l,g}(r_0+l) + \sigma_{l,s}(r_0) + \omega(l)\end{aligned}\quad (2.10)$$

where

$$\omega(l) = \frac{1}{A(r_0)}\bar{\omega}(l).\quad (2.11)$$

The geometrical prefactors $V_{liq}/A(r_0)$ and $A(r_0+l)/A(r_0)$ have the following explicit forms:

$$\frac{V_{liq}}{A(r_0)} = \frac{r_0}{\tau+1} \left(\left(1 + \frac{l}{r_0}\right)^{\tau+1} - 1 \right)\quad (2.12)$$

and

$$\frac{A(r_0+l)}{A(r_0)} = \left(1 + \frac{l}{r_0}\right)^\tau\quad (2.13)$$

with $\tau = 2$ for a sphere and $\tau = 1$ for a cylinder. Before determining the surface phase diagrams from the minimization of $\Omega_s(l)$ we first discuss the two l -dependent terms $\Sigma_{l,g}$ and $\omega(l)$, which are interesting in their own right and allow for a comparison with results obtained by other approaches.

B. Liquid-vapor and solid-liquid surface tension

From $\Sigma_{l,g}$ we obtain an expression for the curvature dependence of the liquid-vapor surface tension of a spherical drop and of a liquid thread. Whereas apart from Ref. [57] we are not aware of studies of liquid fibers, the surface tension of liquid drops has been subject to partially controversial discussions [58]. Here we calculate the surface tension within our approach for both cases explicitly in order to work out the influence of the curvature.

Within the sharp-kink approximation of Eq. (2.1) the planar liquid-vapor surface tension is given by [30]

$$\sigma_{l,g}^{(p)} = \frac{1}{A} \Sigma_{l,g}^{(p)} = -\frac{1}{2} (\Delta\rho)^2 \int_0^\infty dz t^{(p)}(z), \quad (2.14)$$

where $t^{(p)}(z)$ is the interaction potential of a fluid particle at distance $z > 0$ of a half-space filled with fluid particles, too, interacting with a pair potential \tilde{w} :

$$t^{(p)}(z) = \int_z^\infty dz' \int_{R^2} d^2 r_{\parallel} \tilde{w} \left(\sqrt{\mathbf{r}_{\parallel}^2 + z'^2} \right), \quad (2.15)$$

$\mathbf{r}_{\parallel}^2 = x^2 + y^2$. If one inserts the intermolecular potential \tilde{w} chosen above, one obtains for the surface tension of the planar interface $\sigma_{l,g}^{(p)} = \frac{3}{4} \pi \epsilon \sigma^4 (\Delta\rho)^2$. Close to T_c this expression for $\sigma_{l,g}$ vanishes $\sim \tilde{t}$ where $\tilde{t} = (T_c - T)/T_c \rightarrow 0$ instead of the expected mean-field behavior $\tilde{t}^{3/2}$ because the sharp-kink approximation fails to take into account the broadening of the interface on the scale of the bulk correlation length $\xi \sim \tilde{t}^{-1/2}$. Thus Eq. (2.14) takes into account the long-ranged character of the forces but should not be used close to T_c . The corresponding expressions for a cylinder and a sphere of radius h have a similar form:

$$\sigma_{l,g}^{(c)}(h) = \frac{1}{2M\pi h} \Sigma_{l,g}^{(c)} = -\frac{1}{2} (\Delta\rho)^2 \int_h^\infty dr \frac{r}{h} t^{(c)}(r; h) \quad (2.16)$$

and

$$\sigma_{l,g}^{(s)}(h) = \frac{1}{4\pi h^2} \Sigma_{l,g}^{(s)} = -\frac{1}{2} (\Delta\rho)^2 \int_h^\infty dr \left(\frac{r}{h} \right)^2 t^{(s)}(r; h). \quad (2.17)$$

$t^{(c)}(r; h)$ is the interaction potential at distance $r > h$ from the axis of an infinite liquid cylinder of radius h :

$$t^{(c)}(r; h) = \int_{-\infty}^{+\infty} dz \int_0^{2\pi} d\phi \int_0^h r' dr' \tilde{w} \left(\sqrt{r^2 + r'^2 - 2rr' \cos \phi + z^2} \right). \quad (2.18)$$

Correspondingly, $t^{(s)}(r; h)$ is the interaction potential at distance $r > h$ from the center of a liquid drop of radius h :

$$t^{(s)}(r; h) = \frac{2\pi}{r} \int_0^h dr' r' \int_{r-r'}^{r+r'} ds s \tilde{w}(s). \quad (2.19)$$

If one inserts Eqs. (2.3) and (2.4) into Eq. (2.19), one obtains for $r \gg h$

$$t^{(s)}(r; h) \xrightarrow{r \gg h} -\frac{4\pi}{3} h^3 \frac{4\epsilon}{(r/\sigma)^6} + \mathcal{O}\left(\frac{1}{r^8}\right), \quad (2.20)$$

i. e., viewed from a large distance the liquid drop appears as a single molecule with an effective radius h , exerting a van-der-Waals interaction on any other fluid particle. Equations (2.16) and (2.17) are valid for a general form of the interaction potential $w(r)$. For the specific choice given by Eqs. (2.3) and (2.4) the expansion in powers of the curvature $1/h$ yields the following expressions for the surface tensions (see Eqs. (A7) and (B35) in Appendices A and B, respectively):

$$\frac{1}{A} \Sigma_{l,g}^{(p)} = \sigma_{l,g}^{(p)}, \quad (2.21)$$

$$\sigma_{l,g}^{(c)}(h) = \sigma_{l,g}^{(p)} \left(1 - \frac{1}{6} \frac{\ln(h/\sigma)}{(h/\sigma)^2} - \frac{1}{(h/\sigma)^2} \left(\frac{5}{3} \ln 2 + \frac{1}{144} \right) - \mathcal{O}\left(\frac{1}{(h/\sigma)^4}\right) \right), \quad (2.22)$$

and

$$\sigma_{l,g}^{(s)}(h) = \sigma_{l,g}^{(p)} \left(1 - \frac{2}{9} \frac{\ln(h/\sigma)}{(h/\sigma)^2} - \frac{1}{(h/\sigma)^2} \left(\frac{2}{9} \ln 2 + \frac{4}{27} \right) - \mathcal{O}\left(\frac{1}{(h/\sigma)^8}\right) \right). \quad (2.23)$$

If one compares these results with the usual ansatz for the surface tension of a drop [59],

$$\sigma_{l,g}^{(s)}(h) = \sigma_{l,g}^{(p)} \left(1 - \frac{2\delta}{h} + \frac{\alpha}{h^2} + \dots \right), \quad (2.24)$$

first, one notices that our approach predicts that the surface tensions of the curved interfaces are smaller than the planar one and that both attain the latter one asymptotically, $\lim_{h \rightarrow \infty} \sigma_{l,g}^{(s,c)}(h) = \sigma_{l,g}^{(p)}$. Second, since our density profile (Eq.(2.6)) is antisymmetric around $r = h$ and does not contain a symmetric component, within our approach the Tolman length δ must be zero [58]. Third, the long-ranged forces give rise to logarithmic corrections which dominate the usual subdominant term $\sim \alpha h^{-2}$. Within our approach $\sigma_{l,g}^{(i)}$ is invariant with respect to interchanging liquid with vapor and therefore they do not depend on the sign of curvature of the interfaces. The actual behavior of $\sigma_{l,g}^{(s)}(h)$ and $\sigma_{l,g}^{(c)}(h)$ as obtained from Eqs. (2.16) and (2.17) is shown in Fig. 2.

The solid-liquid surface tension entering Eq. (2.10) depends only on r_0 and thus it is constant with respect to the minimization of $\Omega_s(l)$. Within the sharp-kink approximation (Eq. (2.6)) it has the following form ($\tau = 2$ for a sphere, $\tau = 1$ for a cylinder):

$$\begin{aligned} \sigma_{l,s}(r_0) = & -\frac{1}{2}\rho_l^2 \int_{r_1}^{\infty} dr \left(\frac{r}{r_0}\right)^{\tau} t^{(\tau)}(r, r_1) + \rho_l \rho_w \int_{r_1}^{\infty} dr \left(\frac{r}{r_0}\right)^{\tau} v^{(\tau)}(r, r_0) \\ & - \Omega_b(\rho_l) V_{exc}^{(\tau)} / A(r_0) \end{aligned} \quad (2.25)$$

where $v^{(\tau)}(r; r_0)$ is the substrate potential at a distance r of a sphere and a cylinder with radius r_0 , respectively, and with

$$V_{exc}^{(\tau)} / A(r_0) = \frac{r_0}{\tau + 1} \left((1 + d_w / r_0)^{\tau+1} - 1 \right), \quad (2.26)$$

where V_{exc} is the excluded volume due to the repulsive parts of the interaction potentials (see Fig. 1). (For additional information see Ref. [60].)

C. Interaction between the interfaces

For the flat substrate, within the sharp-kink approximation, the correction term $\omega^{(p)}(l) = \frac{1}{A} \bar{\omega}^{(p)}(l)$ is given by

$$\begin{aligned} \omega^{(p)}(l) = & \Delta\rho \left(\rho_l \int_{l-d_w}^{\infty} dz t^{(p)}(z) - \rho_w \int_l^{\infty} dz v^{(p)}(z) \right), \quad l \geq d_w \\ = & \frac{a}{l^2} + \frac{b}{l^3} + \dots, \quad l \gg d_w. \end{aligned} \quad (2.27)$$

Approximately the substrate potential may be expressed in terms of ϕ_{LJ}^{wf} (Eq. (2.5)):

$$v^{(p)}(z) = \int_z^{\infty} dz' \int_{R^2} d^2 r_{\parallel} \phi_{LJ}^{wf} \left(\sqrt{\mathbf{r}_{\parallel}^2 + z'^2} \right). \quad (2.28)$$

In contrast to $t^{(p)}(z)$ the function $v^{(p)}(z)$ diverges for $z \rightarrow 0$. However, according to Eq. (2.6), in Eq. (2.27) one has $l \geq d_w$.

In the case of a planar substrate and for the above parametrization of the interaction in terms of Lennard-Jones potentials the order of the wetting transition and the wetting temperature T_w are determined by ϵ , σ , ϵ_{wf}/ϵ , σ_{wf}/σ , and $\rho_w \sigma_{wf}^3$. In case of a first-order wetting transition $\omega(l)$ has two minima separated by a free energy barrier. One of these minima is localized at a finite value l_0 and represents the global minimum for temperatures $T < T_w$, while the second minimum is given by $l = \infty$ where $\omega(l) = 0$. At $T = T_w$, the minimum at $l = \infty$ changes from a local to a global minimum, so that the film thickness on the planar substrate jumps from a microscopic value to infinity. In case of a second order wetting transition, $\omega(l)$ has only one minimum, which is shifted continuously from a small value l_1 to $l = \infty$ as the temperature is raised from $T < T_w$ towards $T = T_w$ [30,31,54].

For the curved geometries, the systematic analysis of the sharp-kink approximation to the density functional in Eq. (2.1) leads to the result that $\omega(l)$ has essentially the same structure as for the planar system ($l \geq d_w$):

$$\omega^{(\tau)}(l) = \Delta\rho \left(\rho_l \int_{r_0+l}^{\infty} dr \left(\frac{r}{r_0} \right)^{\tau} t(r; r_1) - \rho_w \int_{r_0+l}^{\infty} dr \left(\frac{r}{r_0} \right)^{\tau} v(r; r_0) \right) \quad (2.29)$$

with $\tau = 1$ for the cylindrical and $\tau = 2$ for the spherical system. $t(r; r_1)$ is defined in terms of $\tilde{w}(r)$, and thus $w(r)$, according to Eq. (2.18) and Eq. (2.19), respectively; $v(r; r_0)$ is the substrate potential of a sphere and a cylinder of radius r_0 , respectively. It should be emphasized that Eq. (2.29) is valid for any functional form of $w(r)$ and $v(r)$, provided only that they decay rapidly enough in order to guarantee the convergence of the integrals; Eq. (2.29) also does not depend on the explicit form of Eq. (2.2).

However, due to the unlimited increase of $A(r_0+l)/A(r_0)$ (see Eq. (2.13)) in Eq. (2.10) even at coexistence, i. e., $\Delta\Omega_b = 0$, the film thickness l cannot take on a macroscopic value on cylinders or spheres, so that first order wetting transitions are reduced to a jump from a small to a large but finite value of l . In order to be able to discuss these transitions quantitatively the general expression for the effective interface potential (Eq. (2.29)) must be evaluated for specific interaction potentials $w(r)$ and $v(r)$. According to Appendices A and B the model potentials in Eqs. (2.3)-(2.5) lead to (see Eq. (A13))

$$\omega^{(\tau)}(l) = \omega_{attr}^{(\tau)}(l) + \omega_{rep}^{(\tau)}(l) \quad (2.30)$$

where

$$\begin{aligned} \omega_{rep}^{(s)}(l) = & \frac{1}{r_0^2} \frac{\pi}{540} \Delta\rho (\rho_l \epsilon \sigma^{12} - \rho_w \epsilon_{wf} \sigma_{wf}^{12}) \left(\frac{h^2 + 8hr_0 + r_0^2}{(h+r_0)^8} - \frac{h^2 - 8hr_0 + r_0^2}{(h-r_0)^8} \right) \\ & + \frac{\pi}{90} \Delta\rho \rho_l \epsilon \sigma^{12} \left(\frac{9h-r_0}{(h-r_0)^9} - \frac{9h+r_0}{(h+r_0)^9} \right) \frac{d_w}{r_0} + \mathcal{O} \left(\left(\frac{d_w}{r_0} \right)^2 \right), \end{aligned} \quad (2.31)$$

$$\begin{aligned} \omega_{attr}^{(s)}(l) = & -\frac{1}{r_0^2} \frac{\pi}{3} \Delta\rho (\rho_l \epsilon \sigma^6 - \rho_w \epsilon_{wf} \sigma_{wf}^6) \left(2hr_0 \frac{h^2 + r_0^2}{(h^2 - r_0^2)^2} - \ln \frac{h+r_0}{h-r_0} \right) \\ & - \frac{16\pi}{3} \Delta\rho \rho_l \epsilon \sigma^6 \frac{h^3 r_0}{(h^2 - r_0^2)^3} \frac{d_w}{r_0} + \mathcal{O} \left(\left(\frac{d_w}{r_0} \right)^2 \right), \end{aligned} \quad (2.32)$$

(see Eqs. (B2), (B20), and (B22))

$$\begin{aligned} \omega_{rep}^{(e)}(l) = & \frac{7\pi^2}{64} \Delta\rho (\rho_l \epsilon \sigma^{12} - \rho_w \epsilon_{wf} \sigma_{wf}^{12}) \frac{r_0}{h^9} {}_2F_1 \left(\frac{11}{2}, \frac{9}{2}; 2; \left(\frac{r_0}{h} \right)^2 \right) \\ & + \frac{7\pi^2}{64} \Delta\rho \rho_l \epsilon \sigma^{12} \frac{r_0}{h^9} \left(2 {}_2F_1 \left(\frac{11}{2}, \frac{9}{2}; 2; \left(\frac{r_0}{h} \right)^2 \right) + \frac{99}{4} \frac{r_0^2}{h^2} {}_2F_1 \left(\frac{13}{2}, \frac{11}{2}; 3; \left(\frac{r_0}{h} \right)^2 \right) \right) \frac{d_w}{r_0} \\ & + \mathcal{O} \left(\left(\frac{d_w}{r_0} \right)^2 \right), \end{aligned} \quad (2.33)$$

and

$$\begin{aligned}
\omega_{attr}^{(c)}(l) &= -\frac{\pi^2}{2} \Delta\rho(\rho_l \epsilon \sigma^6 - \rho_w \epsilon_{wf} \sigma_{wf}^6) \frac{r_0}{h^3} {}_2F_1\left(\frac{5}{2}, \frac{3}{2}; 2; \left(\frac{r_0}{h}\right)^2\right) \\
&\quad - \frac{\pi^2}{2} \Delta\rho \rho_l \epsilon \sigma^6 \frac{r_0}{h^3} \left(2 {}_2F_1\left(\frac{5}{2}, \frac{3}{2}; 2; \left(\frac{r_0}{h}\right)^2\right) + \frac{15}{4} \frac{r_0^2}{h^2} {}_2F_1\left(\frac{7}{2}, \frac{5}{2}; 3; \left(\frac{r_0}{h}\right)^2\right) \right) \frac{d_w}{r_0} \\
&\quad + \mathcal{O}\left(\left(\frac{d_w}{r_0}\right)^2\right).
\end{aligned} \tag{2.34}$$

Here we have assumed that the radius of the substrate is large compared with the diameter of the fluid particles. Equations (2.32) and (2.34) can be compared with other approaches [23,34], in particular with the dispersion theory developed in Ref. [34(c)] which considers a system composed of three concentrically arranged media characterized by different dielectric constants ϵ_i . The summation of the electromagnetic surface normal modes yields the dispersion function. Its expansion in powers of the dielectric reflection coefficient $\Delta_{ij} = \frac{\epsilon_i - \epsilon_j}{\epsilon_i + \epsilon_j}$ results in a factorization of the dispersion energies into a frequency-dependent and a geometrical factor. The geometrical factors (Eqs. (6.5) and (6.9) in Ref. [34(c)]) are in full agreement with our results for the attractive contributions (Eqs. (2.32) and (2.34)). It is reassuring to see that despite of the differences between these two approaches as discussed in the Introduction both yield the same functional dependence on the film thickness for large l . Furthermore one should keep in mind that the density functional approach yields a well-defined expression of $\omega(l)$ even for small values of l , whereas the dispersion theory leads to diverging energies in this limit. In addition the density functional can capture subdominant contributions to $\omega(l)$ which arise both from the repulsive parts of the interaction potentials and from detailed structures of the substrate determining the wetting behavior at coexistence. This will be discussed in the following section.

For the model defined by Eqs. (2.4) and (2.5) the effective interface potential of the curved substrates, $\omega^{(\tau)}(l, r_0) = \omega_{attr}^{(\tau)}(l, r_0) + \omega_{rep}^{(\tau)}(l, r_0)$, can be related to that of the planar substrate as follows:

$$\omega^{(\tau)}(l, r_0) = \omega_{attr}^{(p)}(l) \mathcal{S}_{attr}^{(\tau)}\left(\frac{r_0}{l}\right) + \omega_{rep}^{(p)}(l) \mathcal{S}_{rep}^{(\tau)}\left(\frac{r_0}{l}\right) \tag{2.35}$$

where the scaling functions

$$\mathcal{S}_{attr}^{(\tau)}\left(\frac{r_0}{l}\right) = \frac{\omega_{attr}^{(\tau)}(l, r_0)}{\omega_{attr}^{(p)}(l)}, \quad \mathcal{S}_{rep}^{(\tau)}\left(\frac{r_0}{l}\right) = \frac{\omega_{rep}^{(\tau)}(l, r_0)}{\omega_{rep}^{(p)}(l)} \tag{2.36}$$

turn out to depend indeed only on the ratio $x = r_0/l$ so that

$$\omega^{(\tau)}(l, r_0) = \omega^{(p)}(l) \frac{\mathcal{S}_{attr}^{(\tau)}(r_0/l) + \frac{\omega_{rep}^{(p)}(l)}{\omega_{attr}^{(p)}(l)} \mathcal{S}_{rep}^{(\tau)}(r_0/l)}{1 + \frac{\omega_{rep}^{(p)}(l)}{\omega_{attr}^{(p)}(l)}}. \tag{2.37}$$

Since $\omega_{attr}^{(p)}(l) = a/l^2$ and $\omega_{rep}^{(p)}(l) = c/l^8$ with the Hamaker constant $a = \pi\Delta\rho(\rho_w\epsilon_{wf}\sigma_{wf}^6 - \rho_l\epsilon\sigma^6)/3$ and with $c = \pi\Delta\rho(\rho_l\epsilon\sigma^{12} - \rho_w\epsilon_{wf}\sigma_{wf}^{12})/90$, one has $\omega_{rep}^{(p)}(l)/\omega_{attr}^{(p)}(l) = c/(al^6)$ and thus due to $\omega^{(p)}(l) = \omega_{attr}^{(p)}(l) + \omega_{rep}^{(p)}(l)$

$$\omega^{(\tau)}(l, r_0) = \omega^{(p)}(l) \left(\mathcal{S}_{attr}^{(\tau)} + \frac{c}{a} l^{-6} \left(\mathcal{S}_{rep}^{(\tau)} \left(\frac{r_0}{l} \right) - \mathcal{S}_{attr}^{(\tau)} \left(\frac{r_0}{l} \right) \right) \right) + \mathcal{O}(l^{-12}). \quad (2.38)$$

Therefore for $l \gg \sigma$ the effective interface potential attains the scaling form

$$\omega^{(\tau)}(l, r_0) = \omega^{(p)}(l) \mathcal{S}_\tau \left(\frac{r_0}{l} \right), \quad l \gg \sigma, \quad (2.39)$$

where $\mathcal{S}_\tau(x) \equiv \mathcal{S}_{attr}^{(\tau)}(r_0/l)$. These scaling functions exhibit the following limiting behavior:

$$\mathcal{S}_\tau(x \rightarrow \infty) = 1 + \frac{\tau}{2x} + \mathcal{O}(x^{-2}) \quad (2.40)$$

and

$$\mathcal{S}_\tau(x \rightarrow 0) = \alpha_\tau x + \beta_\tau x^2 + \mathcal{O}(x^3) \quad (2.41)$$

where $\alpha_c = \frac{3\pi}{2}$, $\beta_c = -\frac{9\pi}{2}$, $\alpha_s = \frac{16}{3}$, and $\beta_s = -16$. The full scaling function $\mathcal{S}_\tau(x)$ is shown in Fig. 3(a). It exhibits a non-monotonic behavior.

III. Wetting behavior

A. Film thickness at coexistence and above the wetting transition temperature

We consider a curved substrate-fluid system at a temperature $T > T_w^{(\tau)}(r_0)$ above its (quasi-)wetting transition temperature $T_w^{(\tau)}(r_0)$ and at liquid-vapor coexistence. (Typically one has $T_w^{(\tau)}(r_0) > T_w^{(\tau)}(\infty) = T_w^{(p)}$, see below). The curvature prevents the build-up of a macroscopically thick wetting film as it would form on the corresponding planar substrate. If this film thickness is sufficiently large it can be determined from the leading terms in the effective interface potential ($a > 0$):

$$\Omega_s(l) \simeq \frac{a}{l^2} \mathcal{S}_\tau \left(\frac{r_0}{l} \right) + \left(1 + \frac{l}{r_0} \right)^\tau \sigma_{l,g}^{(p)} + \sigma_{l,s}(r_0). \quad (3.1)$$

Due to $T > T_w^{(\tau)}$ and $\mu - \mu_0(T) = 0^-$ the equilibrium thickness corresponding to Eq. (3.1) is the maximum thickness the film can attain and it is given by

$$l_{max}^{(\tau)} = \frac{1}{x_\tau^*(\kappa)} r_0 \quad (3.2)$$

where $x_\tau^*(\kappa)$ is the solution of the implicit equation

$$x = \kappa \left(\frac{\tau}{2} \right)^{1/3} s_\tau(x) \quad (3.3)$$

with (see Eq. (2.36) and Fig. 3(b))

$$s_\tau(x) = (1 + x^{-1})^{(\tau-1)/3} \left(\mathcal{S}_\tau(x) + \frac{x}{2} \mathcal{S}'_\tau(x) \right)^{-1/3}. \quad (3.4)$$

This shows that the limiting thickness of the wetting film above T_w is governed by the dimensionless parameter

$$\kappa = \left(\frac{r_0^2 \sigma_{l,g}^{(p)}}{a} \right)^{1/3}. \quad (3.5)$$

Due to $s_\tau(x \rightarrow \infty) = 1 + \left(\frac{\tau}{4} - \frac{1}{3} \right) x^{-1} + \left(\frac{2}{9} - \frac{\tau}{4} + \frac{\tau^2}{24} \right) x^{-2} + \mathcal{O}(x^{-3})$ one finds

$$x_\tau^*(\kappa \rightarrow \infty) = \left(\frac{\tau}{2} \right)^{1/3} \kappa + \frac{\tau}{4} - \frac{1}{3} + \mathcal{O}(\kappa^{-1}). \quad (3.6)$$

In the limit $x \rightarrow 0$ one has $s_1(x \rightarrow 0) = \left(\frac{4}{9\pi} \right)^{1/3} x^{-1/3} \left(1 + \frac{4}{3}x - \frac{59}{72}x^2 + \mathcal{O}(x^3) \right)$ and $s_2(x \rightarrow 0) = \frac{1}{2}x^{-2/3} \left(1 + \frac{5}{3}x - \frac{4}{9}x^2 + \mathcal{O}(x^3) \right)$ so that

$$x_{\tau=1}^*(\kappa \rightarrow 0) = \left(\frac{2\kappa^3}{9\pi} \right)^{1/4} + \left(\frac{2\kappa^3}{9\pi} \right)^{1/2} + \mathcal{O}(\kappa^{9/4}) \quad (3.7)$$

and

$$x_{\tau=2}^*(\kappa \rightarrow 0) = \left(\frac{\kappa}{2} \right)^{3/5} + \left(\frac{\kappa}{2} \right)^{6/5} + \mathcal{O}(\kappa^{9/5}). \quad (3.8)$$

This implies that for a given system, i. e., $\sigma_{l,g}^{(p)}$ and a fixed and for large r_0 the maximum thickness of the wetting film is given by

$$l_{max}^{(\tau)}(r_0 \rightarrow \infty) = \left(\frac{2ar_0}{\tau \sigma_{l,g}^{(p)}} \right)^{1/3} = \left(\frac{2a}{\Delta \rho \frac{\tau \sigma_{l,g}^{(p)}}{\Delta \rho r_0}} \right)^{1/3}, \quad \kappa \gg 1, \quad (3.9)$$

(see also, c. f., the first paragraph of Subsect. III. B) whereas for a small liquid-vapor surface tension $\sigma_{l,g}^{(p)}$ and a large Hamaker constant a the maximum thicknesses are (see Eq. (3.7))

$$l_{max}^{(c)} \simeq \left(\frac{9\pi a r_0^2}{2\sigma_{l,g}^{(p)}} \right)^{1/4}, \quad \kappa \ll 1, \quad (3.10)$$

and

$$l_{max}^{(s)} \simeq \left(\frac{8a r_0^3}{\sigma_{l,g}^{(p)}} \right)^{1/5}, \quad \kappa \ll 1. \quad (3.11)$$

For large κ l_{max} is larger for a cylinder than for a sphere by a constant factor $2^{1/3} \simeq 1.26$ (Eq. (3.6)) whereas for small κ this ratio diverges weakly as $(9\pi)^{1/4} 2^{-17/20} \kappa^{-3/20}$ (Eqs. (3.7) and (3.8)). The full dependence of $l_{max}^{(\tau)}/r_0 = 1/x_\tau^*$ on κ is shown in Fig. 4.

In principle κ can be any positive number. Typically, at low temperatures, $\sigma_{l,g}^{(p)}$ ranges between $10^{-3} J/m^2$ and $10^{-2} J/m^2$ [61] and a between $10^{-20} J$ and $10^{-19} J$ [61] so that $\kappa = \kappa_0 \cdot (r_0/\text{\AA})^{2/3}$ with $\kappa_0 = 0.05 \dots 0.20$. With $\kappa_0 = 0.05$ according to Fig. 4 this implies that for $r_0 = 100\text{\AA}$ $l_{max}^{(c)} \simeq 130\text{\AA}$ and $l_{max}^{(s)} \simeq 90\text{\AA}$ whereas for $r_0 = 1\mu m$ $l_{max}^{(c)} \simeq 550\text{\AA}$ and $l_{max}^{(s)} \simeq 430\text{\AA}$. Due to finite resolutions for pressure and temperature equilibrium film thicknesses on a planar substrate can be followed up to at most a few hundred \AA , say 500\AA . In this case and for the above quoted values of $\sigma_{l,g}^{(p)}$ and a r_0 must be smaller than $50\mu m$ for a cylinder and $100\mu m$ for a sphere in order to cause a deviation from the corresponding planar film thickness of more than 5%.

If for a given system, i. e. r_0 fixed, the temperature is raised towards T_c , $\sigma_{l,g}^{(p)}$ vanishes as $\sigma_0 \tilde{t}^{2\nu}$, $\nu \simeq 0.632$, where $\tilde{t} = (T_c - T)/T_c \rightarrow 0$, and $a \sim \Delta\rho$ as $a_0 \tilde{t}^\beta$, $\beta \simeq 0.328$, so that κ goes to zero as $\left(\frac{r_0^2 \sigma_0}{a_0} \right)^{1/3} \tilde{t}^{(2\nu-\beta)/3} \sim \tilde{t}^{0.312}$ and Eqs. (3.7) and (3.8) apply. From these one infers that the maximum film thicknesses diverge as $l_{max}^{(c)} \simeq (9\pi r_0^2 a_0 / 2\sigma_0)^{1/4} \tilde{t}^{-(2\nu-\beta)/4} \sim \tilde{t}^{-0.234}$ and $l_{max}^{(s)} \simeq (8r_0^3 a_0 / \sigma_0)^{1/5} \tilde{t}^{-(2\nu-\beta)/5} \sim \tilde{t}^{-0.187}$, respectively. At T_c the critical fluctuations in the bulk lead to a power-law decay of the density profile towards the bulk density. As function of the temperature T this mesoscopic interfacial structure known as critical adsorption emerges from a film whose thickness diverges like the bulk correlation length $\xi = \xi_0^- \tilde{t}^{-\nu} \simeq \xi_0^- \tilde{t}^{-0.632}$ where ξ_0^- is typically of the order of 1.5\AA . This picture for a planar substrate [62] holds also for spherical and cylindrical substrates provided ξ is large compared with their radii of curvature [26]. On this basis we expect that ultimately for $\tilde{t} \rightarrow 0$ both $l_{max}^{(c)}$ and $l_{max}^{(s)}$ should diverge as $\tilde{t}^{-\nu}$. Our above results obtained from the effective interface potential signal such a divergence but the corresponding exponent is smaller. This difference must be attributed to our present sharp-kink approximation of a mean-field theory. Nonetheless one should keep in mind that at least within the mean-field theory for a planar geometry the leading behavior of the effective interface potential is captured correctly by the sharp-kink approximation in spite of the actual broadening of the emerging liquid-vapor interface close to T_c [55]; it is reasonable to expect that this quality of the sharp-kink approximation carries over to the case of curved surfaces. However, as

the discussion of Eqs. (2.46) and (2.47) in Ref. [55(c)] shows even this quality of the sharp-kink approximation does not suffice to describe properly the crossover between complete wetting and critical adsorption. The crossover condition $l \simeq \xi$ must be inserted by hand. Our above findings for $l_{max}^{(\tau)}$ must be judged and augmented similarly.

The above analysis relies on a positive value of a and, because we have considered only the leading terms in $\omega(l)$, on the fact that $l_{max}^{(\tau)}$ is large. This is fulfilled for $T > T_w^{(\tau)}(r_0)$ where $T_w^{(\tau)}(r_0)$ is the thin-thick transition temperature in the case of a (quasi-) first-order wetting transition. If the wetting transition on the planar substrate is continuous, there is no transition at coexistence and we consider simply $T > T_w^{(p)}$, i. e., $a > 0$. The solid-vapor surface tension is the minimum value of $\Omega_s(l)$ so that at coexistence

$$\sigma_{s,g} = \min_l \Omega_s(l) = \Omega_s(l_0) \leq \frac{A(r_0 + l_0)}{A(r_0)} \sigma_{l,g}(r_0 + l_0) + \sigma_{l,s}(r_0) \quad (3.12)$$

because $\omega(\infty) = 0$ so that $\omega(l_0) \leq 0$ (see Eq. (2.10)). One should note that in Eq. (3.12) the inequality never turns into an equality if $r_0 < \infty$ because $l_0(r_0 < \infty) < \infty$ so that $\omega(l_0(r_0 < \infty)) < 0$. Only in the limit $r_0 \rightarrow \infty$ one recovers the standard relation that $\sigma_{s,g}^{(p)} \leq \sigma_{l,g}^{(p)} + \sigma_{l,s}^{(p)}$ turns into an equality at $T = T_w^{(p)}$. Since in Eq. (3.12) the right hand side $\sigma_{l,g}$ is enhanced by the factor $A(r_0 + l_0)/A(r_0)$ as compared with the planar case one can surmise that $T_w^{(\tau)}(r_0)$ is larger than $T_w^{(p)}$. However, this argument must be checked more carefully, because at $T_w^{(\tau)}(r_0)$ the right hand side of Eq. (3.12) is not attained. This will be done in Subsec. III. C.

B. Complete wetting off coexistence and above the wetting transition temperature

According to Eq. (3.9) the thickness $l_{max}^{(\tau)}$ of a wetting film on a curved substrate at liquid-vapor coexistence $\Delta\mu = 0$ is the same as if the identical system in planar geometry is taken off from liquid-vapor coexistence with a $\Delta\mu_{eff}(\Delta\mu = 0) = \frac{\tau\sigma_{l,g}^{(p)}}{r_0\Delta\rho}$. In this subsection we want to discuss how a wetting film on a curved substrate attains this maximum thickness $l_{max}^{(\tau)}$ when one approaches liquid-vapor coexistence, i. e. $\Delta\mu \rightarrow 0$, above $T_w^{(\tau)}(r_0)$. In this case we have (see Eqs. (2.10), (2.12), (2.13), and (3.1)), with $a > 0$,

$$\begin{aligned} \Omega_s(l \gg d_w) &\simeq \frac{a}{l^2} S_\tau \left(\frac{r_0}{l} \right) + \left(1 + \frac{l}{r_0} \right)^\tau \sigma_{l,g}^{(p)} \\ &+ \frac{1}{\tau + 1} \left(\left(1 + \frac{l}{r_0} \right)^{\tau+1} - 1 \right) r_0 \Delta\rho \Delta\mu + \sigma_{l,s}(r_0) \end{aligned} \quad (3.13)$$

so that

$$l_0 = \frac{1}{y_\tau^*(\kappa, \lambda)} r_0 \quad (3.14)$$

where $y_\tau^*(\kappa, \lambda)$ is the solution of the implicit equation

$$y = \kappa \left(\frac{\tau}{2} \right)^{1/3} u_\tau(y, \lambda) \quad (3.15)$$

with

$$u_\tau(y, \lambda) = \left(1 + \frac{\lambda}{\tau} \left(1 + \frac{1}{y} \right) \right)^{1/3} s_\tau(y). \quad (3.16)$$

The dimensionless parameter λ measures the distance from liquid-vapor coexistence,

$$\lambda = \frac{\Delta\rho r_0}{\sigma_{l,g}^{(p)}} \Delta\mu, \quad (3.17)$$

so that $y_\tau^*(\kappa, \lambda = 0) = x_\tau^*(\kappa) = r_0/l_{max}(\kappa)$. With $u_\tau(y \rightarrow \infty, \lambda) = (1 + \frac{\lambda}{\tau})^{1/3} + y^{-1}(\tau + \lambda - \frac{4}{3})/4(1 + \lambda/\tau)^{2/3} + \mathcal{O}(y^{-2})$ one has

$$y_\tau^*(\kappa \rightarrow \infty, \lambda) = \left(\frac{\tau}{2} \right)^{1/3} \kappa \left(1 + \frac{\lambda}{\tau} \right)^{1/3} + \frac{\tau + \lambda - \frac{4}{3}}{1 + \frac{\lambda}{\tau}} + \mathcal{O}(\kappa^{-1}). \quad (3.18)$$

In the limit $\kappa \rightarrow 0$ one finds $u_1(y \rightarrow 0) = (\frac{4}{9\pi})^{1/3} \left(\frac{\lambda}{y^2} \right)^{1/3} \left(1 + \frac{1+5\lambda}{3} \frac{y}{\lambda} + \mathcal{O}\left(\left(\frac{y}{\lambda}\right)^2\right) \right)$ and $u_2(y \rightarrow 0) = (\frac{\lambda}{16})^{1/3} \frac{1}{y} \left(1 + \frac{2+6\lambda}{3} \frac{y}{\lambda} + \mathcal{O}\left(\left(\frac{y}{\lambda}\right)^2\right) \right)$ so that

$$y_1^*(\kappa \rightarrow 0, \lambda) = \left(\frac{2\kappa^3\lambda}{9\pi} \right)^{1/5} + \frac{1+5\lambda}{5\lambda} \left(\frac{2\kappa^3\lambda}{9\pi} \right)^{2/5} + \mathcal{O}(\kappa^{9/5}) \quad (3.19)$$

and

$$y_2^*(\kappa \rightarrow 0, \lambda) = \left(\frac{\kappa^3\lambda}{16} \right)^{1/6} + \frac{1+3\lambda}{3\lambda} \left(\frac{\kappa^3\lambda}{16} \right)^{1/3} + \mathcal{O}(\kappa^{3/2}). \quad (3.20)$$

In the case $\kappa \gg 1$ Eq.(3.16) implies

$$l_0(r_0, \Delta\mu) = \frac{l_{max}}{\left(1 + \frac{\lambda}{\tau} \right)^{1/3}}, \quad \kappa \gg 1, \quad (3.21)$$

whereas for $\kappa \ll 1$ one has

$$l_0^{(c)}(r_0, \Delta\mu) = \left(\frac{9\pi a r_0^2}{2\Delta\rho\Delta\mu} \right)^{1/5}, \quad \kappa \ll 1, \quad (3.22)$$

and

$$l_0^{(s)}(r_0, \Delta\mu) = \left(\frac{16ar_0^3}{\Delta\rho\Delta\mu} \right)^{1/6}, \quad \kappa \ll 1. \quad (3.23)$$

Equations (3.16), (3.22), and (3.23) show that the limits $\lambda \rightarrow 0$ and $\kappa \rightarrow 0$ cannot be interchanged.

Since for a small undersaturation $\Delta\mu$ the thickness of the complete wetting film on the corresponding planar substrate is ($T > T_w^{(p)}$)

$$l_0(r_0 = \infty, \Delta\mu \rightarrow 0) = l_0^{(p)}(\Delta\mu \rightarrow 0) = \left(\frac{2a}{\Delta\rho\Delta\mu} \right)^{1/3}, \quad (3.24)$$

the film thickness on the corresponding curved substrate can be expressed in terms of an effective $\Delta\mu_{eff}(\Delta\mu; r_0, \tau)$:

$$l_0(r_0, \Delta\mu \rightarrow 0) = l_0^{(p)}(\Delta\mu_{eff}), \quad (3.25a)$$

$$\Delta\mu_{eff} = \Delta\mu + \delta\mu(\kappa, \lambda). \quad (3.25b)$$

In the following we determine $\Delta\mu_{eff}$ on the basis of Eq. (3.13) which captures the *leading* behavior of $\Omega_s(l)$ for large l . (One should keep in mind that prewetting phenomena depend also on the behavior of $\Omega_s(l \gtrsim d_w)$ so that one cannot expect that the (quasi-) prewetting line on curved substrates is simply the prewetting line of the planar substrate, $\Delta\mu_{pw}^{(p)}(T)$, shifted upwards by $\Delta\mu_{eff}$. Thus Eq. (3.25a) holds only above the prewetting line where l_0 is sufficiently large. Therefore we concur with Upton et al. (Sect. XI in Ref. [26(b)] in that the effects of curvature cannot be fully subsumed into an effective $\Delta\mu_{eff}$.) With Eqs. (3.14) and (3.17) one has

$$\lambda_{eff}(\kappa, \lambda) = \frac{r_0\Delta\rho\Delta\mu_{eff}}{\sigma_{l,g}^{(p)}} = 2 \left(\frac{y^*(\kappa, \lambda)}{\kappa} \right)^3. \quad (3.26)$$

In the limit $\kappa \gg 1$ Eq. (3.18) applies so that $\Delta\mu_{eff}$ is given by

$$\Delta\mu_{eff}(\Delta\mu; r_0, \tau) = \Delta\mu + \frac{\tau\sigma_{l,g}^{(p)}}{\Delta\rho r_0}, \quad \kappa \gg 1. \quad (3.27)$$

Thus in the limit $\kappa \gg 1$ the curved substrates resemble the same film thickness as the planar substrate if the liquid-vapor coexistence curve $\mu_0(T)$ is shifted upwards by

$$\delta\mu_\infty^{(\tau)} = \frac{\tau\sigma_{l,g}^{(p)}}{\Delta\rho r_0} = \frac{\tau \left(\sigma_{l,g}^{(p)} \right)^{3/2}}{\Delta\rho a^{1/2}} \kappa^{-3/2}, \quad \kappa \gg 1. \quad (3.28)$$

This is in accordance with our previous finding $\Delta\mu_{eff}(\Delta\mu = 0) = \delta\mu_\infty^{(\tau)}$ (see Eq. (3.9)).

From Eq. (3.27) one finds that for spheres ($\tau = 2$) the effect of the curvature is twice as large as for cylinders ($\tau = 1$). It should be emphasized that the shift $\delta\mu_\infty^{(\tau)}$ is independent of the Hamaker constant a and depends on surface properties only via the planar liquid-vapor surface tension.

Equation (3.27) holds only in the limit $\kappa = (\sigma_{l,g}^{(p)} r_0^2/a)^{1/3} \gg 1$, i. e., for $r_0 \rightarrow \infty$ and T fixed. In the opposite case, i. e., for $T \rightarrow T_c$ and r_0 fixed one has $\kappa \sim \tilde{t}^{(2\nu-\beta)/3} \rightarrow 0$ so that the limit $\kappa \ll 1$ must be considered (see Eqs. (3.19) and (3.20)). These latter equations are valid provided that (i) $y^* \ll 1$ and (ii) $(1 + 1/y^*) \lambda/\tau \gg 1$ (compare Eq. (3.16)). Condition (i) is fulfilled if $\kappa \ll (9\pi/2\lambda)^{1/3}$ for a cylinder and if $\kappa \ll 2^{4/3}/\lambda^{1/3}$ for a sphere, respectively. Condition (ii) is always fulfilled for $\lambda > \tau$; for $\lambda < \tau$ it requires $y^* \ll \lambda/(\tau - \lambda)$, i. e., $\kappa \ll (9\pi/2)^{1/3} \lambda^{4/3}/(1 - \lambda)^{5/3}$ for a cylinder and $\kappa \ll 2^{4/3} \lambda^{5/3}/(2 - \lambda)^2$ for a sphere, respectively. In this regime, denoted as I (see Figs. 6(a) and (b)), λ_{eff} is given by

$$\lambda_{eff}^{(c)} \simeq 2 \left(\frac{2\lambda}{9\pi} \right)^{3/5} \kappa^{-6/5}, \quad \text{regime I,} \quad (3.29)$$

and

$$\lambda_{eff}^{(s)} \simeq \left(\frac{\lambda}{4} \right)^{1/2} \kappa^{-3/2}, \quad \text{regime I.} \quad (3.30)$$

On the other hand according to Eq. (3.18) the limit $y^* \gg 1$ applies if $\kappa \gg 2^{1/3}/(\tau + \lambda)^{1/3}$ (regime II); in this case Eq. (3.26) yields

$$\lambda_{eff}^{(\tau)} \simeq \tau + \lambda, \quad \text{regime II,} \quad (3.31)$$

which is equivalent to Eq. (3.27). In the intermediate regime III, i. e., $1 \gg y^* \gg \lambda/(\tau - \lambda)$, the asymptotic formulae in Eqs. (3.19) and (3.20) do not hold. Instead of expanding y^* in powers of κ , in this case one has to evaluate Eqs. (3.15) and (3.16) for small values of λ first and then to consider the limit $\kappa \rightarrow 0$:

$$y_\tau^*(\kappa, \lambda \rightarrow 0) \simeq \kappa \left(\frac{\tau}{2} \right)^{1/3} \left(1 + \frac{\lambda}{3\tau} \left(1 + \frac{1}{y} \right) \right) s_\tau(y). \quad (3.32)$$

With $s_\tau(y)$ taken in the limit $y \rightarrow 0$ one finds in this regime III

$$y_1^* \simeq \left(\frac{2\kappa^3}{9\pi} \right)^{1/4} \left(1 + \frac{\lambda}{4} \left(\left(\frac{2\kappa^3}{9\pi} \right)^{-1/4} + 2 + \mathcal{O}(\kappa^{3/4}) \right) + \mathcal{O}(\lambda^2) \right) \quad (3.33)$$

and

$$y_2^* \simeq \left(\frac{\kappa}{2} \right)^{3/5} \left(1 + \frac{\lambda}{10} \left(\left(\frac{\kappa}{2} \right)^{-3/5} + 2 + \mathcal{O}(\kappa^{3/5}) \right) + \mathcal{O}(\lambda^2) \right), \quad (3.34)$$

respectively, so that

$$\lambda_{eff}^{(c)} \simeq 2 \left(\frac{2}{9\pi\kappa} \right)^{3/4} \left(1 + \frac{3}{4}\lambda \left(\left(\frac{2\kappa^3}{9\pi} \right)^{-1/4} + 4 + \mathcal{O}(\kappa^{3/4}) \right) + \mathcal{O}(\lambda^2) \right),$$

regime III,

(3.35)

and

$$\lambda_{eff}^{(s)} \simeq \left(\frac{1}{16\kappa^6} \right)^{1/5} \left(1 + \frac{3}{10}\lambda \left(\left(\frac{\kappa}{2} \right)^{-3/5} + 4 + \mathcal{O}(\kappa^{3/5}) \right) + \mathcal{O}(\lambda^2) \right),$$

regime III.

(3.36)

Figures 7(a) and (b) visualize this crossover behavior of λ_{eff} as function of κ for λ fixed in the case of a cylinder and a sphere, respectively.

C. First-order wetting transitions

The results of the previous subsection allow us to discuss the effect of curvature on a wetting transition which is first order on a planar substrate. For suitably chosen interaction potentials Fig. 8 shows such a phase diagram and the temperature dependence of the corresponding film thickness at coexistence for a cylinder and a sphere, respectively, as compared to those of the corresponding planar substrate. In accordance with Refs. [63,64] we find for the planar substrate that the prewetting line $\mu_{pw}^{(p)}(T)$ joins the gas-liquid coexistence curve $\mu_0(T)$ tangentially,

$$\mu_{pw}^{(p)}(T \rightarrow T_w^{(p)}) - \mu_0(T) = k_\mu |T - T_w^{(p)}|^{\gamma(\zeta)}, \quad \gamma(\zeta) = \frac{\zeta}{\zeta - 1},$$
(3.37)

if for large distances the pair interaction potentials in the system decay like $r^{-(3+\zeta)}$ [63]. Upon crossing the prewetting line the wetting film thickness undergoes a thin-thick transition where the corresponding jump $\Delta l(T)$ diverges at the first-order transition temperature $T_w^{(p)}$ as

$$\Delta l(T \rightarrow T_w^{(p)}) = k_l |T - T_w^{(p)}|^{-\gamma(\zeta)/\zeta}.$$
(3.38)

In Subsects. III.A and III.B we focused on the region $T > T_w^{(p)}$ of the phase diagram where the behavior of the film thickness is independent of the order of the wetting transition. Since, however, in the region close to $T_w^{(p)}$ the order of the transition plays an essential role, the present and the following subsection are dedicated separately to first- and second-order transitions, respectively. A first-order wetting transition is accompanied by a prewetting line which implies the occurrence of discontinuities in the film thickness

also off coexistence. In the region between the prewetting line and the coexistence curve, i. e., $T > T_w^{(p)}$ and $\Delta\mu \leq \Delta\mu_{pw}^{(p)}(T)$ (see Subsect. III.B), the film thickness on the curved substrates and on the corresponding planar substrate are related to each other via $\Delta\mu_{eff}$. In the limit of large radii, $\kappa \gg 1$, this relationship is given by the shift $\Delta\mu_{eff} = \Delta\mu + \delta\mu$. Thus one is inclined to surmise that for $\kappa \gg 1$ also the prewetting line of the curved substrates can be obtained by shifting the prewetting line of the corresponding planar substrate upwards in the phase diagram by the amount $\delta\mu$. In this case the knowledge of the location of the prewetting lines relative to each other yields information about the shift of the transition temperature, $T_w^{(\tau)}(r_0) - T_w^{(p)}$, and the jump in the film thickness $\Delta l^{(\tau)}$ on the curved substrates. Since Eq. (3.37) holds especially for $T = T_w^{(\tau)}(\kappa \rightarrow \infty)$, one has with $\mu_{pw}^{(p)}(T_w^{(\tau)}(\kappa \rightarrow \infty) \rightarrow T_w^{(p)}) - \mu_0(T_w^{(\tau)}(\kappa \rightarrow \infty)) = \delta\mu_\infty^{(\tau)}$,

$$T_w^{(\tau)}(\kappa \rightarrow \infty) - T_w^{(p)} = \left(\frac{1}{k_\mu} \delta\mu_\infty^{(\tau)} \right)^{1/\gamma(\zeta)} \quad (3.39)$$

so that for the jump in thickness at coexistence on the curved substrate one has

$$\Delta l^{(\tau)}(T_w^{(\tau)}(\kappa \rightarrow \infty)) = k_l \left(\frac{1}{k_\mu} \delta\mu_\infty^{(\tau)} \right)^{-1/\zeta}. \quad (3.40)$$

Thus $\zeta = 3$ implies $T_w^{(\tau)}(\kappa \rightarrow \infty) - T_w^{(p)} = (3\pi\tau/(4k_\mu))^{3/2}(\Delta\rho/r_0)^{3/2}$ and $\Delta l^{(\tau)}(T_w^{(\tau)}(\kappa \rightarrow \infty)) = k_l(4k_\mu/(3\pi\tau))^{1/3}(r_0/\Delta\rho)^{1/3}$.

However, the results of Subsect. III.B hold only for large l whereas the study of the prewetting line involves also the behavior of $\Omega_s(l)$ for $l \gtrsim d_w$. This requires to test the above considerations numerically which takes into account the full function $\Omega_s(l)$. Therefore we have calculated the prewetting lines for the planar, spherical, and cylindrical geometries for fixed fluid-fluid and fluid-substrate interaction potential parameters and for different radii. The analysis of the dependence of the jump in the film thickness and of the shift of the transition temperature yields $(T_w^{(\tau)}(r_0 \rightarrow \infty) - T_w^{(p)})/T_w^{(p)} \sim r_0^{-2/3}$ and $\Delta l^{(\tau)}(r_0 \rightarrow \infty) \sim r_0^{1/3}$ which confirms the above heuristic considerations. However, the inspection of the prewetting lines in Fig. 8(a) demonstrates that the phase diagrams of the curved systems do not correspond to a simple shift of the phase diagram of the planar system.

Since $\kappa = \left(9\left(\frac{r_0}{\sigma}\right)^2 \Delta\rho / \left(4\left(\rho_w \left(\frac{\epsilon_{wf}}{\epsilon}\right) \left(\frac{\sigma_{wf}}{\sigma}\right)^6 - \rho_l \right) \right) \right)^{1/3}$, the limit $\kappa \ll 1$ requires (i) a small radius of the substrate, (ii) large substrate potential parameters $\rho_w \epsilon_{wf} \sigma_{wf}^6$ in comparison to ρ_l , or (iii) T close to T_c . Simultaneously the parameter space of ρ_w , ϵ_{wf} , and σ_{wf} is restricted by the requirement to have a first-order wetting transition in the temperature interval between the triple point temperature T_3 and T_c . Within the framework of our numerical analysis a set of parameters which fulfills these conditions has not been found. Thus a numerical analysis of the case $\kappa \ll 1$ would require to enlarge the parameter space considered here which we have not pursued.

D. Critical wetting transitions at coexistence

Up to now we have considered the case that the Hamaker constant a of the planar system (Eq. (2.27)) is positive. This is always valid for $T > T_w^{(p)}$. If the wetting transition is first order this holds even for $T = T_w^{(p)}$. In the latter case the description of the system for $T < T_w^{(p)}$ requires one to consider the full effective interface potential and not only its leading behavior for large film thicknesses (Eq. (2.27)).

If, however, the substrate potential is sufficiently weak, a favorable choice of interaction potentials allows for the occurrence of a continuous, so-called critical wetting transition such that a changes sign at $T_w^{(p)}$ and the coefficient b of the next-to-leading order term in $\omega(l)$ is positive at that temperature [30] (Eq. (2.27)):

$$a(T \lesssim T_w) \lesssim 0, \quad a(T = T_w) = 0, \quad b(T_w) > 0 \quad (\text{critical wetting}). \quad (3.41)$$

For critical wetting there is no prewetting line. Recently such a continuous wetting transition at coexistence has been observed experimentally [65]. This implies that on a curved substrate any wetting transitions, which are continuous in the planar geometry, are wiped out. Due to the effective upward shift of the bulk phase diagram caused by curvature (see Subsect. III.B), the wetting behavior on a curved substrate upon raising the temperature along the liquid-vapor coexistence curve $\mu = \mu_0(T) - 0$ is that of the corresponding planar substrate if in the latter case one passes the critical wetting transition at $T_w^{(p)}$ with a constant undersaturation $\delta\mu_\infty^{(\tau)}$ parallel and below $\mu_0(T)$ (Eq. (3.28)). This results in a steep but smooth increase of the thickness of the wetting film on a curved substrate upon passing $T_w^{(p)}$ at $\mu_0(T)$ and a levelling off at a finite value for $T > T_w^{(p)}$ (see Fig. 9) for which the previous considerations (Subsects. III.B and C) hold. Since, however, these previous results have been derived for the case $a > 0$, this analysis must be refined in order to cover the case that a changes sign at T_w .

To this end we first consider the circumstances under which critical wetting transitions can occur. As mentioned above, the substrate potential must be sufficiently weak so that $a(T) < 0$ for T close to the triple point. However, for pure Lennard-Jones interactions (see Eqs. (2.4) and (2.5)), it is well known that the excluded volume effect near the substrate (i. e., $d_w > 0$) leads to $b(T_w) < 0$ and thus induces a first-order wetting transition [30,55]. One can fulfill the necessary condition $b(T_w) > 0$ (Eq. (3.45)) by coating the substrate with an appropriate thin film consisting of a different material which leaves the *leading* asymptotic behavior of the substrate potential and thus a unchanged but introduces a suitable subdominant contribution which can overcompensate the effect of the excluded volume within the effective interface potential.

Therefore we consider a planar substrate filling the half-space $z \leq 0$ and consisting of two types of particles which are located in the region $z \leq -\delta$ and in the film $-\delta < z \leq 0$ and which interact with the fluid particles according to Eq. (2.5) with interaction potential parameters $\{\sigma_{wf}^{(0)}, \epsilon_{wf}^{(0)}\}$ and $\{\sigma_{wf}^{(1)}, \epsilon_{wf}^{(1)}\}$, respectively. With the simple assumption that

the two species exhibit the same number density ρ_w this leads to a substrate potential (Eq. (2.28)) $V^{(p)}(z) = \rho_w v^{(p)}(z)$ with

$$v^{(p)}(z \rightarrow \infty) = - \left[\frac{u_3}{z^3} + \frac{u_4}{z^4} + \dots \right] \quad (3.42)$$

where

$$u_3 = \frac{2\pi}{3} \epsilon_{wf}^{(0)} \left(\sigma_{wf}^{(0)} \right)^6, \quad u_4 = 2\pi \delta \left(\epsilon_{wf}^{(1)} (\sigma_{wf}^{(1)})^6 - \epsilon_{wf}^{(0)} (\sigma_{wf}^{(0)})^6 \right). \quad (3.43)$$

(This expression for u_4 does not yet include contributions due to a discrete arrangement of the substrate atoms on a lattice; in this respect see Ref. [30].) Thus with (see Eqs. (2.4) and (2.15))

$$t^{(p)}(z \rightarrow \infty) = - \left[\frac{t_3}{z^3} + \mathcal{O}(z^{-5}) \right] \quad (3.44)$$

and

$$t_3 = \frac{2\pi}{3} \epsilon \sigma^6, \quad t_4 = 0, \quad (3.45)$$

one has

$$a = \frac{1}{2} \Delta \rho (u_3 \rho_w - t_3 \rho_l) \quad (3.46)$$

$$b = \frac{1}{3} \Delta \rho (u_4 \rho_w - 3d_w t_3 \rho_l). \quad (3.47)$$

Thus $b > 0$ is realized for a sufficient large value of u_4 which is, e. g., the case if the coating of the substrate consists of particles whose interaction with the fluid particles is stronger than that of the particles in the main part of the substrate beneath.

Analogously, for curved substrates we consider coated spheres and cylinders which consist of particles characterized by interaction potential parameters $\{\epsilon_{wf}^{(0)}, \sigma_{wf}^{(0)}\}$ and $\{\epsilon_{wf}^{(1)}, \sigma_{wf}^{(1)}\}$ for $0 \leq r \leq r_0 - \delta$ and $r_0 - \delta < r \leq r_0$, respectively. Based on the results of Appendix C Eq. (2.35) can be generalized in order to be able to describe continuous wetting transitions:

$$\omega^{(\tau)}(l, r_0) = \frac{a}{l^2} \mathcal{S}_\tau \left(\frac{r_0}{l} \right) + \frac{b}{l^3} \mathcal{R}_\tau \left(\frac{r_0}{l} \right) + \mathcal{O}(l^{-4}) \quad (3.48)$$

where the scaling function $\mathcal{R}_\tau(x)$ (see Fig. 10 and Eqs. (C4)-(C7)) is given by ($x = r_0/l$)

$$\mathcal{R}_\tau(x) = \lim_{l \rightarrow \infty} \left[\frac{l^3}{b} \left(\omega^{(\tau)}(l, r_0) - \frac{a}{l^2} \mathcal{S}_\tau(x) \right) \right]. \quad (3.49)$$

For large x , $\mathcal{R}_\tau(x)$ takes on the form

$$\mathcal{R}_\tau(x \rightarrow \infty) = 1 + \frac{3\tau}{4x} + \mathcal{O}(x^{-2}) \quad (3.50)$$

whereas for $x \rightarrow 0$ one has

$$\mathcal{R}_c(x \rightarrow 0) = \frac{3\pi}{2} (1 - 3x + \mathcal{O}(x^2)) \quad (3.51)$$

and

$$\mathcal{R}_s(x \rightarrow 0) = 8 (1 - 3x + \mathcal{O}(x^2)). \quad (3.52)$$

The minimization of the corresponding effective interface potential

$$\Omega_s(l) = \frac{a}{l^2} \mathcal{S}_\tau \left(\frac{r_0}{l} \right) + \frac{b}{l^3} \mathcal{R}_\tau \left(\frac{r_0}{l} \right) + \sigma_{l,g}^{(p)} \left(1 + \frac{l}{r_0} \right)^\tau + \sigma_{l,s} \quad (3.53)$$

yields for the equilibrium film thickness the implicit equation (note that here $\kappa \leq 0$ is possible)

$$x = \kappa \left(\frac{\tau}{2} \right)^{1/3} r_\tau(x, \gamma) \quad (3.54)$$

with

$$r_\tau(x, \gamma) = (1 + \gamma x q_\tau(x))^{-1/3} s_\tau(x) \quad (3.55)$$

and

$$q_\tau(x) = \frac{\mathcal{R}_\tau(x) + \frac{x}{3} \mathcal{R}'_\tau(x)}{\mathcal{S}_\tau(x) + \frac{x}{2} \mathcal{S}'_\tau(x)}. \quad (3.56)$$

The functions $s_\tau(x)$ and $q_\tau(x)$ depend only on the geometrical properties of the substrate whereas the fluid-fluid and fluid-substrate interaction potential parameters enter in form of the dimensionless numbers $\kappa = \left(r_0^2 \sigma_{l,g}^{(p)} / a \right)^{1/3}$ and $\gamma = 3b / (2ar_0)$. For the explicit forms of the functions $q_\tau(x)$ see Eqs. (C6) and (C7). The knowledge of the behavior of $q_\tau(x)$ and $s_\tau(x)$ in the limits $x \rightarrow 0$ and $x \rightarrow \infty$ allows one to solve Eq. (3.54) approximately for specific regions of the (κ, γ) parameter space (see Fig. 11). Since, however, one has $x = r_0/l \geq 0$, only the regions $(\kappa < 0, \gamma < 0)$ (for $T \geq T_w^{(p)}$) and $(\kappa \geq 0, \gamma \geq 0)$ (for $T \geq T_w^{(p)}$) are of interest.

With $q_\tau(x \rightarrow \infty) = 1 + \frac{\tau}{4}x^{-1} + \frac{\tau^2}{16}x^{-2} + \mathcal{O}(x^{-3})$ and $s_\tau(x \rightarrow \infty) = 1 + \left(\frac{\tau}{4} - \frac{1}{3}\right)x^{-1} + \left(\frac{2}{9} - \frac{\tau}{4} + \frac{\tau^2}{24}\right)x^{-2} + \mathcal{O}(x^{-3})$ one has for $|\gamma| \gg \frac{1}{x}$:

$$r_\tau(x \rightarrow \infty, |\gamma| \gg \frac{1}{x}) = \frac{1}{(\gamma x)^{1/3}} \left(1 + \frac{1}{\gamma x} \frac{\gamma\tau - 2\gamma - 2}{6} + \mathcal{O}\left((\gamma x^2)^{-1}\right) \right) \quad (3.57)$$

so that the solution $x_\tau^*(\kappa, \gamma)$ of Eq. (3.54) reads (note that κ^3/γ is always positive)

$$x_\tau^*(|\kappa| \rightarrow \infty, |\gamma| \rightarrow \infty) = \left(\frac{\tau \kappa^3}{2 \gamma} \right)^{1/4} - \frac{1}{4\gamma} \left(1 + \frac{\gamma}{2}(2 - \tau) \right) + \mathcal{O}\left((\kappa\gamma)^{-1}\right). \quad (3.58)$$

Thus in the limit of fixed but large r_0 and $a \rightarrow 0$ one finds for the film thickness $l_0^{(\tau)} = r_0/x_\tau^*$ (b must be positive for critical wetting to occur)

$$l_0^{(\tau)} = \left(\frac{3 br_0}{\tau \sigma_{l,g}^{(p)}} \right)^{1/4} = \left(\frac{3b}{\Delta\rho \delta\mu_\infty^{(\tau)}} \right)^{1/4}, \quad T = T_w^{(p)}, \quad r_0 \gg \left(\frac{3b}{2\sigma_{l,g}^{(p)}} \right)^{1/3}, \quad (3.59)$$

where $\delta\mu_\infty^{(\tau)}$ is defined by Eq. (3.28). For the corresponding planar substrate the film thickness along a complete wetting path $\Delta\mu \rightarrow 0$ approaching the transition temperature $T = T_w^{(p)}$ of the second order wetting transition is given by $l_0(r_0 = \infty, \Delta\mu, T = T_w^{(p)}) = (\frac{3b}{\Delta\mu\Delta\rho})^{1/4} = l_0^{(p)}(T = T_w^{(p)}, \Delta\mu)$ due to $a(T = T_w^{(p)}) = 0$ (see Eq. (2.27)). Thus in the limit considered in Eq. (3.58) the film thickness at coexistence on a curved substrate equals the film thickness of the corresponding planar system which is off coexistence at $\Delta\mu = \delta\mu_\infty^{(\tau)}$. This implies that the picture, which has emerged in the previous subsection for $a > 0$, carries over to the case $a = 0$.

For $x \rightarrow \infty$, $|\gamma| \ll \frac{1}{x}$ the sign of γ has to be considered. If γ is positive, i. e., $T > T_w^{(p)}$, one can expand $r_\tau(x)$ in powers of γx as before, which leads to

$$r_\tau(x \rightarrow \infty, \gamma x \ll 1) = 1 + \frac{3\tau - 4}{12} x^{-1} + \frac{\gamma x}{3} \left(1 + \frac{3\tau - 2}{6} x^{-1} + \mathcal{O}(x^{-2}) \right) + \mathcal{O}(x^{-2}, \gamma^2 x^2) \quad (3.60)$$

so that one finds for the solution of Eq. (3.54)

$$x_\tau^*(\kappa \rightarrow +\infty, \gamma \rightarrow 0^+) = \kappa \left(\frac{\tau}{2} \right)^{1/3} + \frac{3\tau - 4}{12} - \frac{\gamma\kappa}{3} \left(\frac{\tau}{2} \right)^{1/3} \left(\kappa \left(\frac{\tau}{2} \right)^{1/3} + \frac{3\tau - 2}{6} + \mathcal{O}(\kappa^{-1}) \right) + \mathcal{O}(\kappa^{-1}, \gamma^2 \kappa^3), \quad \gamma\kappa \ll 1. \quad (3.61)$$

Hence for large r_0 and $b/a \rightarrow 0$ the film thickness attains its asymptotic value given by Eq. (3.9) as

$$l_0^{(\tau)}(T) = \frac{r_0}{\kappa} \left(\frac{2}{\tau} \right)^{1/3} \left[1 + \frac{\gamma}{3} \left(\left(\frac{\tau}{2} \right)^{1/3} \kappa + \frac{1}{3} \right) + \mathcal{O}(\kappa^{-1}, \gamma^2) \right] \\ T > T_w^{(p)}, \quad r_0 \gg \frac{3b}{2a} > 0. \quad (3.62)$$

For $\gamma \rightarrow 0^-$, $\kappa \rightarrow -\infty$, i. e., for $T < T_w^{(p)}$, $r_0 \rightarrow \infty$, and a fixed, the film thickness is determined by the equation

$$x^3 + \gamma x^4 = \frac{\tau}{2} \kappa^3. \quad (3.63)$$

Since $x^3 + \gamma x^4$ has zeros at $x = 0$ and $x = -1/\gamma$ and a maximum at $x = -3/(4\gamma)$, Eq. (3.63) implies $x^* > -1/\gamma \equiv r_0/l_0^{(p)}$ and thus $l_0^{(p)} > l_0^{(\tau)}$. With the ansatz $x^* = -1/\gamma + \delta x$ Eq. (3.63) leads to

$$x^* = -\frac{1}{\gamma} \left(1 + \frac{\tau}{2} \gamma^3 \kappa^3 + \mathcal{O}((\gamma\kappa)^6) \right), \quad \gamma\kappa \ll 1, \quad (3.64)$$

so that one has for the film thickness

$$l_0^{(\tau)}(T) = l_0^{(p)}(T, \Delta\mu = 0) \left(1 - \frac{27\tau b^3 \sigma_{l,g}^{(p)}}{16 r_0 a^4} \right),$$

$$T < T_w^{(p)}, \quad r_0 \gg \left(\frac{3b}{2\sigma_{l,g}^{(p)}} \right)^{1/3}. \quad (3.65)$$

So far we have discussed the limit $x \rightarrow \infty$. For $x \rightarrow 0$ one has $s_c(x \rightarrow 0) = \left(\frac{4}{9\pi}\right) \frac{1}{x^{1/3}} \left(1 + \frac{4}{3}x - \frac{59}{72}x^2 + \mathcal{O}(x^3)\right)$, $s_s(x \rightarrow 0) = \frac{1}{2x^{2/3}} \left(1 + \frac{5}{3}x - \frac{4}{9}x^2 + \mathcal{O}(x^3)\right)$ and $q_c(x \rightarrow 0) = \frac{2}{3x} \left(1 + \frac{25}{8}x^2 + \mathcal{O}(x^3)\right)$, $q_s(x \rightarrow 0) = \frac{1}{x} \left(1 + 2x^2 + \mathcal{O}(x^3)\right)$. Thus $r_\tau(x \rightarrow 0, \gamma)$ is given by $r_c(x \rightarrow 0, \gamma) = \left(\frac{4}{9\pi}\right)^{1/3} \left(1 + \frac{2}{3}\gamma\right)^{-1/3} \frac{1}{x^{1/3}} \left(1 + \frac{4}{3}x\right)$ and $r_s(x \rightarrow 0, \gamma) = \frac{1}{2} (1 + \gamma)^{-1/3} \frac{1}{x^{2/3}} \left(1 + \frac{5}{3}x\right)$ which leads to

$$x_c^*(|\kappa| \ll 1, \gamma) = \left(\frac{2}{9\pi} \frac{\kappa^3}{1 + \frac{2}{3}\gamma}\right)^{1/4} + \left(\frac{2}{9\pi} \frac{\kappa^3}{1 + \frac{2}{3}\gamma}\right)^{1/2} + \mathcal{O}\left(\left(\frac{\kappa^3}{1 + \frac{2}{3}\gamma}\right)^{3/4}\right) \quad (3.66)$$

for a cylinder ($\tau = 1$) and

$$x_s^*(|\kappa| \ll 1, \gamma) = \left(\frac{1}{8} \frac{\kappa^3}{1 + \gamma}\right)^{1/5} + \left(\frac{1}{8} \frac{\kappa^3}{1 + \gamma}\right)^{2/5} + \mathcal{O}\left(\left(\frac{\kappa^3}{1 + \gamma}\right)^{3/5}\right) \quad (3.67)$$

for a sphere ($\tau = 2$), respectively. Obviously for $a < 0$ there exists a physically meaningful solution only if $\gamma < -\frac{4-\tau}{2}$. The film thicknesses are thus given by

$$l_0^{(c)} = \left(\frac{9\pi a r_0^2}{2 \sigma_{l,g}^{(p)}} \left(1 + \frac{b}{a r_0}\right)\right)^{1/4}, \quad r_0 \ll \left(\frac{|a|}{\sigma_{l,g}^{(p)}}\right)^{1/2} \quad (3.68)$$

and

$$l_0^{(s)} = \left(8 \frac{ar_0^3}{\sigma_{l,g}^{(p)}} \left(1 + \frac{3b}{2ar_0} \right) \right)^{1/5}, \quad r_0 \ll \left(\frac{|a|}{\sigma_{l,g}^{(p)}} \right)^{1/2}. \quad (3.69)$$

Upon crossing $T_w^{(p)}$ the parameter γ jumps from $-\infty$ at $T_w^{(p)} - 0$ to $+\infty$ at $T_w^{(p)} + 0$ because at $T = T_w^{(p)}$ the Hamaker constant a changes sign. At $T_w^{(p)}$ x_τ^* depends only on the parameter $\kappa^3/\gamma = 2r_0^3\sigma_{l,g}^{(p)}/(3b)$ which is positive both above and below $T_w^{(p)}$:

$$x_c^*(|\kappa| \ll 1, |\gamma| \rightarrow \infty) = \left(\frac{\kappa^3}{3\pi\gamma} \right)^{1/4} + \left(\frac{\kappa^3}{3\pi\gamma} \right)^{1/2} + \mathcal{O} \left(\left(\frac{\kappa^3}{\gamma} \right)^{3/4} \right),$$

$$\frac{\kappa^3}{\gamma} \ll 1, \quad (3.70)$$

and

$$x_s^*(|\kappa| \ll 1, |\gamma| \rightarrow \infty) = \left(\frac{\kappa^3}{8\gamma} \right)^{1/5} + \left(\frac{\kappa^3}{8\gamma} \right)^{2/5} + \mathcal{O} \left(\left(\frac{\kappa^3}{\gamma} \right)^{3/5} \right),$$

$$\frac{\kappa^3}{\gamma} \ll 1, \quad (3.71)$$

so that one obtains for the film thicknesses at $T_w^{(p)}$ the results

$$l_0^{(c)} = \left(\frac{9\pi br_0}{2\sigma_{l,g}^{(p)}} \right)^{1/4}, \quad T = T_w^{(p)}, \quad r_0 \ll \left(\frac{3b}{2\sigma_{l,g}^{(p)}} \right)^{1/3}, \quad (3.72)$$

and

$$l_0^{(s)} = \left(\frac{12r_0b}{\sigma_{l,g}^{(p)}} \right)^{1/5}, \quad T = T_w^{(p)}, \quad r_0 \ll \left(\frac{3b}{2\sigma_{l,g}^{(p)}} \right)^{1/3}. \quad (3.73)$$

In the limit $\gamma \rightarrow 0^+$, i. e., r_0 fixed but small and $b/a \rightarrow 0$, one recovers the first-order results given by Eqs. (3.10) and (3.11), respectively:

$$l_0^{(c)}(|\kappa| \ll 1, \gamma \rightarrow 0^+) = r_0 \left(\frac{9\pi}{2\kappa^3} \right)^{1/4} \left[\left(1 + \frac{1}{6}\gamma + \mathcal{O}(\gamma^2) \right) + \mathcal{O}(\kappa^{3/4}) \right]$$

$$T > T_w^{(p)}, \quad 0 < \frac{b}{a} \ll \frac{2r_0}{3} \quad (3.74)$$

and

$$l_0^{(s)}(|\kappa| \ll 1, \gamma \rightarrow 0^+) = r_0 \left(\frac{2}{\kappa} \right)^{3/5} \left[\left(1 + \frac{1}{5}\gamma + \mathcal{O}(\gamma^2) \right) + \mathcal{O}(\kappa^{3/5}) \right]$$

$$T > T_w^{(p)}, \quad 0 < \frac{b}{a} \ll \frac{2r_0}{3}. \quad (3.75)$$

For those regions of the (κ, γ) parameter space which are not covered by the above considerations of the limits $x \rightarrow 0$ and $x \rightarrow \infty$ the solution of Eq. (3.54) requires a numerical treatment of Eqs. (3.54) - (3.65) using the full expressions for the functions $q_\tau(x)$ and $s_\tau(x)$.

IV. Finite-size effects

In Sect. III we have shown that the positive curvature of a substrate prevents the formation of infinitely thick wetting films. At coexistence a critical wetting transition is smeared out whereas a first-order wetting transition is reduced to a discontinuous transition between a thin and a thick, but finite, film. However, the latter nonanalytic behavior as well as the discontinuities associated with the corresponding prewetting line are artefacts of the mean-field theory we have used. Since the surface area of spheres is quasi-zero-dimensional and that of cylinders quasi-one-dimensional, fluctuations erase any phase transition and lead to a rounding of the above mentioned discontinuities. With increasing radii of the spheres and cylinders this rounding sharpens and a first-order transition emerges gradually. In this sense our mean-field results become increasingly more accurate as the size of the spherical and cylindrical substrates becomes larger.

Based on the results of Privman and Fisher [66] for the influence of finite-size effects on first-order transitions we are able to estimate the rounding of the first-order wetting transitions described above (see also Refs. [25] and [26]). In Ref. [66] the scaling functions for the singular part of the free energy and the magnetization in an external field of a finite Ising spin lattice, i. e., a stripe and a block geometry, are derived. The shape of these functions allows one to determine the region over which the phase transition is smeared out. In order to translate the results of Ref. [66] onto the case of the prewetting transition we analyze the effective interface potential $\Omega_s(l)$ given by Eq. (2.10). In the vicinity of the prewetting line $\mu_{pre}(T)$ $\Omega_s(l)$ exhibits two local minima, $l_<(T, \mu)$ and $l_>(T, \mu)$ with the corresponding values $\Omega_s(l_<(T, \mu)) =: \Omega_s^<(T, \mu)$ and $\Omega_s(l_>(T, \mu)) =: \Omega_s^>(T, \mu)$ of the effective interface potential. One of the two thicknesses $l_<(T, \mu)$ and $l_>(T, \mu)$ corresponds to the global minimum which represents the equilibrium film thickness $l^{(0)}(T, \mu)$ at the point (T, μ) of the phase diagram. On the prewetting line one has $\Omega_s^<(T, \mu_{pre}(T)) = \Omega_s^>(T, \mu_{pre}(T))$ so that the thin film ($l_<^{(0)}(T, \mu_{pre}(T))$) and the thick film ($l_>^{(0)}(T, \mu_{pre}(T))$) coexist. We now consider the difference $\Delta\Omega_s(T, \mu) = \Omega_s^>(T, \mu) - \Omega_s^<(T, \mu)$ between the two minimum values for a given temperature T as a function of the chemical potential μ . According to Ref. [66] the width $\delta\mu(T)$ of the rounding region for a spherical substrate is given implicitly by the inequality

$$|\Delta\Omega_s(T, \mu = \mu_{pre}(T) + \delta\mu(T))| r_0^2 \lesssim k_B T. \quad (4.1)$$

On a cylinder along its axis the liquidlike film is expected to break up into domains with small ($l_<^{(0)}$) and large ($l_>^{(0)}$) film thickness, respectively. The corresponding kinks at the

domain boundaries are accompanied by an additional free energy per unit length, i. e., a line tension Σ_l . Following Ref. [26] we estimate Σ_l by the product $\Sigma_l \simeq \Delta l \sigma_{l,g}^{(p)} \equiv (l_{>} - l_{<}) \sigma_{l,g}^{(p)} \simeq l_{>} \sigma_{l,g}^{(p)}$. Reference [67] provides a more detailed picture of the line tension associated with the coexistence of thin and thick films on a planar substrate along the prewetting line. We note that from these analyses one expects that in systems governed by nonretarded van der Waals forces Σ_l diverges logarithmically upon approaching coexistence at T_w . Since for large r_0 one has $\Delta l \sim |T - T_w|^{-\frac{1}{2}}$ (Eq. (3.38)), our ansatz for Σ_l overestimates the actual value. Since we aim only for a rough estimate we refrain from a more detailed analysis along these lines. (For a discussion of finite-size effects on the line tension see the work by Indekeu and Dobbs in Ref. [67].) The rounding region of the prewetting phase transition on a cylindrical substrate is then given by [66]

$$|\Delta\Omega_s(T, \mu = \mu_{pre}(T) + \delta\mu(T))| r_0 \xi \exp(r_0 \Sigma_l(T, \mu = \mu_{pre}(T))/k_B T) \lesssim k_B T, \quad (4.2)$$

where ξ is the bulk correlation length. The width $\delta\mu(T)$ as determined by Eqs. (4.1) and (4.2) can be translated into a temperature interval $\delta T(T)$ by taking into account the slope $m_{pre}^{(\tau)}(T) = \partial(\mu_{pre}^{(\tau)}(T)/\epsilon) / \partial(k_B T/\epsilon)$ of the prewetting line:

$$|k_B \delta T| \simeq |m_{pre}^{(\tau)}(T)|^{-1} |\delta\mu(T)|. \quad (4.3)$$

Now consider $\Delta\Omega_s$ at a point $(T, \mu_{pre}(T) + \delta\mu(T))$ on the boundary of the rounding region given by Eqs. (4.1) and (4.2), respectively. The calculation of $\Delta\Omega_s(T, \mu_{pre}(T) + \delta\mu(T))$ requires the evaluation of the effective interface potential for the two minima at $l_{>}$ and $l_{<}$. Whereas Ω_s in the asymptotic form (Eq. (3.13)) of Eq. (2.10) yields sufficient information about the second minimum $l_{>}$, this is less transparent for $l_{<}(T, \mu)$ and $\Omega_s^<(T, \mu)$. However, because $\Omega_s^<(T, \mu)$ varies only weakly upon a deviation $\delta\mu$ from the prewetting line $\mu = \mu_{pre}(T)$ [25], one has $\Omega_s^<(T, \mu_{pre}(T) + \delta\mu) \simeq \Omega_s^<(T, \mu_{pre}(T)) = \Omega_s^>(T, \mu_{pre}(T))$. Thus one obtains

$$|\Delta\Omega_s(T, \mu_{pre}(T) + \delta\mu)| \simeq |\delta\mu| \left| \frac{\partial\Omega_s^>(T, \mu)}{\partial\mu} \right|_{\mu=\mu_{pre}(T)}. \quad (4.4)$$

With Eqs. (4.1) - (4.3) this implies

$$|k_B \delta T| \lesssim \frac{k_B T}{r_0^2} |m_{pre}^{(s)}|^{-1} \left| \frac{\partial\Omega_s^>(T, \mu)}{\partial\mu} \right|_{\mu=\mu_{pre}(T)}^{-1} \quad (4.5)$$

for a sphere and

$$|k_B \delta T| \lesssim \frac{k_B T}{r_0 \xi} |m_{pre}^{(c)}|^{-1} \left| \frac{\partial\Omega_s^>(T, \mu)}{\partial\mu} \right|_{\mu=\mu_{pre}(T)}^{-1} \exp(-r_0 \Sigma_s/k_B T) \quad (4.6)$$

for a cylinder, respectively. The factor $\partial\Omega_s^>/\partial\mu$ consists of four contributions:

$$\begin{aligned} \frac{\partial \Omega_s^>}{\partial \mu} = & \left(\frac{\partial \Omega_s^>}{\partial \mu} \right)_{l_>, \rho_l, \rho_g} + \left(\frac{\partial \Omega_s^>}{\partial l_>} \right)_{\mu, \rho_l, \rho_g} \frac{\partial l_>}{\partial \mu} + \\ & + \left(\frac{\partial \Omega_s^>}{\partial \rho_l} \right)_{\mu, l_>, \rho_g} \frac{\partial \rho_l}{\partial \mu} + \left(\frac{\partial \Omega_s^>}{\partial \rho_g} \right)_{\mu, l_>, \rho_l} \frac{\partial \rho_g}{\partial \mu}. \end{aligned} \quad (4.7)$$

Since the variation of $(\rho_g(\mu = \mu_0) - \rho_g(\mu))/\rho_g(\mu = \mu_0)$ and $(\rho_l(\mu = \mu_0) - \rho_l(\mu))/\rho_l(\mu = \mu_0)$ are both of the order 10^{-3} along the whole prewetting line, the last two terms of Eq. (4.7) can be neglected. With Eq. (3.13) for the effective interface potential $\Omega_s(l)$ one obtains

$$\begin{aligned} \frac{\partial \Omega_s^>}{\partial \mu} = & \frac{r_0 \Delta \rho}{\tau + 1} \left(\left(1 + \frac{1}{y} \right)^{\tau+1} - 1 \right) \\ & - \frac{\tau r_0 \Delta \rho}{y^2} \left(1 + \frac{1}{y} \right)^{\tau-1} \left(1 + \frac{\lambda}{\tau} \left(1 + \frac{1}{y} \right) - \frac{2 y^3}{\tau \kappa^3} s_\tau^{-3}(y) \right) \frac{\partial y}{\partial \lambda} \end{aligned} \quad (4.8)$$

with $y = r_0/l_>$. The second minimum $l_>$ is given as the solution of the implicit equation (3.15). Depending on the value of the dimensionless parameters $\kappa = (r_0^2 \sigma_{l,g}^{(p)}/a)$ and $\lambda = (3b/(2ar_0))$ there are three different regimes in each of which the implicit equation (3.15) provides an approximate solution $l_>$ (see Sect. III.B and Fig. 6). Accordingly, this leads to three different limiting cases of the estimates (4.5) and (4.6) for the rounded regions.

1. In region I one has $\kappa \rightarrow 0$, λ fixed, and y given by Eqs. (3.19) and (3.20) which leads to $\left| \frac{\partial \Omega_s^>}{\partial \mu} \right|^{-1} \simeq \frac{3}{2} \left(\frac{r_0 \Delta \mu}{a \Delta \rho} \right)^{\frac{1}{2}}$ for a sphere and $\left| \frac{\partial \Omega_s^>}{\partial \mu} \right|^{-1} \simeq 5 \left(\left(\frac{2 \Delta \mu}{9 \pi a} \right)^2 \frac{r_0}{\Delta \rho^3} \right)^{1/5}$ for a cylinder, respectively. Thus with $\Delta \mu_{pre} = \mu_0 - \mu_{pre}$ one finds for the width of the rounding region $|k_B \delta T|$:

$$|k_B \delta T| \lesssim \frac{3}{2} \frac{k_B T}{|m_{pre}^{(s)}|} \left(\frac{\Delta \mu_{pre}}{r_0^3 a \Delta \rho} \right)^{1/2} \quad (4.9)$$

for a sphere and

$$\begin{aligned} |k_B \delta T| \lesssim & 5 \frac{k_B T}{\xi |m_{pre}^{(c)}|} \left(\frac{2 \Delta \mu_{pre}}{9 \pi a} \right)^{2/5} \left(\frac{1}{r_0^4 \Delta \rho^3} \right)^{1/5} \times \\ & \times \exp \left(- \frac{\sigma_{l,g}^{(p)}}{k_B T} \left(\frac{9 \pi}{2} \frac{a r_0^7}{\Delta \rho \Delta \mu_{pre}} \right)^{1/5} \right) \end{aligned} \quad (4.10)$$

for a cylinder.

2. For film thicknesses $l_>$ small compared with the radius r_0 (region II) one has $\kappa \rightarrow \infty$, λ fixed, and y is given by Eq. (3.32). With $\left| \frac{\partial \Omega_s^>}{\partial \mu} \right|^{-1} = \frac{3}{r_0 \Delta \rho} \left(\frac{2 \sigma_{l,g}^{(p)}}{\tau r_0 a} \right)^{1/3} \left(1 + \frac{r_0 \Delta \rho \Delta \mu}{\tau \sigma_{l,g}^{(p)}} \right)^{1/3}$ one finds

$$|k_B \delta T| \lesssim \frac{3k_B T}{\Delta \rho |m_{pre}^{(s)}| r_0^2} \left(\frac{\frac{2\sigma_{l,g}^{(p)}}{r_0} + \Delta \rho \Delta \mu_{pre}}{2a} \right)^{1/3} \quad (4.11)$$

for a sphere and

$$|k_B \delta T| \lesssim \frac{3k_B T}{\Delta \rho \xi |m_{pre}^{(c)}| r_0} \left(\frac{\frac{\sigma_{l,g}^{(p)}}{r_0} + \Delta \rho \Delta \mu_{pre}}{2a} \right)^{1/3} \times \\ \times \exp \left(-\frac{r_0 \sigma_{l,g}^{(p)}}{k_B T} \left(\frac{2a}{\frac{\sigma_{l,g}^{(p)}}{r_0} + \Delta \rho \Delta \mu_{pre}} \right)^{1/3} \right) \quad (4.12)$$

for a cylinder, respectively.

3. In region III one has $\lambda/\kappa \rightarrow 0$ and y given by Eqs. (3.33) and (3.34), so that one finds

$$|k_B \delta T| \lesssim 3 \frac{k_B T}{|m_{pre}^{(s)}| \Delta \rho} \frac{1}{\left(\frac{\sigma_{l,g}^{(p)}}{8ar_0^3} \right)^{3/5}} \left(1 + \frac{3}{10} \left(\frac{8ar_0^3}{\sigma_{l,g}^{(p)^6}} \right)^{1/5} \Delta \rho \Delta \mu_{pre} \right) \quad (4.13)$$

for a sphere and

$$|k_B \delta T| \lesssim 2 \frac{k_B T}{\xi |m_{pre}^{(c)}| \Delta \rho} \frac{1}{\left(\frac{2}{9\pi} \frac{\sigma_{l,g}^{(p)}}{r_0^2 a} \right)^{1/2}} \left(1 + \left(\frac{9\pi}{32} \frac{r_0^2 a}{\sigma_{l,g}^{(p)^5}} \right)^{1/4} \Delta \rho \Delta \mu_{pre} \right) \times \\ \times \exp \left(-\frac{1}{k_B T} \left(\frac{9\pi}{2} r_0^6 a \sigma_{l,g}^{(p)^3} \right)^{1/4} \left(1 + \left(\frac{9\pi}{512} \frac{r_0^2 a}{\sigma_{l,g}^{(p)^5}} \right)^{1/4} \Delta \rho \Delta \mu_{pre} \right)^{-1} \right) \quad (4.14)$$

for a cylinder, respectively.

From Eqs. (4.9)-(4.14) one infers that for a sphere the width of the rounded region shrinks for $r_0 \rightarrow \infty$ always algebraically but exponentially for a cylinder. In the case of large radii and small film thickness (region II) our result for δT for a sphere agrees with Eq. (5.5) in Ref. [25]. As already stated in this reference it is difficult to obtain a general expression for $\mu_{pre}(T)$ and $m_{pre}^{(\tau)}$. However, our microscopic model allows us to obtain quantitative estimates for $\mu_{pre}(T)$ and $m_{pre}^{(\tau)}$ for specific interaction potentials of the system. From the first-order wetting phase diagram of a cylinder and a sphere of radius $r_0 = 100\sigma$ (see Fig. 8) one can infer $\Delta \mu_{pre}$ directly as a function of the temperature. If

one chooses $k_B T = 0.95\epsilon$, one has $k_B T_w^{(p)} \simeq 0.785\epsilon$, $\Delta\mu_{pre}^{(s)} \simeq 0.01\epsilon$, $|m_{pre}^{(s)}|^{-1} \simeq 1.65$, and $\Delta\mu_{pre}^{(c)} \simeq 0.026\epsilon$, $|m_{pre}^{(c)}|^{-1} \simeq 1.45$, respectively. Thus with $\rho_g \sigma^3 (k_B T = 0.95\epsilon) \simeq 0.076$, $\rho_l \sigma^3 (k_B T = 0.95\epsilon) \simeq 0.551$, as well as the substrate parameters $\epsilon_{wf} = 0.625\epsilon$, $\sigma_{wf} = 1.35\sigma$, and $\rho_w \sigma^3 = 1.0$, Eq. (4.11) yields

$$\frac{|\delta T|}{T_w^{(p)}} \simeq 2.3 \cdot 10^{-4} \quad (\text{sphere, region II}). \quad (4.15)$$

Equation (4.12) for a cylindrical substrate involves also the bulk correlation length ξ defined as $\xi^2 = \frac{1}{6} \int d^3 r r^2 \mathcal{G}(r) / \int d^3 r \mathcal{G}(r)$ where $\mathcal{G}(|\mathbf{r} - \mathbf{r}'|) = \langle \hat{\rho}(\mathbf{r}) \hat{\rho}(\mathbf{r}') \rangle - \langle \hat{\rho}(\mathbf{r}) \rangle \langle \hat{\rho}(\mathbf{r}') \rangle$ is the two-point correlation function of the fluctuating number density $\hat{\rho}(\mathbf{r})$. Within our model this leads to $\xi^2 = \frac{1}{6} |w_2| \rho^2 \kappa_T$ with the isothermal compressibility $\kappa_T = \rho^{-2} \left(\frac{\partial^2 f_h}{\partial \rho^2} + w_0 \right)^{-1}$ and $w_i = \int d^3 r r^i \tilde{w}(r)$. For the model potential of the fluid-fluid interaction given by Eqs. (2.3) and (2.4) one obtains $\xi(T = 0.95\epsilon/k_B) \simeq 1.7\sigma$ which implies

$$\frac{|\delta T|}{T_w^{(p)}} \simeq 10^{-140} \quad (\text{cylinder, region II}). \quad (4.16)$$

We conclude that for $r_0 = 100\sigma$ the rounding of the prewetting transition on a sphere is at the lower end of the experimentally accessible temperature resolution whereas for a cylinder the rounding cannot be detected.

V. Summary

We have studied wetting phenomena on cylindrical and spherical substrates (Fig. 1) for simple fluids whose particles are governed by dispersion forces and are exposed to long-ranged substrate potentials. Our approach is based on a microscopic density functional theory. Using a sharp-kink approximation for the density profile (Sect. II A), we have determined the effective interface potential $\Omega_s(l)$ (Eq. (2.10)) for the emerging liquidlike film of thickness l . From a detailed analytical as well as numerical discussion of $\Omega_s(l)$ for a cylinder ($\tau = 1$) and a sphere ($\tau = 2$) of radius r_0 we have obtained the following main results:

1. As a contribution to $\Omega_s(l)$ we have determined the liquid-vapor surface tension $\sigma_{l,g}^{(\tau)}(h)$ of a spherical drop and a liquid thread of radius h (see Subsec. II B). For small values of $\frac{1}{h}$ it approaches its planar value $\sigma_{l,g}^{(p)} = \sigma_{l,g}^{(\tau)}(h = \infty)$ nonanalytically: the next-to-leading order term beyond the contribution $\sim \frac{1}{h}$ is proportional to $\ln(h)/h^2$ (see Eqs. (2.21) - (2.23) and Fig. 2).

2. The interaction contribution $\omega^{(\tau)}(l, r_0)$ to the effective interface potential $\Omega_s(l)$ has been determined in closed form (Eq. (2.29)). It can be expressed in terms of the corresponding planar quantity $\omega^{(p)}(l)$ (Eq. (2.27)) by scaling functions $\mathcal{S}_\tau(r_0/l)$ and $\mathcal{R}_\tau(r_0/l)$ (see Eqs. (2.35), (2.39), and (3.48) and Figs. 3 and 10). These scaling functions are universal, i. e. independent of interaction potential parameters, and reflect the geometrical properties of the substrate (see Eqs. (A16), (B30), (C4), and (C5)).
3. At liquid-vapor coexistence $\mu = \mu_0(T)$ and above the wetting temperature $T_w^{(\tau)}(r_0)$ (Sect. III A) the maximum film thickness l_{max} is determined by Eq. (3.2) depending on the dimensionless parameter $\kappa = (r_0^2 \sigma_{l,g}^{(p)}/a)^{1/3}$ with the Hamaker constant a (see Fig. 4). In the limiting cases $\kappa \gg 1$ and $\kappa \ll 1$ one obtains for l_{max} power laws as given by Eqs. (3.9) - (3.11).
4. For a small undersaturation $\Delta\mu = \mu_0(T) - \mu > 0$ and above the wetting temperature $T_w^{(\tau)}(r_0)$ the equilibrium film thickness l_0 on curved substrates equals the equilibrium film thickness on the corresponding planar substrate for the fluid taken to be off coexistence at an effective undersaturation $\Delta\mu_{eff}$. In the particular case of large radii r_0 , i. e., $\kappa \rightarrow \infty$, the film thickness on a curved substrate equals that on the corresponding planar substrate as if the liquid-vapor coexistence curve was shifted by a constant value $\delta\mu_\infty^{(\tau)} = \tau\sigma_{l,g}^{(p)}/(r_0\Delta\rho)$ into the vapor phase (see Eqs. (3.9) and (3.28) and Fig. 5). In general, however, l_0 and $\Delta\mu_{eff}$ are determined by κ and the additional dimensionless parameter $\lambda = r_0\Delta\rho\Delta\mu/\sigma_{l,g}^{(p)}$ (Eq. (3.14)) which measures the actual distance $\Delta\mu$ from liquid-vapor coexistence in terms of the difference $\Delta\rho = \rho_l - \rho_g$ of the liquid and vapor number densities. This (κ, λ) parameter space separates into three regions (Fig. 6) in each of which $\Delta\mu_{eff}$ and thus the film thickness l_0 reveals a characteristic power law behavior as function of κ and λ (see Eqs. (3.29) - (3.31), (3.35), and (3.36) and Fig. 7).
5. For suitably chosen interaction potential parameters the numerical analysis of the effective interface potential in its full form (Eqs. (2.10), (2.16), (2.17), and (2.29)) renders the phase diagram for first-order wetting of curved substrates (see Fig. 8(a)). The curvature of the substrate raises the wetting temperature $T_w^{(\tau)}(r_0)$ compared to the wetting temperature $T_w^{(p)}$ of the corresponding planar substrate. In the limit of large radii r_0 this shift vanishes as $T_w^{(\tau)}(r_0) - T_w^{(p)} \sim r_0^{-3/2}$. At $T_w^{(\tau)}(r_0)$ the jump Δl_0 in the film thickness is finite (Fig. 8(b)) and diverges for $r_0 \rightarrow \infty$ as $\Delta l_0 \sim r_0^{1/3}$.
6. The curvature of a substrate erases a critical wetting transition such that there is a continuous and smooth increase of the film thickness (see Fig. 9). Even for very large radii r_0 the effects of curvature on the film thickness near this smeared out critical wetting transition are still significant (see Eq. (3.59) and Fig. 9(b)). At coexistence this film thickness is determined by the two dimensionless parameters $\kappa = (r_0^2 \sigma_{l,g}^{(p)}/a)^{1/3}$ and $\gamma = 3b/(2ar_0)$ formed from the expansion coefficients a and b

of the planar effective interface potential (Eq. (2.27)). This (κ, γ) parameter space separates into a rich structure (Fig. 11) such that its various regions correspond to different power laws for l_0 (see Eqs. (3.59), (3.65), (3.68), (3.69), and (3.72) - (3.75)).

7. Since the surface of a sphere and a cylinder is quasi-zero- and quasi-onedimensional, respectively, finite size effects smear out the first-order phase transitions shown in Fig. 8(b) as obtained by mean-field theory. However, according to the estimates in Sect. IV, these finite-size induced fluctuation effects are confined to a very narrow temperature interval δT around the prewetting line. For a typical spherical substrate with a radius $r_0 = 100\sigma$ where σ denotes the diameter of the fluid particles one finds $\delta T/T_w^{(p)} \sim 10^{-4}$. For a cylindrical substrate with the same radius δT is vanishingly small.

Acknowledgements

We thank R. Evans, A. Hanke, and M. Napiórkowski for many helpful discussions.

APPENDIX A: EXPLICIT FORM OF THE EFFECTIVE INTERFACE POTENTIAL FOR A SPHERE

According to Eqs. (2.17) and (2.29) $\sigma_{l,g}^{(s)}$ and part of $\omega^{(s)}(l)$ are determined by $t^{(s)}(r; a)$ which represents the interaction potential of a fluid particle at distance r outside a sphere of radius a filled with the same fluid particles. In polar coordinates $t^{(s)}(r; a)$ takes on the following form:

$$\begin{aligned} t^{(s)}(r; a) &= \int_{|\mathbf{r}'| \leq a} d^3 r' \tilde{w}(|\mathbf{r} - \mathbf{r}'|) \\ &= 2\pi \int_0^a dr' r'^2 \int_0^\pi d\theta \sin \theta \tilde{w} \left(\sqrt{r^2 + r'^2 - 2rr' \cos \theta} \right), \end{aligned} \quad (\text{A1})$$

where we have already used the rotational invariance of $t^{(s)}(r; a)$. With the substitution $s^2 = r^2 + r'^2 - 2rr' \cos \theta$, Eq. (A1) yields

$$\begin{aligned} t^{(s)}(r; a) &= 2\pi \int_0^a dr' \frac{r'}{r} \int_{r-r'}^{r+r'} ds s \tilde{w}(s) \\ &= \frac{2\pi}{r} \int_{r-a}^{r+a} dr' (r - r') \int_{r'}^\infty ds s \tilde{w}(s). \end{aligned} \quad (\text{A2})$$

Equation (2.3) leads to (on physical grounds only the case $a \geq \sigma$ is of interest)

$$\begin{aligned} t^{(s)}(r \geq a ; a \geq \sigma) &= \\ &= \begin{cases} t_{>}^{(s)}(r; a) = \frac{2\pi}{r} \int_{r-a}^{r+a} dr' (r - r') \int_{r'}^\infty ds s \phi_{LJ}(s), & r \geq a + \sigma \\ t_{<}^{(s)}(r; a) = \frac{2\pi}{r} \int_{r-a}^{r+a} dr' (r - r') \int_{r'}^\infty ds s \phi_{LJ}(s) \\ \quad + \frac{2\pi}{r} \int_{r-a}^\sigma dr' (r - r') \int_\sigma^\infty ds s \phi_{LJ}(s), & a < r < a + \sigma \end{cases} \end{aligned} \quad (\text{A3})$$

One has $t_{>}^{(s)}(a + \sigma, a) = t_{<}^{(s)}(a + \sigma, a)$. In the next step we now explicitly use Eq. (2.4) so that

$$\begin{aligned} t_{>}^{(s)}(r; a) &= 2\pi\epsilon \left[\frac{\sigma^{12}}{20} \left(\frac{1}{r(r+a)^8} - \frac{1}{r(r-a)^8} \right) - \frac{2\sigma^{12}}{45} \left(\frac{1}{(r+a)^9} - \frac{1}{(r-a)^9} \right) \right. \\ &\quad \left. - \frac{\sigma^6}{2} \left(\frac{1}{r(r+a)^2} - \frac{1}{r(r-a)^2} \right) + \frac{\sigma^6}{3} \left(\frac{1}{(r+a)^3} - \frac{1}{(r-a)^3} \right) \right] \end{aligned} \quad (\text{A4})$$

and

$$\begin{aligned} t_{<}^{(s)}(r; a) &= \pi\epsilon \left(-\frac{16}{9}\sigma^3 + \frac{3}{5}r\sigma^2 - \frac{3}{5}\frac{a^2\sigma^2}{r} + \frac{3}{2}\frac{\sigma^4}{r} \right) + \frac{4\epsilon\sigma^{12}\pi}{5} \left(\frac{1}{8r(r+a)^8} \right. \\ &\quad \left. - \frac{1}{9(r+a)^9} \right) - 2\epsilon\sigma^6\pi \left(\frac{1}{2r(r+a)^2} - \frac{1}{3(r+a)^3} \right). \end{aligned} \quad (\text{A5})$$

The integral $\int_b^\infty dr r^2 t^{(s)}(r; a)$, $b \geq a$, is given as

$$\int_b^\infty dr r^2 t^{(s)}(r; a) = \begin{cases} \int_b^\infty dr r^2 t_{>}^{(s)}(r; a) & , b \geq a + \sigma \\ \int_b^{a+\sigma} dr r^2 t_{<}^{(s)}(r; a) + \int_{a+\sigma}^\infty dr r^2 t_{>}^{(s)}(r; a) & , b < a + \sigma. \end{cases} \quad (\text{A6})$$

From Eq. (A6) one can directly infer the liquid-gas surface tension $\sigma_{l,g}^{(s)}$ (Eq. (2.17))

$$\sigma_{l,g}^{(s)}(h) = \sigma_{l,g}^{(p)} \left(1 - \frac{2 \ln(h/\sigma)}{9 (h/\sigma)^2} - \frac{1}{(h/\sigma)^2} \left(\frac{2}{9} \ln 2 + \frac{4}{27} \right) - \frac{1}{20736} \frac{1}{(h/\sigma)^8} \right), \quad (\text{A7})$$

where $\sigma_{l,g}^{(p)} = \frac{3\pi}{4} \epsilon \sigma^4 (\Delta\rho)^2$. According to Eqs. (2.29) and (A6) one has to distinguish the cases $l > d_w + \sigma$ and $d_w \leq l \leq d_w + \sigma$. For $l > d_w + \sigma$ one has

$$\begin{aligned} \omega^{(s)}(l > d_w + \sigma) &= \\ &= \Delta\rho \left(\rho_l \int_h^\infty dr \left(\frac{r}{r_0} \right)^2 t_{>}^{(s)}(r; r_1) - \rho_w \int_h^\infty dr \left(\frac{r}{r_0} \right)^2 v^{(s)}(r; r_0) \right), \end{aligned} \quad (\text{A8})$$

whereas for $d_w \leq l \leq d_w + \sigma$

$$\begin{aligned} \omega^{(s)}(d_w \leq l \leq d_w + \sigma) &= \\ &= \Delta\rho \left(\rho_l \int_h^{r_1+\sigma} dr \left(\frac{r}{r_0} \right)^2 t_{<}^{(s)}(r; r_1) + \rho_l \int_{r_1+\sigma}^\infty dr \left(\frac{r}{r_0} \right)^2 t_{>}^{(s)}(r; r_1) \right. \\ &\quad \left. - \rho_w \int_h^\infty dr \left(\frac{r}{r_0} \right)^2 v^{(s)}(r; r_0) \right). \end{aligned} \quad (\text{A9})$$

If $v^{(s)}(r; r_0)$ is approximated as the linear superposition of $\phi_{LJ}^{wf}(r)$ (Eq. (2.5)) it has the same form as $t_{>}^{(s)}(r; r_0)$ with (ϵ, σ) replaced by $(\epsilon_{wf}, \sigma_{wf})$. For additional simplifications see Ref. [34(b)]. In this case and with Eq. (A4) we obtain

$$\begin{aligned} \omega^{(s)}(l > d_w + \sigma) &= \Delta\rho \left[\rho_l \epsilon \sigma^{12} f_{rep}^{(s)}(r_1, h) - \rho_w \epsilon_{wf} \sigma_{wf}^{12} f_{rep}^{(s)}(r_0, h) \right. \\ &\quad \left. - \rho_l \epsilon \sigma^6 f_{attr}^{(s)}(r_1, h) + \rho_w \epsilon_{wf} \sigma_{wf}^6 f_{attr}^{(s)}(r_0, h) \right] \end{aligned} \quad (\text{A10})$$

where

$$f_{rep}^{(s)}(a, b) = \frac{\pi}{540r_0^2} \left(\frac{b^2 + 8ab + a^2}{(b+a)^8} - \frac{b^2 - 8ab + a^2}{(b-a)^8} \right) \quad (\text{A11})$$

and

$$f_{attr}^{(s)}(a, b) = \frac{\pi}{3r_0^2} \left(2ab \frac{b^2 + a^2}{(b^2 - a^2)^2} - \ln \frac{b+a}{b-a} \right). \quad (\text{A12})$$

Expansion in powers of $\frac{d_w}{r_0}$ yields

$$\omega^{(s)}(l) = \omega_{rep}^{(s)}(l) + \omega_{attr}^{(s)}(l) \quad (\text{A13})$$

where

$$\begin{aligned} \omega_{rep}^{(s)}(l) &= \frac{\pi}{540r_0^2} \Delta\rho (\rho_l \epsilon \sigma^{12} - \rho_w \epsilon_{wf} \sigma_{wf}^{12}) \left(\frac{h^2 + 8hr_0 + r_0^2}{(h+r_0)^8} - \frac{h^2 - 8hr_0 + r_0^2}{(h-r_0)^8} \right) \\ &+ \frac{\pi}{90} \Delta\rho \rho_l \epsilon \sigma^{12} \left(\frac{9h-r_0}{(h-r_0)^9} - \frac{9h+r_0}{(h+r_0)^9} \right) \frac{d_w}{r_0} \\ &+ \mathcal{O} \left(\left(\frac{d_w}{r_0} \right)^2 \right) \end{aligned} \quad (\text{A14})$$

and

$$\begin{aligned} \omega_{attr}^{(s)}(l) &= -\frac{\pi}{3r_0^2} \Delta\rho (\rho_l \epsilon \sigma^6 - \rho_w \epsilon_{wf} \sigma_{wf}^6) \left(2hr_0 \frac{h^2 + r_0^2}{(h^2 - r_0^2)^2} - \ln \frac{h+r_0}{h-r_0} \right) \\ &- \frac{d_w}{r_0} \frac{16}{3} \pi \rho_l \Delta\rho \frac{r_0 h^3}{(h^2 - r_0^2)^3} + \mathcal{O} \left(\left(\frac{d_w}{r_0} \right)^2 \right). \end{aligned} \quad (\text{A15})$$

In the limit $l \gg \sigma$ the functions $\mathcal{S}_s(r_0/l) = \omega_{attr}^{(s)}(l)/\omega_{attr}^{(p)}(l)$ and $s_s(x) = ((1+x^{-1})/(\mathcal{S}_s(x) + \frac{x}{2}\mathcal{S}'_s(x)))^{1/3}$ are given by

$$\mathcal{S}_s(x) = \frac{1}{x^2} \left(2x(x+1)^2 \frac{2x^2 + 2x + 1}{(1+2x)^2} - \ln(2x+1) \right) \quad (\text{A16})$$

and

$$s_s(x) = \frac{1}{2} \frac{1+2x}{(x^2(1+x))^{1/3}} \quad , \quad (\text{A17})$$

respectively.

APPENDIX B: THE EFFECTIVE INTERFACE POTENTIAL OF A CYLINDRICAL SUBSTRATE

For a cylinder the calculation of the l -dependent terms $\sigma_{l,g}^{(c)}$ and $\omega^{(c)}(l)$ is somewhat more complicated than in the case of a sphere. They have the form

$$\sigma_{l,g}^{(c)} = -\frac{1}{2} (\Delta\rho)^2 f^{(c)}(h, h; [\tilde{w}]) \quad (\text{B1})$$

and

$$\omega^{(c)}(l) = \Delta\rho \left(\rho_l f^{(c)}(r_1, h; [\tilde{w}]) - \rho_w g^{(c)}(r_0, h; [v]) \right), \quad (\text{B2})$$

with

$$f^{(c)}(a, b; [\tilde{w}]) = \frac{1}{2\pi M r_0} \int_{\mathcal{C}(b, \infty)} d^3 r \int_{\mathcal{C}(0, a)} d^3 r' \tilde{w}(|\mathbf{r} - \mathbf{r}'|) \quad (\text{B3})$$

and

$$g^{(c)}(a, b; [v]) = \frac{1}{2\pi M r_0} \int_{\mathcal{C}(b, \infty)} d^3 r \int_{\mathcal{C}(0, a)} d^3 r' v(|\mathbf{r} - \mathbf{r}'|) \quad (\text{B4})$$

where $\mathcal{C}(r_<, r_>)$ denotes the region between two cylinders of radii $r_<$ and $r_>$. Eq. (B3) can be rewritten in the form

$$f^{(c)}(a, b; [\tilde{w}]) := I(a, \infty) - I(a, b) \quad (\text{B5})$$

where

$$I(a, b) = \frac{1}{2\pi M r_0} \int_{\mathcal{C}(0, b)} d^3 r \int_{\mathcal{C}(0, a)} d^3 r' \tilde{w}(|\mathbf{r} - \mathbf{r}'|). \quad (\text{B6})$$

With $\mathbf{r} = (\mathbf{r}_\perp, z)$ where the z -axis is the cylinder axis and \mathbf{r}_\perp orthogonal to it one has

$$\begin{aligned} I(a, b) &= \frac{1}{\pi r_0} \int_0^\infty dz \int_{0 \leq |\mathbf{r}_\perp| \leq b} d^2 r_\perp \int_{0 \leq |\mathbf{r}'_\perp| \leq a} d^2 r'_\perp \tilde{w} \left(\sqrt{(\mathbf{r}_\perp - \mathbf{r}'_\perp)^2 + z^2} \right) \\ &=: \frac{1}{\pi r_0} \int_0^\infty dz J(z) \end{aligned} \quad (\text{B7})$$

with

$$J(z) = \int_{0 \leq |\mathbf{r}_\perp| \leq b} d^2 r_\perp \int_{0 \leq |\mathbf{r}'_\perp| \leq a} d^2 r'_\perp \tilde{w} \left(\sqrt{(\mathbf{r}_\perp - \mathbf{r}'_\perp)^2 + z^2} \right). \quad (\text{B8})$$

The coordinate transformation

$$\begin{aligned} \mathbf{R} &= \frac{1}{2}(\mathbf{r}_\perp + \mathbf{r}'_\perp), & \tilde{\mathbf{r}} &= \mathbf{r}_\perp - \mathbf{r}'_\perp \\ \mathbf{r}_\perp &= \mathbf{R} + \frac{1}{2}\tilde{\mathbf{r}}, & \mathbf{r}'_\perp &= \mathbf{R} - \frac{1}{2}\tilde{\mathbf{r}}, \end{aligned} \quad (\text{B9})$$

yields

$$J(z) = 2\pi \int_0^{a+b} d\tilde{r} \tilde{r} \tilde{w} \left(\sqrt{\tilde{r}^2 + z^2} \right) \int_D d^2R. \quad (\text{B10})$$

Equation (B9) provides the following limits of integration for \mathbf{R} :

$$0 \leq \left(\mathbf{R} + \frac{1}{2}\tilde{\mathbf{r}} \right)^2 \leq b^2, \quad 0 \leq \left(\mathbf{R} - \frac{1}{2}\tilde{\mathbf{r}} \right)^2 \leq a^2. \quad (\text{B11})$$

This corresponds to two circles, one with radius b centered at $\mathbf{R} = -\frac{1}{2}\tilde{\mathbf{r}}$, the other with radius a centered at $\mathbf{R} = +\frac{1}{2}\tilde{\mathbf{r}}$. Thus $\int_D d^2R =: D(\tilde{r}, a, b)$ is the area of intersection of these two circles which depends on $\tilde{\mathbf{r}}$ for $b - a \leq |\tilde{\mathbf{r}}| \leq b + a$ and equals πa^2 for $0 \leq |\tilde{\mathbf{r}}| \leq b - a$:

$$D(\tilde{r}, a, b) = \begin{cases} g_{a,b}(\tilde{r}), & b - a \leq |\tilde{\mathbf{r}}| \leq b + a \\ \pi a^2, & 0 \leq |\tilde{\mathbf{r}}| < b - a \\ 0, & \text{otherwise} \end{cases} \quad (\text{B12})$$

where $g_{a,b}(\tilde{r}) := \frac{\pi}{2}n^2 - \frac{1}{2}\sqrt{-\tilde{r}^4 + 2n^2\tilde{r}^2 - m^4} + a^2 \arcsin \frac{m^2 - \tilde{r}^2}{2\tilde{r}a} - b^2 \arcsin \frac{m^2 + \tilde{r}^2}{2\tilde{r}b}$ with $m^2 = b^2 - a^2$ and $n^2 = b^2 + a^2$. One has $g_{a,\infty} = \pi a^2$ because the smaller circle lies always within the larger one and

$$D(\tilde{r}, a, a) = \begin{cases} g_{a,a}(\tilde{r}), & 0 \leq |\tilde{\mathbf{r}}| \leq 2a \\ 0, & |\tilde{\mathbf{r}}| > 2a. \end{cases} \quad (\text{B13})$$

with $g_{a,a}(\tilde{r}) = \pi a^2 - \frac{\tilde{r}}{2}\sqrt{4a^2 - \tilde{r}^2} - 2a^2 \arcsin \frac{\tilde{r}}{2a}$. Inserting Eq. (B12) into Eq. (B10) yields

$$J(z) = 2\pi^2 a^2 \int_{|z|}^{\sqrt{(b-a)^2 + z^2}} dss\tilde{w}(s) + 2\pi \int_{\sqrt{(b-a)^2 + z^2}}^{\sqrt{(b+a)^2 + z^2}} dss\tilde{w}(s)g_{a,b} \left(\sqrt{s^2 - z^2} \right) \quad (\text{B14})$$

so that

$$I(a, b) = \frac{2\pi a^2}{r_0} \int_0^\infty dz \int_{|z|}^{\sqrt{(b-a)^2 + z^2}} dss\tilde{w}(s) + \frac{2}{r_0} \int_0^\infty dz \int_{\sqrt{(b-a)^2 + z^2}}^{\sqrt{(b+a)^2 + z^2}} dss\tilde{w}(s)g_{a,b} \left(\sqrt{s^2 - z^2} \right) \quad (\text{B15})$$

and especially

$$I(a, \infty) = \frac{2\pi a^2}{r_0} \int_0^\infty dz \int_{|z|}^\infty dss\tilde{w}(s). \quad (\text{B16})$$

Thus independent of the explicit form of \tilde{w} $f^{(c)}(a, b; [\tilde{w}])$ is given by

$$\begin{aligned} f^{(c)}(a, b; [\tilde{w}]) &= \frac{2\pi a^2}{r_0} \int_0^\infty dz \int_{\sqrt{(b-a)^2+z^2}}^\infty ds s \tilde{w}(s) \\ &\quad - \frac{2}{r_0} \int_0^\infty dz \int_{\sqrt{(b-a)^2+z^2}}^{\sqrt{(b+a)^2+z^2}} ds s \tilde{w}(s) g_{a,b}(\sqrt{s^2 - z^2}). \end{aligned} \quad (\text{B17})$$

Equation (2.3) requires the consideration of two cases:

$$\begin{aligned} f^{(c)}(b > a + \sigma) &= \frac{2}{r_0} \left(\pi a^2 \int_0^\infty dz \int_{\sqrt{(b-a)^2+z^2}}^\infty ds s w(s) \right. \\ &\quad \left. - \int_0^\infty dz \int_{\sqrt{(b-a)^2+z^2}}^{\sqrt{(b+a)^2+z^2}} ds s w(s) g_{a,b}(\sqrt{s^2 - z^2}) \right) \end{aligned} \quad (\text{B18})$$

and

$$\begin{aligned} f^{(c)}(a \leq b \leq a + \sigma) &= \\ &= \frac{2\pi a^2}{r_0} \left(\int_0^{\sqrt{\sigma^2 - (b-a)^2}} dz \int_\sigma^\infty ds + \int_{\sqrt{\sigma^2 - (b-a)^2}}^\infty dz \int_{\sqrt{(b-a)^2+z^2}}^\infty ds \right) s w(s) \\ &\quad - \frac{2}{r_0} \left(\int_0^{\sqrt{\sigma^2 - (b-a)^2}} dz \int_\sigma^{\sqrt{(b+a)^2+z^2}} ds + \int_{\sqrt{\sigma^2 - (b-a)^2}}^\infty dz \int_{\sqrt{(b-a)^2+z^2}}^{\sqrt{(b+a)^2+z^2}} ds \right) \times \\ &\quad \times s w(s) g_{a,b}(\sqrt{s^2 - z^2}). \end{aligned} \quad (\text{B19})$$

For $a = b$ one obtains

$$\begin{aligned} f^{(c)}(a = b) &= \frac{2\pi a^2}{r_0} \left(\int_0^\sigma dz \int_\sigma^\infty ds + \int_\sigma^\infty dz \int_z^\infty ds \right) s w(s) \\ &\quad - \frac{2}{r_0} \left(\int_0^\sigma dz \int_\sigma^{\sqrt{4a^2+z^2}} ds + \int_\sigma^\infty dz \int_z^{\sqrt{4a^2+z^2}} ds \right) \times \\ &\quad \times s w(s) g_{a,a}(\sqrt{s^2 - z^2}). \end{aligned} \quad (\text{B20})$$

If we now adopt the Lennard-Jones form for $w(r)$ (Eq. (2.4)) $f^{(c)}$ separates into a contribution $f_{rep}^{(c)}$ from the repulsive part proportional to r^{-12} and into a contribution $f_{attr}^{(c)}$ due to the attractive part $\sim r^{-6}$ of this potential so that

$$f^{(c)} = \epsilon \sigma^{12} f_{rep}^{(c)} - \epsilon \sigma^6 f_{attr}^{(c)} \quad (\text{B21})$$

and

$$f_{rep}^{(c)} = \frac{\pi}{20r_0} \int_0^\infty \frac{dz}{z^{10}} \left(\frac{\sum_{i=0}^9 a_{2i}(m, n) z^{2i}}{(z^4 + 2n^2 z^2 + m^4)^{9/2}} - 8m^2 \right) \quad (\text{B22})$$

with the coefficients $a_0 = 8m^{20}$, $a_2 = 72m^{16}n^2$, $a_4 = 36m^{16} + 252m^{12}n^4$, $a_6 = 252m^{12}n^2 + 420m^8n^6$, $a_8 = 63m^{12} + 630m^8n^4 + 315m^4n^8$, $a_{10} = 70n^{10} + 620m^4n^6 + 318m^8n^2$, $a_{12} = 155n^8 + 55m^8 + 462m^4n^4$, $a_{14} = 132n^6 + 156m^4n^2$, $a_{16} = 52n^4 + 20m^4$, $a_{18} = 8n^2$ where $m^2 = b^2 - a^2$ and $n^2 = b^2 + a^2$. By using a symbol-manipulation program one can show that the latter expression is identical with

$$f_{rep}^{(c)} = \frac{7\pi^2}{64r_0} \frac{a^2}{b^9} {}_2F_1 \left(\frac{11}{2}, \frac{9}{2}; 2; \left(\frac{a}{b}\right)^2 \right). \quad (\text{B23})$$

The attractive contribution has a similar form:

$$\begin{aligned} f_{attr}^{(c)} &= \frac{\pi}{2r_0} \int_0^\infty \frac{dz}{z^4} \left(\frac{n^2 z^6 + z^4 (2n^4 + m^4) + 3m^4 n^2 z^2 + m^8}{(z^4 + 2n^2 z^2 + m^4)^{3/2}} - m^2 \right) \\ &= \frac{\pi^2}{2r_0} \frac{a^2}{b^3} {}_2F_1 \left(\frac{5}{2}, \frac{3}{2}; 2; \frac{a^2}{b^2} \right). \end{aligned} \quad (\text{B24})$$

For $a = r_1$ and $b = h$ one obtains $f^{(c)}(r_1, h; [\tilde{w}])$.

In order to provide an explicit formula for the effective interface potential $\omega^{(c)}(l)$ one finally has to specify the contribution $g^{(c)}$ from the substrate potential (see Eqs. (B2) and (B4)). If the substrate potential is approximated as the linear superposition of Lennard-Jones interaction potentials between pairs of substrate atoms and fluid atoms (see Eq. (2.5)), $g^{(c)}$ has the same functional as $f^{(c)}$ with ϵ and σ replaced by ϵ_{wf} and σ_{wf} , respectively:

$$g^{(c)}(r_0, h) = f^{(c)}(a = r_0, b = h; \epsilon \rightarrow \epsilon_{wf}, \sigma \rightarrow \sigma_{wf}). \quad (\text{B25})$$

Equations (B23) and (B24) are only valid for $h > r_0 + d_w + \sigma$, because due to the Heaviside function entering Eq. (2.3) $f^{(c)}$ changes its form for $d_w < l < d_w + \sigma$. Since in the substrate potential there is no such Heaviside function, $g^{(c)}$ retains its form for *all* values of h . Keeping this in mind one has

$$\omega^{(c)}(l > d_w + \sigma) = \Delta\rho (\rho_l f^{(c)}(r_1, h) - \rho_w f^{(c)}(r_0, h; \epsilon \rightarrow \epsilon_{wf}, \sigma \rightarrow \sigma_{wf})). \quad (\text{B26})$$

In the limit $\frac{d_w}{r_0} \rightarrow 0$ Eq. (B26) yields explicitly

$$\omega^{(c)}(l) = \omega_{rep}^{(c)}(l) + \omega_{attr}^{(c)}(l), \quad d_w/r_0 \ll 1, \quad (\text{B27})$$

where

$$\begin{aligned}
\omega_{rep}^{(c)}(l) &= \frac{7\pi^2}{64} \Delta\rho (\rho_l \epsilon \sigma^{12} - \rho_w \epsilon_{wf} \sigma_{wf}^{12}) \frac{r_0}{h^9} {}_2F_1\left(\frac{11}{2}, \frac{9}{2}; 2; \left(\frac{r_0}{h}\right)^2\right) \\
&+ \frac{7\pi^2}{64} \Delta\rho \rho_l \epsilon \sigma^{12} \frac{r_0}{h^9} \left({}_2F_1\left(\frac{11}{2}, \frac{9}{2}; 2; \left(\frac{r_0}{h}\right)^2\right) + \frac{99}{4} \frac{r_0^2}{h^2} {}_2F_1\left(\frac{13}{2}, \frac{11}{2}; 3; \left(\frac{r_0}{h}\right)^2\right) \right) \frac{d_w}{r_0} \\
&+ \mathcal{O}\left(\left(\frac{d_w}{r_0}\right)^2\right)
\end{aligned} \tag{B28}$$

and

$$\begin{aligned}
\omega_{attr}^{(c)}(l) &= -\frac{\pi^2}{2} \Delta\rho (\rho_l \epsilon \sigma^6 - \rho_w \epsilon_{wf} \sigma_{wf}^6) \frac{r_0}{h^3} {}_2F_1\left(\frac{5}{2}, \frac{3}{2}; 2; \left(\frac{r_0}{h}\right)^2\right) \\
&- \frac{\pi^2}{2} \Delta\rho \rho_l \epsilon \sigma^6 \frac{r_0}{h^3} \left({}_2F_1\left(\frac{5}{2}, \frac{3}{2}; 2; \left(\frac{r_0}{h}\right)^2\right) + \frac{15}{4} \frac{r_0^2}{h^2} {}_2F_1\left(\frac{7}{2}, \frac{5}{2}; 3; \left(\frac{r_0}{h}\right)^2\right) \right) \frac{d_w}{r_0} \\
&+ \mathcal{O}\left(\left(\frac{d_w}{r_0}\right)\right).
\end{aligned} \tag{B29}$$

The functions $\mathcal{S}_c(x)$ and $s_c(x)$ (Eqs. (2.36) and (3.4)) are thus given by

$$\mathcal{S}_c(x) = \frac{3\pi}{2} \frac{x}{(x+1)^2} {}_2F_1\left(\frac{5}{2}, \frac{3}{2}; 2; \left(\frac{x}{x+1}\right)^2\right) \tag{B30}$$

and

$$s_c(x) = \frac{\left(\frac{4(1+x)^4}{9\pi x}\right)^{1/3}}{\left({}_2F_1\left(\frac{5}{2}, \frac{3}{2}; 2; \left(\frac{x}{x+1}\right)^2\right) + \frac{5x^2}{4(x+1)^2} {}_2F_1\left(\frac{7}{2}, \frac{5}{2}; 3; \left(\frac{x}{x+1}\right)^2\right)\right)^{1/3}}, \tag{B31}$$

respectively.

The liquid-vapor surface tension follows from Eqs. (B1) and (B20). A lengthy calculation yields the following result based on Eqs. (2.3) and (2.4):

$$\sigma_{l,g}^{(c)} = -(\Delta\rho)^2 \epsilon \sigma^4 K\left(\frac{h}{\sigma}\right) \tag{B32}$$

where

$$K(x) = \sum_{i=1}^4 K_i(x) \tag{B33}$$

with

$$\begin{aligned}
K_1(x) = & -\frac{2}{5}(\Delta\rho)^2 \left[\pi\sqrt{4x^2+1} \left(\frac{35}{2048x} - \frac{125}{49152x^3} + \frac{337}{786432x^5} - \frac{209}{2097152x^7} \right. \right. \\
& + \frac{1}{1024x^3(4x^2+1)^3} + \frac{1}{12288x^5(4x^2+1)^2} + \left. \left. \frac{3}{16384x^7(4x^2+1)} \right) \right. \\
& \left. - \pi \frac{175}{4194304} \frac{\ln(2x + \sqrt{4x^2+1})}{x^8} \right], \tag{B34}
\end{aligned}$$

$$\begin{aligned}
K_2(x) = & -\frac{4}{5}x \int_0^1 dz \left\{ \frac{35x^6 + 30x^4z^2 + 9x^2z^4 + z^6}{z^9(4x^2+z^2)^{7/2}} \times \right. \\
& \times \left(\frac{\pi}{2} - \arcsin \left(\sqrt{(1-z^2) \left(1 + \frac{z^2}{4x^2} \right)} \right) \right) + \arcsin \left(\frac{\sqrt{1-z^2}}{2x} \right) \\
& + \frac{1}{4x^2} \sqrt{(1-z^2)(4x^2+z^2-1)} \left(1 - \frac{1}{4z^2} - \frac{14x^2+3z^2}{12z^4(4x^2+z^2)} \right. \\
& \left. \left. - \frac{70x^4+32x^2z^2+3z^4}{12z^6(4x^2+z^2)^2} - \frac{420x^6+290x^4z^2+62x^2z^4+3z^6}{12z^8(4x^2+z^2)^3} \right) \right\}, \tag{B35}
\end{aligned}$$

$$K_3(x) = \frac{\pi}{8x} \sqrt{4x^2+1} - \frac{\pi}{16x^2} \ln \frac{\sqrt{4x^2+1}+2x}{\sqrt{4x^2+1}-2x}, \tag{B36}$$

and

$$\begin{aligned}
K_4(x) = & 2x \int_0^1 dz \left\{ \arcsin \left(\frac{\sqrt{1-z^2}}{2x} \right) - \frac{1}{4x^2} \frac{(1-z^2)^{3/2} \sqrt{4x^2+z^2-1}}{z^2} \right. \\
& \left. + \frac{1}{2z^3 \sqrt{4x^2+z^2}} \left(\frac{\pi}{2} - \arcsin \frac{(2x^2+z^2)(1-z^2) - 2x^2z^2}{2x^2} \right) \right\}. \tag{B37}
\end{aligned}$$

In the asymptotic limit $h \rightarrow \infty$ this expression reduces to

$$\begin{aligned}
& \sigma_{l,g}^{(c)}(h \gg \sigma) = \\
& \sigma_{l,g}^{(p)} \left(1 - \frac{1}{6} \frac{\ln(h/\sigma)}{(h/\sigma)^2} - \frac{1}{(h/\sigma)^2} \left(\frac{5}{3} \ln 2 + \frac{1}{144} \right) \right. \\
& \left. - \frac{5}{1536} \frac{1}{(h/\sigma)^4} + \mathcal{O} \left(\frac{1}{(h/\sigma)^6} \right) \right). \tag{B38}
\end{aligned}$$

APPENDIX C: EFFECTIVE INTERFACE POTENTIAL FOR COATED SPHERES AND CYLINDERS

We consider spherical and cylindrical substrates which are composed of two different species for $0 \leq r \leq r_0 - \delta$ and $r_0 - \delta < r \leq r_0$. They interact with the fluid particles according to pair potentials $\phi_{wf}^{(0)}(r)$ and $\phi_{wf}^{(1)}(r)$, respectively. For reasons of simplicity we assume that the number density of the substrate particles ρ_w is constant. If one approximates the substrate potential $V(\mathbf{r}; r_0) = \rho_w v(\mathbf{r}; r_0)$ by the homogeneous (i. e. disregarding the discrete arrangement of the substrate atoms) linear superposition of these pair potentials one has $v(\mathbf{r}; r_0) = v(r; r_0)$ with

$$\begin{aligned} v(r; r_0) &= \int_{\mathcal{S}(r_0 - \delta)} d^3 r' \phi_{wf}^{(0)}(|\mathbf{r} - \mathbf{r}'|) + \int_{\mathcal{S}(r_0) \setminus \mathcal{S}(r_0 - \delta)} d^3 r' \phi_{wf}^{(1)}(|\mathbf{r} - \mathbf{r}'|) \\ &= \int_{\mathcal{S}(r_0)} d^3 r' \phi_{wf}^{(1)}(|\mathbf{r} - \mathbf{r}'|) + \int_{\mathcal{S}(r_0 - \delta)} d^3 r' \left(\phi_{wf}^{(0)}(|\mathbf{r} - \mathbf{r}'|) - \phi_{wf}^{(1)}(|\mathbf{r} - \mathbf{r}'|) \right) \\ &=: v_1(r; r_0) + v_{0,1}(r; r_0 - \delta) \end{aligned} \quad (\text{C1})$$

where $\mathcal{S}(r)$ denotes a substrate of radius r . If the functions $\phi_{wf}^{(0)}(r)$ and $\phi_{wf}^{(1)}(r)$ are approximated by Eq. (2.5) with interaction potential parameters $\{\epsilon_{wf}^{(0)}, \sigma_{wf}^{(0)}\}$ and $\{\epsilon_{wf}^{(1)}, \sigma_{wf}^{(1)}\}$, respectively, the computation of $v_1(r; r_0)$ and $v_{0,1}(r; r_0 - \delta)$ can be carried out along the lines of the Appendices A and B. On this basis we obtain

$$\begin{aligned} \omega^{(c,s)}(l) &= \\ &= \left(\rho_w \left(\epsilon_{wf}^{(1)} (\sigma_{wf}^{(1)})^{12} - \epsilon_{wf}^{(0)} (\sigma_{wf}^{(0)})^{12} \right) f_{rep}^{(c,s)}(r_0 - \delta, h) - \rho_w \epsilon_{wf}^{(1)} (\sigma_{wf}^{(1)})^{12} f_{rep}^{(c,s)}(r_0, h) \right. \\ &\quad \left. - \rho_w \left(\epsilon_{wf}^{(1)} (\sigma_{wf}^{(1)})^6 - \epsilon_{wf}^{(0)} (\sigma_{wf}^{(0)})^6 \right) f_{attr}^{(c,s)}(r_0 - \delta, h) + \rho_w \epsilon_{wf}^{(1)} (\sigma_{wf}^{(1)})^6 f_{attr}^{(c,s)}(r_0, h) \right. \\ &\quad \left. + \rho_l \epsilon \sigma^{12} f_{rep}^{(c,s)}(r_1, h) - \rho_l \epsilon \sigma^6 f_{attr}^{(c,s)}(r_1, h) \right). \end{aligned} \quad (\text{C2})$$

The expansions of the effective interface potentials $\omega^{(\tau)}(l, r_0)$ into powers of r_0/l under the condition that both $\delta \ll r_0, l$ and $d_w \ll r_0, l$ can be calculated straightforwardly. As a generalization of Eq. (2.27) one obtains

$$\omega^{(\tau)}(l, r_0) = \frac{a}{l^2} \mathcal{S}_\tau \left(\frac{r_0}{l} \right) + \frac{b}{l^3} \mathcal{R}_\tau \left(\frac{r_0}{l} \right) + \mathcal{O} \left(\frac{1}{l^4} \right) \quad (\text{C3})$$

where $\mathcal{S}_\tau(x)$ and $\mathcal{R}_\tau(x)$ are given by Eqs. (2.36) and (3.51), respectively, and with the constants a and b given by Eqs. (3.44), (3.47), and (3.48); they are identical to those of the corresponding planar substrate. For the model potentials given by Eqs. (2.4) and (2.5) one has

$$\mathcal{R}_c(x) = \frac{3\pi}{2} \frac{1}{(1+x)^3} {}_2F_1 \left(\frac{5}{2}, \frac{3}{2}; 2; \left(\frac{x}{x+1} \right)^2 \right) \quad (\text{C4})$$

for a cylinder and

$$\mathcal{R}_s(x) = \frac{8(1+x)^3}{(1+2x)^3} \quad (\text{C5})$$

for a sphere, respectively. From these results one can infer the explicit form of the functions $q_\tau(x, \gamma)$ (Eqs. (3.55) and (3.56)):

$$\begin{aligned} q_c(x) = & \frac{2}{3x} \left[{}_2F_1 \left(\frac{5}{2}, \frac{3}{2}, 2, \left(\frac{x}{x+1} \right)^2 \right) + \frac{5}{4} \frac{x^2}{(x+1)^2} {}_2F_1 \left(\frac{7}{2}, \frac{5}{2}, 3, \left(\frac{x}{x+1} \right)^2 \right) \right]^{-1} \times \\ & \times \left[{}_2F_1 \left(\frac{5}{2}, \frac{3}{2}, 2, \left(\frac{x}{x+1} \right)^2 \right) + \frac{35}{8} \frac{x^2}{(x+1)^2} {}_2F_1 \left(\frac{7}{2}, \frac{5}{2}, 3, \left(\frac{x}{x+1} \right)^2 \right) + \right. \\ & \left. + \frac{175}{48} \frac{x^4}{(x+1)^4} {}_2F_1 \left(\frac{9}{2}, \frac{7}{2}, 4, \left(\frac{x}{x+1} \right)^2 \right) \right] \quad (\text{C6}) \end{aligned}$$

for a cylinder and

$$q_s(x) = \frac{1}{x} \frac{1+2x+2x^2}{1+2x} \quad (\text{C7})$$

for a sphere, respectively.

REFERENCES

- [1] D. Beysens and D. Estève, *Phys. Rev. Lett.* **54**, 2123 (1985); V. Gurfein, D. Beysens, and F. Perrot, *Phys. Rev. A* **40**, 2543 (1989); J. S. van Duijneveldt, and D. Beysens, *J. Chem. Phys.* **94**, 5222 (1991); V. Gurfein, F. Perrot, and D. Beysens, *J. Colloid Interf. Sci* **149**, 373 (1992); T. Narayanan, A. Kumar, E. S. R. Gopal, D. Beysens, P. Guenoun, and G. Zalczer, *Phys. Rev. E* **48**, 1989 (1993); D. Beysens, J.-M. Petit, T. Narayanan, A. Kumar, and M. L. Broide, *Ber. Bunsenges. Phys. Chem.* **98**, 382 (1994); A. Kumar and D. Beysens, *Physica A* **224**, 68 (1996).
- [2] P. D. Gallagher and J. V. Maher, *Phys. Rev. A* **46**, 2012 (1992); M. L. Kurnaz and J. V. Maher, *Phys. Rev. E* **51**, 5916 (1995).
- [3] Z. Király, L. Turi, I. Dékány, K. Bean, and B. Vincent, *Colloid Polym. Sci.* **274**, 779 (1996); and references therein.
- [4] Y. Jayalakshmi and E. W. Kaler, *Phys. Rev. Lett.* **78**, 1379 (1997).
- [5] H. Grill and D. Woermann, *Ber. Bunsenges. Phys. Chem.* **101**, 814 (1997).
- [6] Y. Pomeau, *J. Colloid Interf. Sci.* **113**, 5 (1986); G. Mason and N. R. Morrow, *J. Colloid Interf. Sci.* **168**, 130 (1994).
- [7] E. A. Boucher, *J. Chem. Soc. Faraday Trans. I* **85**, 2963 (1989); T. J. Sluckin, *Phys. Rev. A* **41**, 960 (1990).
- [8] H. T. Dobbs, G. A. Darbellay, and J. M. Yeomans, *Europhys. Lett.* **18**, 439 (1992); H. T. Dobbs and J. M. Yeomans, *J. Phys.: Condens. Matter* **4**, 10133 (1992).
- [9] H. T. Dobbs and J. M. Yeomans, *Mol. Phys.* **80**, 877 (1993); W. R. Osborn and J. M. Yeomans, *Phys. Rev. E* **51**, 2053 (1995).
- [10] S. L. Carnie and D. Y. C. Chan, *J. Colloid Interf. Sci.* **155**, 297 (1993).
- [11] H. Löwen, *Phys. Rev. Lett.* **74**, 1028 (1995); *Z. Physik B* **97**, 269 (1995); R. Netz, *Phys. Rev. Lett.* **76**, 3646 (1996).
- [12] P. G. de Gennes, *C. R. Acad. Sci. Paris II* **292**, 701 (1981); P. Attard, C. P. Ursenbach, and G. N. Patey, *Phys. Rev. A* **45**, 7621 (1992); D. Henderson and M. Plischke, *J. Chem. Phys.* **97**, 7822 (1992); T. W. Burkhardt and E. Eisenriegler, *Phys. Rev. Lett.* **74**, 3189 (1995); E. Eisenriegler and U. Ritschel, *Phys. Rev. B* **51**, 13717 (1995).
- [13] D. Henderson and M. Lozada-Cassou, *J. Colloid Interf. Sci.* **114**, 180 (1986); D. Henderson, *J. Colloid Interf. Sci.* **121**, 486 (1988); S. T. Chui, *Phys. Rev. B* **43**, 10655 (1991); D. Henderson, *J. Chem. Phys.* **97**, 1266 (1992); D. Henderson, *Fluid Phase Equilibria* **76**, 1 (1992); L. Degève and D. Henderson, *J. Chem. Phys.* **100**, 1606 (1994); D. Henderson, K. Chan, and L. Degève, *J. Chem. Phys.* **101**, 6975 (1994); M. Ginoza, T. Kinjo, and M. Yasutomi, *J. Phys.: Condens. Matter* **6**, 8383 (1994); M. Yasutomi and M. Ginoza, *J. Phys.: Condens. Matter* **7**, 3845 (1995).
- [14] A. E. Saez and R. G. Carbonelle, *J. Colloid Interf. Sci.* **140**, 408 (1990); D. Langebein, *Adv. Coll. Interf. Sci.* **46**, 91 (1993); G. Lian, C. Thornton, and M. Adams, *J. Colloid Interf. Sci.* **161**, 138 (1993); D. Li, *J. Colloid Interf. Sci.* **163**, 108 (1994); N. D. Denkov, D. N. Petsev, and K. D. Danov, *Phys. Rev. Lett.* **71**, 3226 (1993).
- [15] H. Lee, H. Tamura, and M. Doi, *J. Phys. D* **26**, 746 (1993); and references therein.

- [16] T. Gil and J. H. Ipsen, Phys. Rev. E **55**, 1713 (1997); T. Gil, M. C. Sabra, J. H. Ipsen, and O. G. Mouritsen, Biophysical Journal, to appear (1997).
- [17] H. K. Christenson, J. Colloid Interf. Sci. **121**, 170 (1988); M. J. Matthewson, Phil. Mag. A **57**, 207 (1988); M. L. Gee, P. Tong, J. N. Israelachvili, and T. A. Witten, J. Chem. Phys. **93**, 6057 (1990); Y. I. Rabinovich, T. G. Movchan, N. Churaev, and P. G. Ten, Langmuir **7**, 817 (1991); M. L. Forcada, M. M. Jakas, and A. Gras-Martí, J. Chem. Phys. **95**, 706 (1991); V. N. Paunov, P. A. Kralchevsky, N. D. Denkov, I. B. Ivanov, and K. Nagayama, Colloids and Surf. **67**, 119 (1992); A. Mamur, Langmuir **9**, 1922 (1993); Y. Q. Li, N. J. Tao, J. Pan, A. A. Garcia, and S. M. Lindsay, Langmuir **9**, 637 (1993); J. Crassous, E. Charlaix, and J. L. Loubet, Europhys. Lett. **28**, 37 (1994); S. Biggs, Ber. Bunsenges. Phys. Chem. **98**, 636 (1994).
- [18] C. M. Mate, J. Appl. Phys. **72**, 3084 (1992).
- [19] P. Basa, J. C. Schön, R. S. Berry, J. Bernholc, J. Jellinek, and P. Salamon, Phys. Rev. B **43**, 8113 (1991).
- [20] F. Lin and D. J. Meier, Langmuir **11**, 2726 (1995).
- [21] M. H. Al-Dahhan and M. P. Duduković, Chem. Engineering Sci. **50**, 2377 (1995).
- [22] F. De Bisschop, J. Adhesion Sci. Technol. **9**, 873 (1995).
- [23] J. R. Philip, J. Chem. Phys. **67**, 1732 (1977).
- [24] R. Holyst and A. Poniewierski, Phys. Rev. B **36**, 5628 (1987); Physica A **149**, 622 (1988).
- [25] M. P. Gelfand and R. Lipowsky, Phys. Rev. B **36**, 8725 (1987).
- [26] (a) J. O. Indekeu, P. J. Upton, and J. M. Yeomans, Phys. Rev. Lett. **61**, 2221 (1988); (b) P. J. Upton, J. O. Indekeu, and J. M. Yeomans, Phys. Rev. B **40**, 666 (1989).
- [27] M. Swift and J. M. Yeomans, J. Phys. A **23**, 5655 (1990).
- [28] T. Gil and L. V. Mikheev, Phys. Rev. E **52**, 772 (1995).
- [29] I. Hadjiagapiou, J. Chem. Phys. **105**, 2927 (1996).
- [30] S. Dietrich, in *Phase Transitions and Critical Phenomena*, edited by C. Domb and J. L. Lebowitz (Academic, London, 1988), Vol. 12, p. 1.
- [31] M. Schick, in *Liquids at Interfaces*, Les Houches Summer School Lectures, Session XLVIII, edited by J. Charvolin, J. F. Joanny, and J. Zinn-Justin (Elsevier, Amsterdam, 1990), p. 416.
- [32] S. Dietrich and M. Napiórkowski, Physica A **177**, 437 (1991); M. Napiórkowski and S. Dietrich, Z. Physik B **89**, 263 (1992); Phys. Rev. E **47**, 1836 (1993); Z. Physik B **97**, 511 (1995).
- [33] I. E. Dzyaloshinskii, E. M. Lifshitz, and L. P. Pitaevskii, Adv. Phys. **10**, 165 (1961).
- [34] (a) V. A. Parsegian and G. H. Weiss, J. Chem. Phys. **60**, 5080 (1974); (b) M. W. Cole and M. Schmeits, Surf. Sci. **75**, 529 (1978); (c) N. S. Witte, J. Chem. Phys. **99**, 8168 (1993).
- [35] R. Evans, Adv. Phys. **28**, 143 (1979); in *Liquids at Interfaces*, Les Houches Summer School Lectures, Session XLVIII, edited by J. Charvolin, J. F. Joanny, and J. Zinn-Justin (Elsevier, Amsterdam, 1990), p. 3.
- [36] M. Connor, P. H. Harding, J.-A. E. Månson, and J. C. Berg, J. Adhesion Sci. Technol. **9**, 983 (1995).

- [37] P. Levinson, J. Jouffroy, and F. Brochard, *J. Physique Lett.* **46**, L21 (1985); F. Brochard, *J. Chem. Phys.* **84**, 4664 (1986).
- [38] D. Quéré, J.-M. di Meglio, and F. Brochard-Wyart, *Revue Phys. Appl.* **23**, 1023 (1988); *Europhys. Lett.* **10**, 335 (1989); *Science* **249**, 1256 (1990), and references therein; A. de Ryck and D. Quéré, *C. R. Acad. Sci. Paris, Série II*, **316**, 1045 (1993); *ibid* **317**, 891 (1993); V. I. Ivanov, D. Quéré, J.-M. di Meglio, and V. M. Starov, *Colloid J. Russian Acad. Sci.* **54**, 346 (1992); D. Quéré and J.-M. di Meglio, *Adv. Colloid Interf. Sci.* **48**, 141 (1994).
- [39] S. Rooks, L. M. Racz, J. Szekely, B. Benhabib, and A. W. Neumann, *Langmuir* **7**, 3222 (1991).
- [40] H. D. Wagner, *J. Appl. Phys.* **67**, 1352 (1990); *ibid* **70**, 495 (1991); B. J. Carroll, *J. Appl. Phys.* **70**, 493 (1991).
- [41] A. L. Yarin, A. Oron, P. Rosenau, *Phys. Fluids A* **5**, 91 (1993).
- [42] B. J. Carroll, in *Contact Angle, Wettability and Adhesion*, edited by K. L. Mittal (VSP Utrecht, 1993), p. 235.
- [43] Y.-N. Lee and S.-M. Chiao, *J. Colloid Interf. Sci.* **181**, 378 (1996).
- [44] G. A. Darbellay and J. M. Yeomans, *J. Phys. A* **23**, 5655 (1990).
- [45] R. D. Groot, N. M. Faber, and J. P. van der Eerden, *Mol. Phys.* **62**, 861 (1987); R. Pospíšil, J. Sýs, A. Malijevský, and S. Labík, *Mol. Phys.* **75**, 261 (1992).
- [46] G. McHale, N. A. Käb, M. I. Newton, and S. M. Rowan, *J. Colloid Interf. Sci.* **186**, 453 (1997).
- [47] J. R. de Bruyn, *Phys. Fluids* **9**, 1599 (1997).
- [48] C. E. Bartosch and S. Gregory, *Phys. Rev. Lett.* **54**, 2513 (1985); S. Kumar, T. Brosius, G. Torzo, D. Finotello, and J. D. Maynard, *Phys. Rev. B* **37**, 7352 (1988); L. Bruschi, G. Torzo, and M. H. W. Chan, *Europhys. Lett.* **6**, 541 (1988); G. Zimmerli and M. H. W. Chan, *Phys. Rev. B* **38**, 8760 (1988).
- [49] L. Wilen and E. Polturak, *Phys. Rev. A* **41**, 6838 (1990).
- [50] J. Czarnecki, *Adv. Colloid Interf. Sci.* **24**, 283 (1986).
- [51] J. A. Barker and D. Henderson, *J. Chem. Phys.* **47**, 4714 (1967).
- [52] N. F. Carnahan and K. E. Starling, *J. Chem. Phys.* **51**, 635 (1969).
- [53] W. Koch, PhD thesis, Bergische Universität Wuppertal (1993).
- [54] S. Dietrich, in *Phase Transitions in Surface Films 2*, Proceedings of the NATO ASI (Series B) held in Erice, Italy, 19-30 June 1990, edited by H. Taub, G. Torzo, H. J. Lauter, and S. C. Fain (Plenum, New York, 1991), Vol. B **267**, p. 391; *Phys. Script. T* **49**, 519 (1993).
- [55] (a) M. Napiórkowski and S. Dietrich, *Phys. Rev. B* **34**, 6469 (1986); (b) *Europhys. Lett.* **9**, 361 (1989); (c) S. Dietrich and M. Napiórkowski, *Phys. Rev. A* **43**, 1861 (1991).
- [56] D. Henderson, S. Sokołowski, and A. Patrykiewicz, *Mol. Phys.* **85**, 745 (1995).
- [57] R. Lovett and M. Baus, *J. Chem. Phys.* **106**, 635 (1997); M. Mareschal, M. Baus, and R. Lovett, *J. Chem. Phys.* **106**, 645 (1997).
- [58] F. B. Buff, *J. Chem. Phys.* **19**, 1591 (1951); *ibid* **23**, 419 (1955); S. M. Thompson, K. E. Gubbins, J. P. R. B. Walton, R. A. R. Chantry, and J. S. Rowlinson,

- J. Chem. Phys. **81**, 530 (1984); M. P. A. Fisher and M. Wortis, Phys. Rev. B **29**, 6252 (1984); J. R. Henderson and J. S. Rowlinson, J. Phys. Chem. **88**, 6484 (1984); D. J. Lee, M. M. Telo da Gama, and K. E. Gubbins, J. Chem. Phys. **85**, 490 (1986); D. Oxtoby and R. Evans, J. Chem. Phys. **89**, 7521 (1988); G. Gompfer and S. Zschokke, Europhys. Lett. **18**, 731 (1991); M. J. P. Nijmeijer, C. Bruin, A. F. van Woerkom, A. F. Bakker, and J. M. J. van Leeuwen, J. Chem. Phys. **96**, 565 (1992); E. M. Blokhuis and D. Bedeaux, Mol. Phys. **80**, 705 (1993); J. S. Rowlinson, J. Phys.: Condens. Matt. **6**, A1 (1994); I. Hadjiagapiou, J. Phys.: Condens. Matt. **6**, 5303 (1994); *ibid* **7**, 547 (1995); V. Talanquer and D. Oxtoby, J. Chem. Phys. **100**, 5190 (1994); M. Iwamatsu, Chin. J. Phys. **33**, 139 (1995); M. Baus and R. Lovett, J. Chem. Phys. **103**, 377 (1995); C. Varea and A. Robledo, Mol. Phys. **85**, 477 (1995); J. W. P. Schmelzer, I. Gutzow, and J. Schmelzer Jr., J. Colloid Interf. Sci. **178**, 657 (1996); A. Laaksonen and R. McGraw, Europhys. Lett. **35**, 367 (1996); V. I. Kalikmanov, Phys. Rev. E **55**, 3068 (1997).
- [59] As described in J. R. Henderson, in *Fluid Interfacial Phenomena*, edited by C. A. Croxton (Wiley, Chichester, 1986), p. 555, Sect. 12. 2. 6, under certain assumptions a hard-sphere fluid exposed to a hard cavity w of radius R is expected to exhibit the behavior $\sigma_w^{(s)}(R \rightarrow \infty) = \sigma_w^{(p)}(1 - \frac{2\delta}{R} + \alpha \frac{\ln(R/\sigma)}{R^2} + \dots)$ and $\sigma_w^{(c)}(R \rightarrow \infty) = \sigma_w^{(p)}(1 + \alpha \frac{\ln(R/\sigma)}{R} + \dots)$. These results indicate that one should be prepared to expect logarithmic corrections even in systems with short-ranged interactions and that the Tolman length for a cylinder might not exist. However, at present it is unclear whether these results are also valid if the hard spheres are replaced by soft interaction potentials, and whether these results remain valid for the liquid-vapor interfaces considered here.
- [60] A. Poniewierski and J. Stecki, J. Chem. Phys. **106**, 3358 (1997).
- [61] J. Israelachvili, *Intermolecular and Surface Forces* (Academic, London, 1985), Chaps. 11.5 and 15.1.
- [62] G. Flöter and S. Dietrich, Z. Phys. B **97**, 213 (1995); and references therein.
- [63] E. H. Hauge and M. Schick, Phys. Rev. B **27**, 4288 (1983).
- [64] M. P. Nightingale, W. F. Saam, and M. Schick, Phys. Rev. B **30**, 3830 (1984).
- [65] K. Ragil, J. Meunier, D. Brosseta, J. O. Indekeu, and D. Bonn, Phys. Rev. Lett. **77**, 1532 (1996).
- [66] V. Privman and M. E. Fisher, J. Stat. Phys. **33**, 385 (1983); J. Appl. Phys. **57**, 3327 (1985).
- [67] B. Widom and A. S. Clarke, Physica A **168**, 149 (1990); C. Varea and A. Robledo, Phys. Rev. A **45**, 2645 (1992); J. O. Indekeu, Physica A **183**, 439 (1992); B. Widom, in *Condensed Matter Theories*, edited by L. Blum and F. B. Malik (Plenum, New York, 1993), Vol. 8, p. 589; C. Varea and A. Robledo, Phys. Rev. E **47**, 3772 (1993); S. Perković, I. Szleifer, and B. Widom, Mol. Phys. **80**, 729 (1993); H. T. Dobbs and J. O. Indekeu, Physica A **201**, 457 (1993); E. M. Blokhuis, Physica A **202**, 402 (1994); A. Robledo and J. O. Indekeu, Europhys. Lett. **25**, 17 (1994); J. O. Indekeu, Int. J. Mod. Phys. B **8**, 309 (1994); J. O. Indekeu and H. T. Dobbs, J. Phys. I France **4**, 77 (1994); S. Perković, E. M. Blokhuis, and G. Han, J. Chem. Phys. **102**, 400

(1995); S. Perković, E. M. Blokhuis, E. Tessler, and B. Widom, *J. Chem. Phys.* **102**, 7585 (1995); T. Getta and S. Dietrich, *Phys. Rev. E*, in press (1997).

Figure captions

FIG. 1. (a) Cross section of the density configuration around a sphere or a cylinder of radius r_0 with a number density ρ_w . The gas phase with number density ρ_g is truncated for $r > L$. The liquidlike film with number density ρ_l has a radius of curvature given by h and a thickness $l = h - r_0$. The density distribution vanishes within an excluded volume $r_0 < r < r_1 = r_0 + d_w$. (b) Corresponding density configuration close to a planar wall.

FIG. 2. Liquid-vapor surface tension of a liquid drop (s) and thread (c) as compared with the planar surface tension (p) as function of their radius h in units of the diameter σ of the fluid particles based on Eqs. (2.16) and (2.17) for the model potential given in Eq. (2.4) with the parameters $\sigma = 1.0$ and $\epsilon = 1.0$. Within the sharp-kink approximation the ratios $\sigma_{l,g}^{(\tau)}(h)/\sigma_{l,g}^{(p)}$ are constant as function of the temperature and behave asymptotically for $\sigma/h \rightarrow 0$ as given in Eqs. (2.22) and (2.23). For $\sigma/h < 1.89 \cdot 10^{-7}$ one has $\sigma_{l,g}^{(c)}(h) < \sigma_{l,g}^{(s)}(h)$; otherwise $\sigma_{l,g}^{(s)}(h)$ is smaller than $\sigma_{l,g}^{(c)}(h)$. Beyond the sharp-kink approximation the ratio $\sigma_{l,g}^{(s)}(h)/\sigma_{l,g}^{(p)}$ for a sphere is expected to approach 1 linearly as function of $\sigma/h \rightarrow 0$ with a slope $-2\delta/\sigma$ given by the Tolman length δ . (See also Ref. [59].)

FIG. 3. (a) Scaling function $\mathcal{S}_\tau(x) \equiv \mathcal{S}_{attr}^{(\tau)}(x)$ of the effective interface potential (see Eqs. (2.29), (2.30), (2.32), (2.34), (2.36), and (2.39)) as function of $x = r_0/l$. $\mathcal{S}_\tau(x)$ vanishes linearly for $x \rightarrow 0$ (Eq. (2.41)) and approaches 1 for $x \rightarrow \infty$ proportional to x^{-1} (Eq. (2.40)). The maxima (\bullet) and the inflection points (\times) are located at $x_{max}^{(c)} \simeq 2.56$, $x_{max}^{(s)} \simeq 1.85$, and $x_t^{(c)} \simeq 4.24$, $x_t^{(s)} \simeq 3.18$, respectively. (b) Corresponding scaling functions $s_\tau(x)$ (see Eq. (3.41)). According to this figure Eq. (3.3) has indeed one unique solution.

FIG. 4. Ratios $l_{max}/r_0 = 1/x_\tau^*$ as a function of $\kappa = (r_0^2 \sigma_{l,g}^{(p)}/a)^{1/3}$ obtained by solving Eq. (3.3) numerically for the same interaction potential parameters as those used in Fig. 2. According to Eqs. (3.6) and (3.7) both ratios vanish for $\kappa \rightarrow \infty$ proportional to κ^{-1} whereas for $\kappa \rightarrow 0$ they diverge proportional to $\kappa^{-3/4}$ and $\kappa^{-3/5}$ for the cylinder and the sphere, respectively.

FIG. 5. Complete wetting film thickness along an isotherm $k_B T/\epsilon = 0.94$ for a sphere and cylinder, respectively, of radius 1000σ , compared with that of a planar wall ($r_0 = \infty$). The curves correspond to Eq. (3.14) with the interaction parameters chosen to be the same as in Fig. 2. In this case $\kappa \simeq 75.5$ so that Eqs. (3.21), (3.25), and (3.26) apply. Therefore the complete wetting film thickness on a curved substrate resembles that on the corresponding planar substrate as if liquid-vapor coexistence would occur at $\Delta\mu(\kappa, \lambda) = -\delta\mu(\kappa, \lambda = -\tau) < 0$ (see Eqs. (3.17) and (3.27)) instead of at $\Delta\mu = 0$. ($\Delta\mu_{eff} = 0$ implies $\lambda = -\tau$, see Eqs. (3.24)-(3.26).)

FIG. 6. According to Eqs. (3.25) and (3.26) the thickness of a complete wetting film on a curved substrate is given by the film thickness on the corresponding planar substrate for an effective undersaturation $\Delta\mu_{eff}(\Delta\mu; r_0, \tau)$. In terms of the relevant dimensionless

parameters $\kappa = (\sigma_{l,g}^{(p)} r_0^2 / a)^{1/3}$ and $\lambda = \Delta \rho r_0 \Delta \mu / \sigma_{l,g}^{(p)}$ one finds three distinct regimes I, II, and III within which $\lambda_{eff}(\kappa, \lambda)$ exhibits the characteristic power laws given by Eqs. (3.29), (3.30), (3.31), (3.35), and (3.36), respectively. (a) shows the crossover lines $\kappa_{I,II}$, $\kappa_{II,III}$, and $\kappa_{I,III}$ between these regimes for a cylinder, (b) the corresponding ones for a sphere. Their amplitudes are chosen such that they meet in a single point. The variation of $\lambda_{eff}(\kappa, \lambda)$ along the dashed-dotted paths is shown in Fig. 7

FIG. 7. (a) shows the effective undersaturation $\lambda_{eff}(\kappa, \lambda)$ for a cylinder along the dashed-dotted path in Fig. 6(a), i. e., for $\lambda = 0.35$, and (b) for a sphere along the dashed-dotted path in Fig. 6(b), i. e., for $\lambda = 0.5$, as function of κ . The full curves correspond to the full solution determined by Eq. (3.26). These solutions display the crossover behaviors which occur according to the corresponding vertical paths in Fig. 6. For large values of κ one is in regime II where $\lambda_{eff}^{(\tau)} \simeq \tau + \lambda$ is constant as function of κ (dashed curves). Upon decreasing κ one enters regime III where Eqs. (3.35) and (3.36) (dashed-dotted curves) hold. Ultimately for $\kappa \rightarrow 0$ one reaches regime I where Eqs. (3.29) and (3.30) (dotted curves) are valid. λ_{eff} is raised to the powers $-5/6$ and $-2/3$, respectively, so that the dotted curves are straight lines.

FIG. 8. (a) Phase diagram of a first-order wetting transition on a cylindrical and a spherical substrate of radii $r_0/\sigma = 100$ obtained by a numerical minimization of Eq. (2.10) with the substrate potential parameters $\sigma_{wf}/\sigma = 1.35$, $\epsilon_{wf}/\epsilon = 0.625$, $d_w/\sigma = 1.175$, and $\rho_w \sigma^3 = 1.0$. The prewetting line of the corresponding planar substrate (solid curve) joins the liquid-vapor coexistence curve $\mu - \mu_0(T) = 0$ tangentially at the first-order transition temperature $T_w^{(p)}$. The wetting behavior on a curved substrate is similar to that of a planar substrate whose coexistence curve is shifted upwards. Consequently for a curved substrate at coexistence there is a thin-thick transition at $T_w^{(\tau)}(\kappa)$ where the remaining part of the prewetting line intersects the coexistence curve *linearly*. Note, however, that along the prewetting line of the curved substrates κ varies as function of the temperature and is thus not a constant; for the given parameter values κ ranges between 13.8 and 17.1 for $0.78 \leq k_B T / \epsilon \leq 1.0$. Therefore the prewetting lines belonging to the curved surfaces are not parallel to the corresponding prewetting line of the flat substrate. The thin-thick transition can be traced into the oversaturated vapor region (dashed-dotted lines) provided it is possible to maintain the thermodynamically instable vapor phase for these values of μ . At the upper end points of these curves the minimum in $\Omega_s(l)$ corresponding to the thicker film ceases to exist. Each prewetting line ends at its lower end in a critical point. However, in the present model and approximation the prewetting lines of both the planar and the curved substrates can only be followed up to the dotted curve which denotes the loci where in the bulk the metastable liquid phase ceased to exist. Therefore beyond the dotted curve the present sharp-kink approximation (Eq. (2.6)) for the density distribution close to the wall is no longer applicable. In that region of the phase diagram for the present choice of interaction potentials the thicknesses of the wetting films are so small that these films cannot be described adequately by a liquidlike layer with a number density ρ_l which corresponds to that of the metastable bulk liquid phase. (b) Temperature dependence of the equilibrium film thickness l_0 at coexistence for the systems described

by the phase diagram in (a). It illustrates the shift of the wetting transition temperature and the finite discontinuity induced by the curvature of the substrate.

FIG. 9. (a) Schematic phase diagram for a planar substrate exhibiting a second-order wetting transition at $T_w^{(p)}$. At $\mu = \mu_0(T)$ and for $T \leq T_c$ the bulk liquid and gas phases coexist; only temperatures above the triple point are considered. If one records the film thickness l/σ as function of the temperature $k_B T/\epsilon$ along a path slightly below coexistence (thin line) and at a fixed undersaturation $\delta\mu_\infty^{(\tau)} > 0$ (dotted line) for a given set of interaction parameters (see below) one obtains the curves shown in (b). For the film thickness on a cylinder or a sphere the path along the coexistence curve across $T_w^{(p)}$ is equivalent to the dotted path for the corresponding planar substrate because of the effective upward shift of the bulk phase diagram due to the curvature (see main text). (b) Film thickness l/σ as function of the temperature $k_B T/\epsilon$ for a planar substrate and for a cylinder and a sphere of radius $r_0/\sigma = 10^8$, respectively, on a thermodynamic path along the coexistence line, $\mu = \mu_0(T)$, crossing the second order wetting transition of the planar substrate. The interaction parameters have been chosen such that for the planar substrate there is a wetting transition at $k_B T_w^{(p)}/\epsilon = 0.9$. This requires (Eqs. (3.41) - (3.46)) $\epsilon_{wf}^{(0)}/\epsilon = (\sigma/\sigma_{wf}^{(0)})^6 \rho_l(T_w^{(p)})/\rho_w \simeq 0.6002$ and $\sigma_{wf}^{(0)}/\sigma = 1.0$ so that $a(T = T_w^{(p)}) = 0$ (Eq. (3.41)) is fulfilled. In order to satisfy the remaining conditions for a critical wetting transition (Eq. (3.41)) one may choose, e. g., $\epsilon_{wf}^{(1)}/\epsilon = 1.4$, $\sigma_{wf}^{(1)}/\sigma = 1.0$, and $\delta/\sigma = 1.5$. The inflection points (\bullet) in the film thickness $l^{(\tau)}(T)$ on the curved substrates occur *below* the wetting temperature $T_w^{(p)}$ of the planar substrate. The levelling off of the curves for the cylinder and the sphere is not yet complete even at T_c . It is remarkable that for $(T_w^{(p)} - T)/T_w^{(p)} \lesssim 10^{-2}$ even for radii of the order of 1cm the effect of the curvature on the wetting film thickness as compared with a truly planar geometry is still visible. We have checked that the above choice of interaction potential parameters is not atypical in the sense that they cause an unusually small temperature gradient of the Hamaker constant at T_w as compared with the experimental observation of critical wetting [65]. Therefore we conclude that this extraordinarily strong sensitivity of critical wetting to curvature is a generic feature.

FIG. 10. Scaling function $\mathcal{R}_\tau(x)$ given by Eqs. (3.49), (C4), and (C5), as function of $x = r_0/l$. $\mathcal{R}_\tau(x)$ rises linearly to a finite value for $x \rightarrow 0$ ($\mathcal{R}_c(x = 0) = \frac{3\pi}{2}$ and $\mathcal{R}_s(x = 0) = 8$, respectively; Eqs. (3.51) and (3.52)) and approaches 1 for $x \rightarrow \infty$ proportional to x^{-1} (Eq. (3.50)).

FIG. 11 In the case of critical wetting at coexistence the film thickness on the curved substrates is determined by Eq. (3.54) with the dimensionless parameters $\kappa = (r_0^2 \sigma_{l,g}^{(p)}/a)^{1/3}$ and $\gamma = 3b/(2ar_0)$. Since $x = r_0/l$ is positive, it is sufficient to consider the regions ($\kappa \geq 0$, $\gamma \geq 0$) and ($\kappa < 0$, $\gamma < 0$) which correspond to $T > T_w^{(p)}$ and $T < T_w^{(p)}$, respectively. The limits $T = T_w^{(p)} \pm 0$ correspond to $\gamma \rightarrow \pm\infty$ whereas on the line $\gamma = 0$ one has, apart from possible multicritical wetting transitions, first-order wetting which we have studied in Subsect. IIIC. By means of the limits $x \rightarrow 0$ and $x \rightarrow \infty$ of the functions $q_\tau(x)$ and $s_\tau(x)$

entering into Eq. (3.55) one can evaluate Eq. (3.54) for the regions I, II, and III of the (κ, γ) parameter space. In the regions Ia,b one has $|\kappa| \gg 1$ and $|\gamma| \gg 1$ so that $\gamma \ll \kappa^3$, i. e., $T \rightarrow T_w^{(p)} \pm 0$ and $r_0 \gg \left(3b/(2\sigma_{l,g}^{(p)})\right)^{1/3}$, which corresponds to film thicknesses given by Eqs. (3.57) - (3.59). For $|\kappa| \gg 1$ and $|\gamma| \ll 1$ with $\kappa\gamma \ll 1$ (large r_0 and $b/a \rightarrow 0$) the film thicknesses are determined by Eqs. (3.60)-(3.62) for positive γ (region IIa) and by Eqs. (3.64)-(3.65) for negative γ (region IIb). In the case $|\kappa| \ll 1$ (regions IIIa,b), i. e. $r_0 \ll \left(|a|/\sigma_{l,g}^{(p)}\right)^{1/2}$, Eqs. (3.66) - (3.69) are valid. For $|\gamma| \rightarrow \infty$ (regions IIIa₁,b₁), i. e. $T \rightarrow T_w^{(p)} \pm 0$, one can expand Eqs. (3.66) and (3.67) into powers of $\kappa^3/\gamma = 2r_0^3\sigma_{l,g}^{(p)}/(3b)$ which leads to Eqs. (3.70) - (3.73). The opposite limit, $\gamma \rightarrow 0$ makes sense only for $\gamma \geq 0$ (region IIIa₂) where the film thicknesses are determined by Eqs. (3.74) and (3.75). In the remaining regions IVa,b and Va,b there is no suitable expansion parameter so that there Eq. (3.54) can only be solved numerically.

Fig. 1(a)

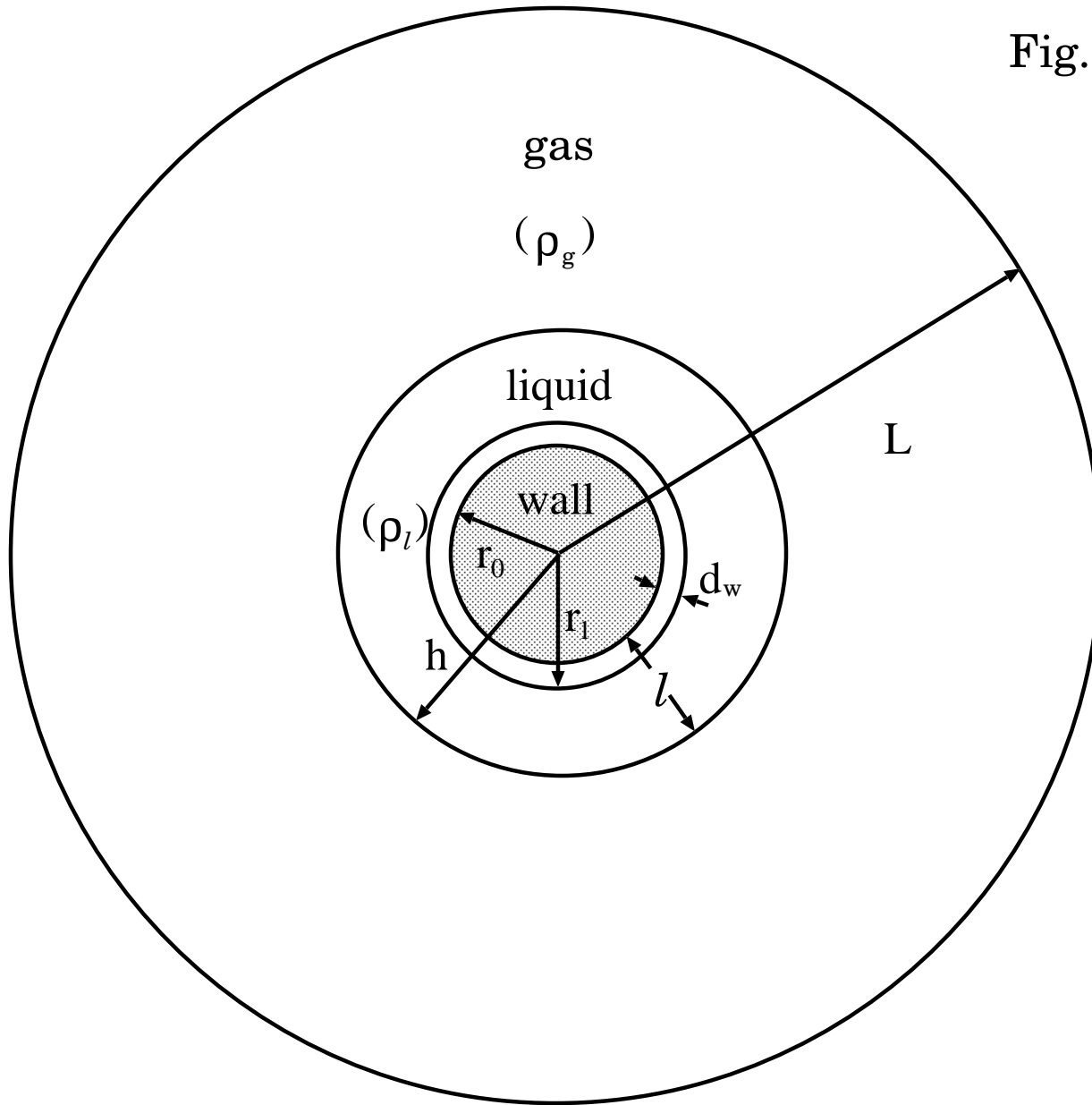
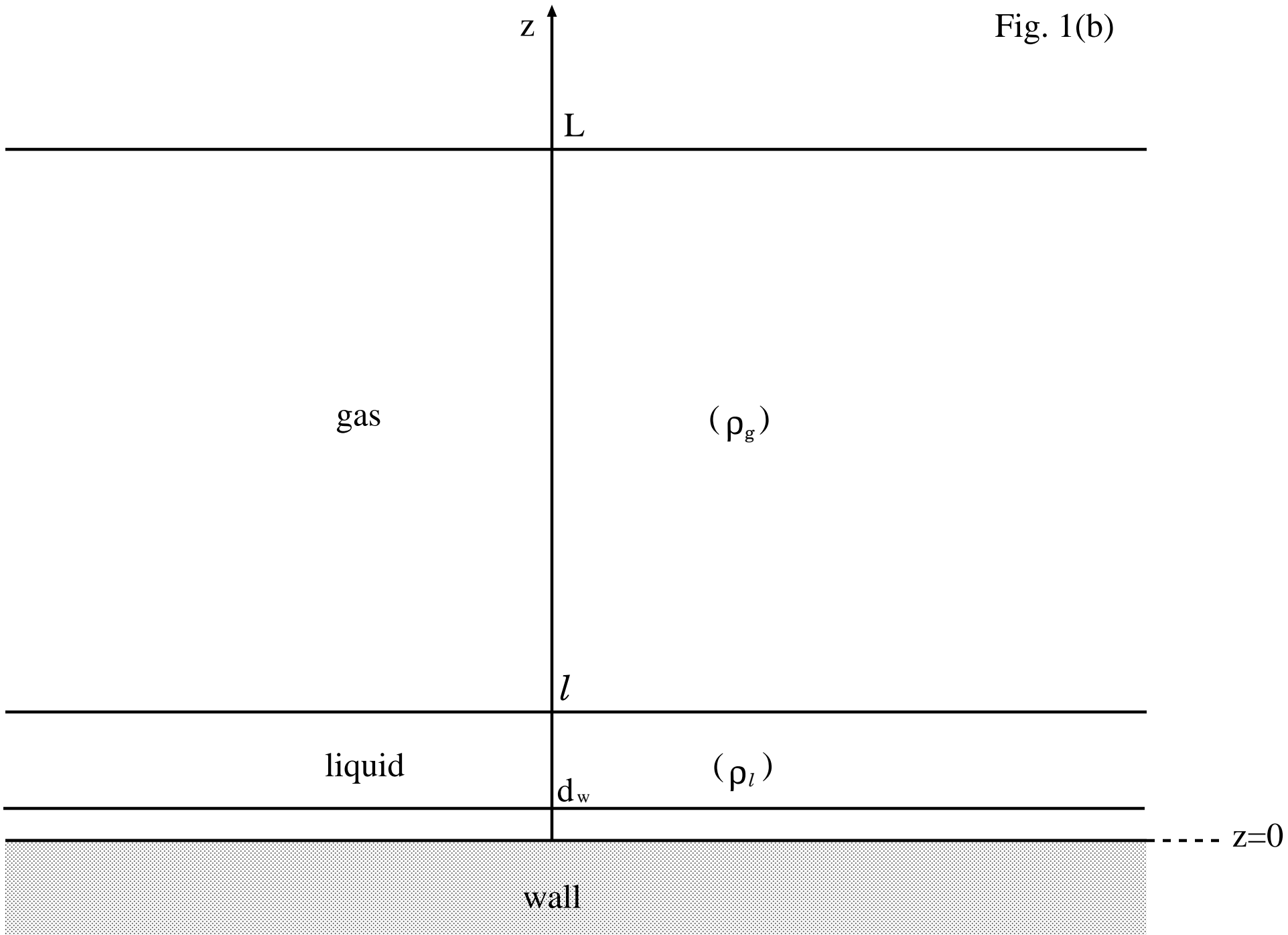
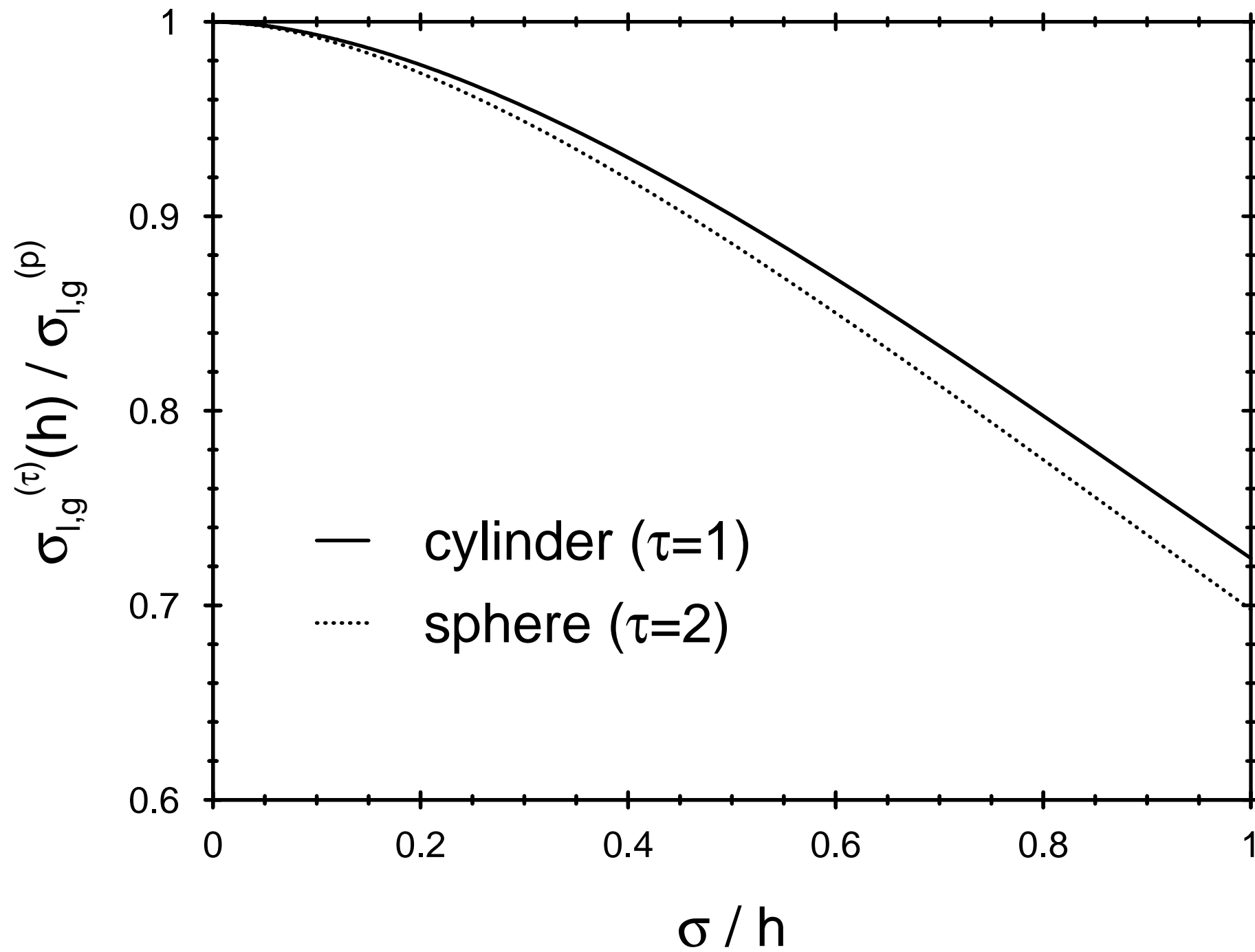


Fig. 1(b)





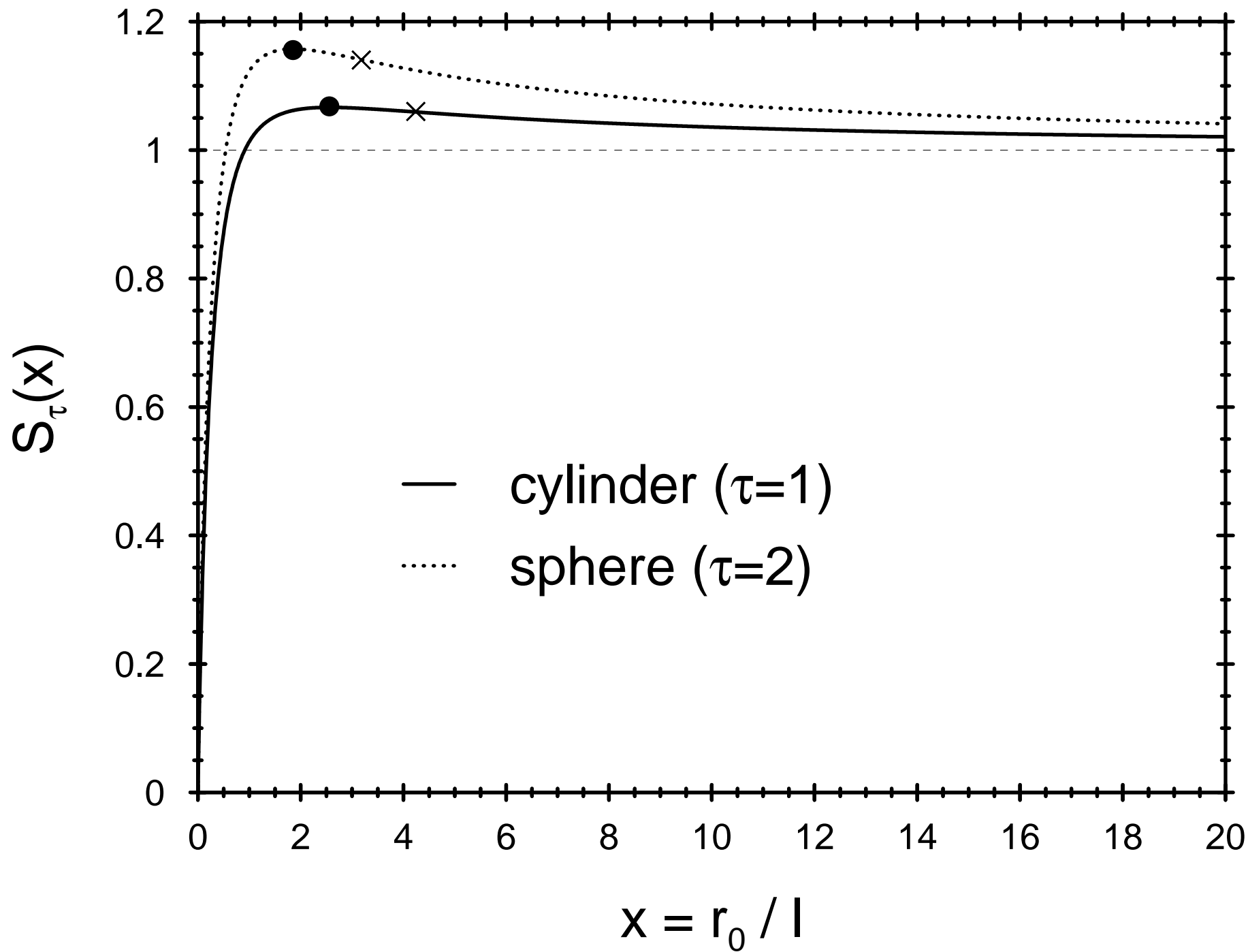


Fig. 3(

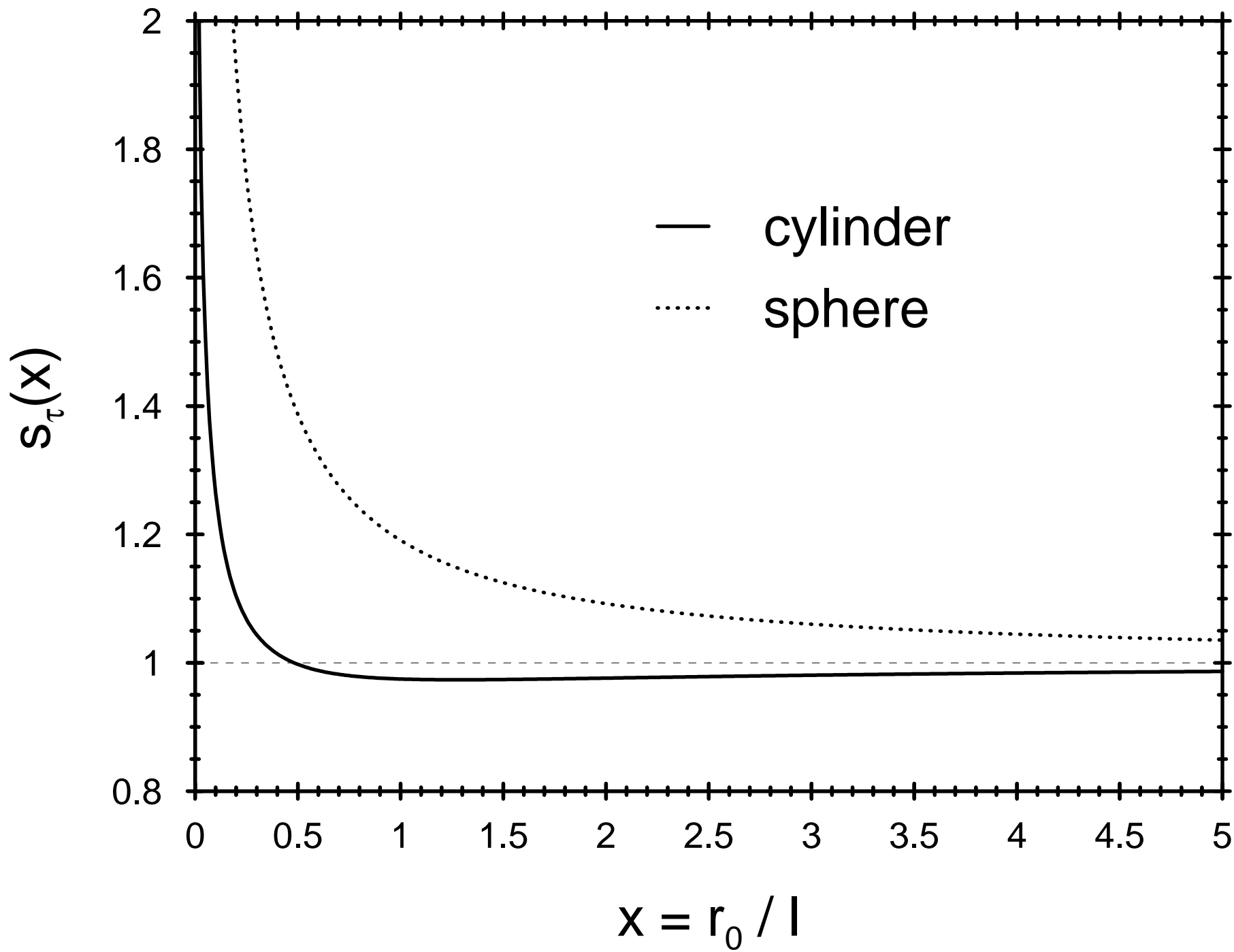


Fig. 4

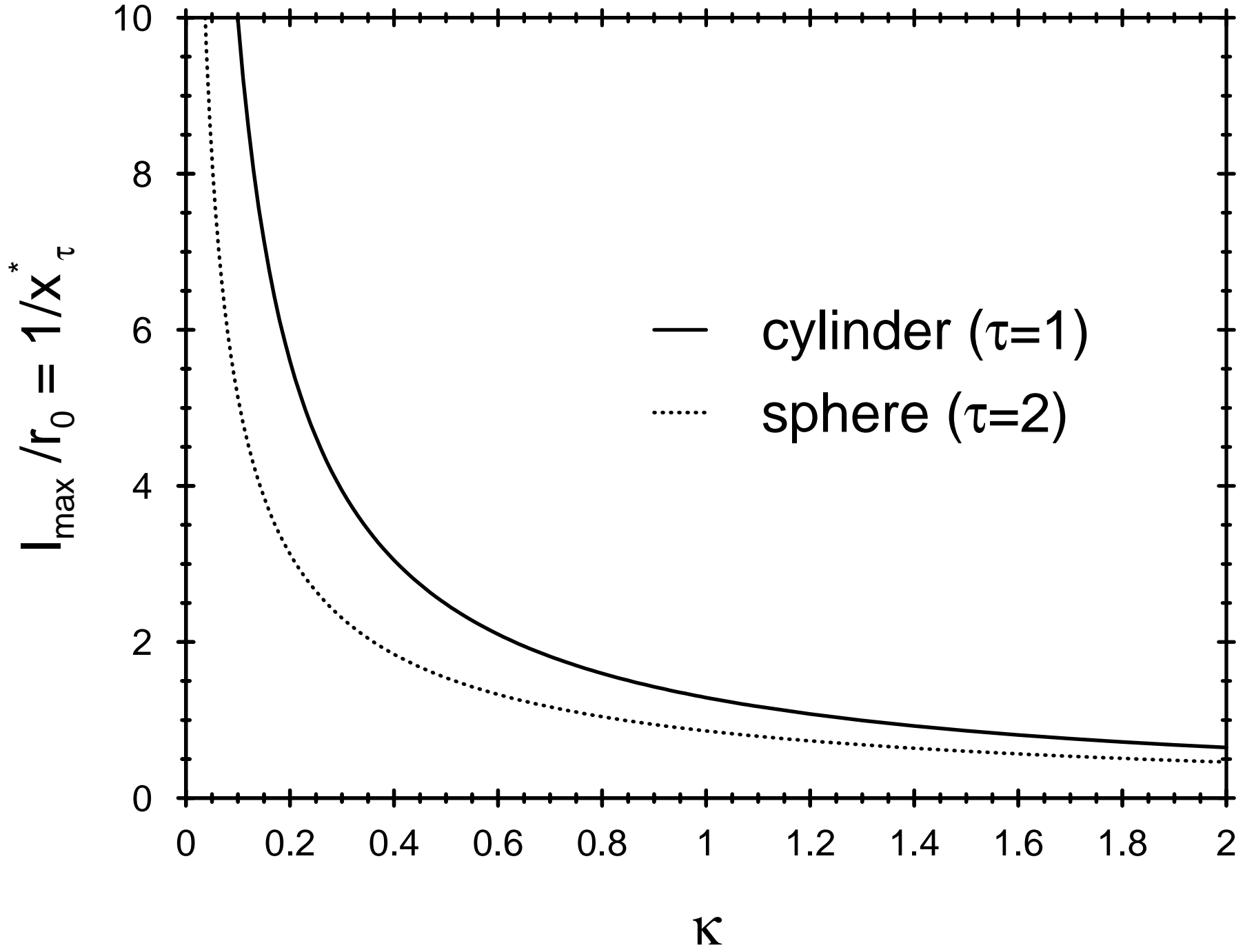


Fig. 5

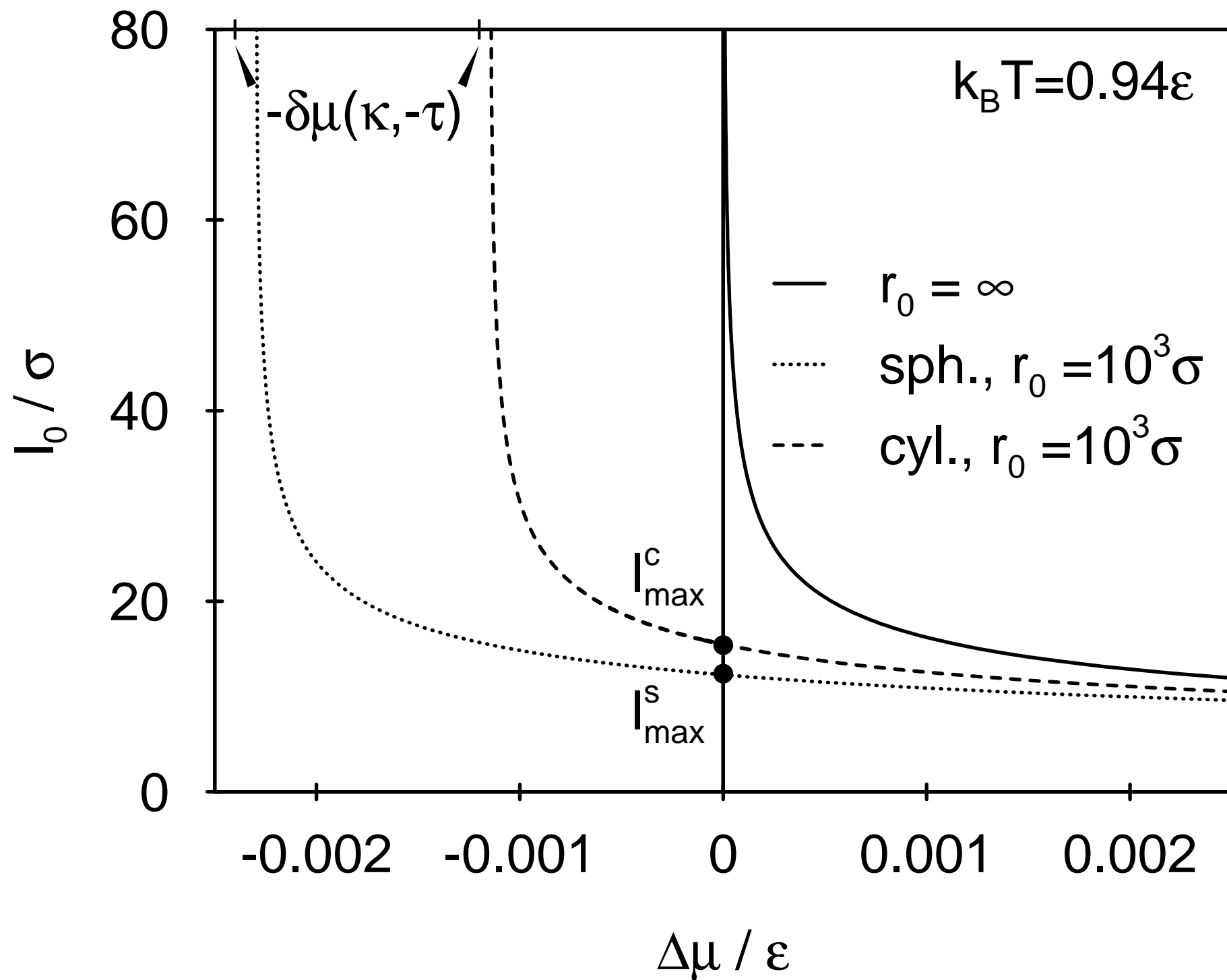


Fig. 6

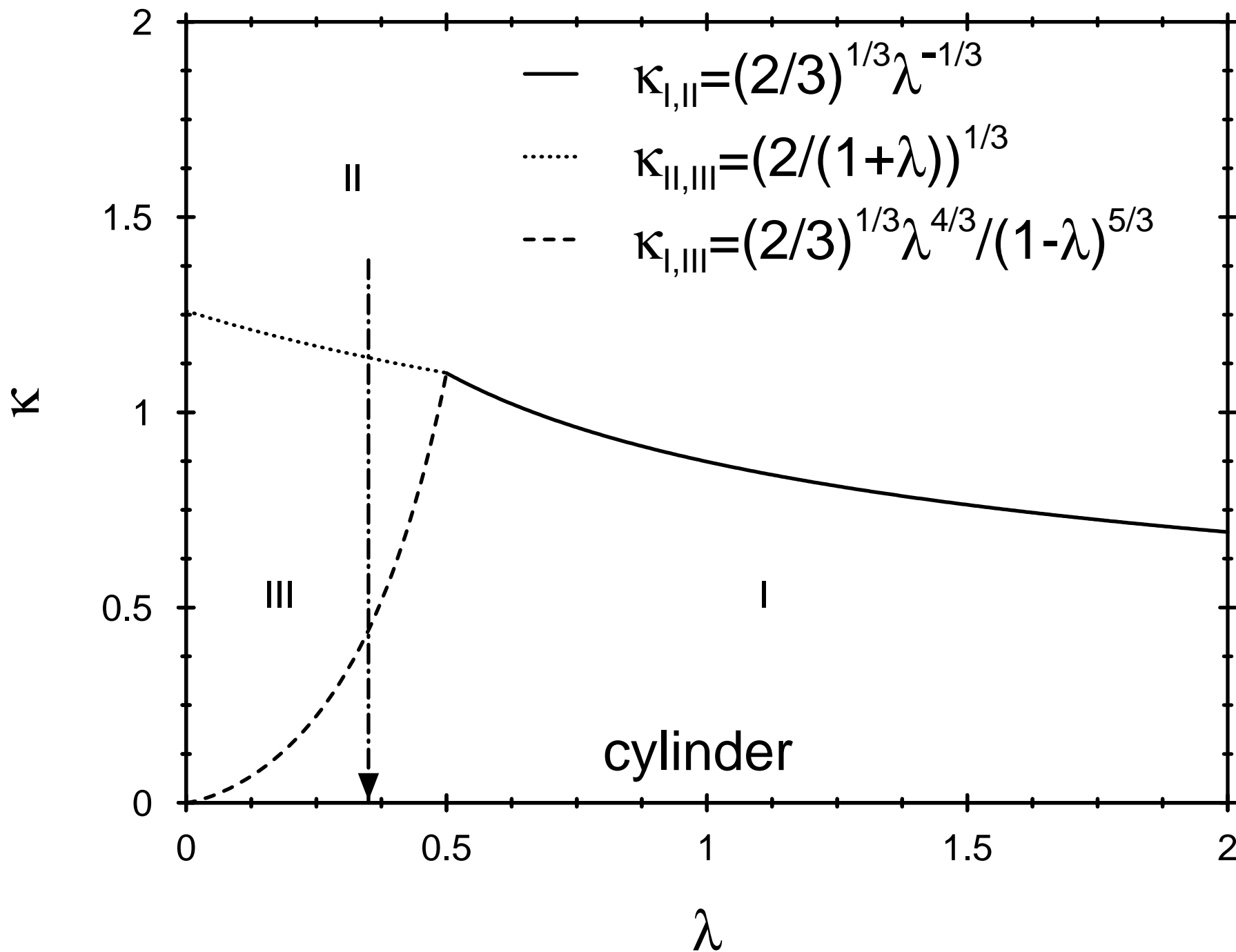


Fig. 6

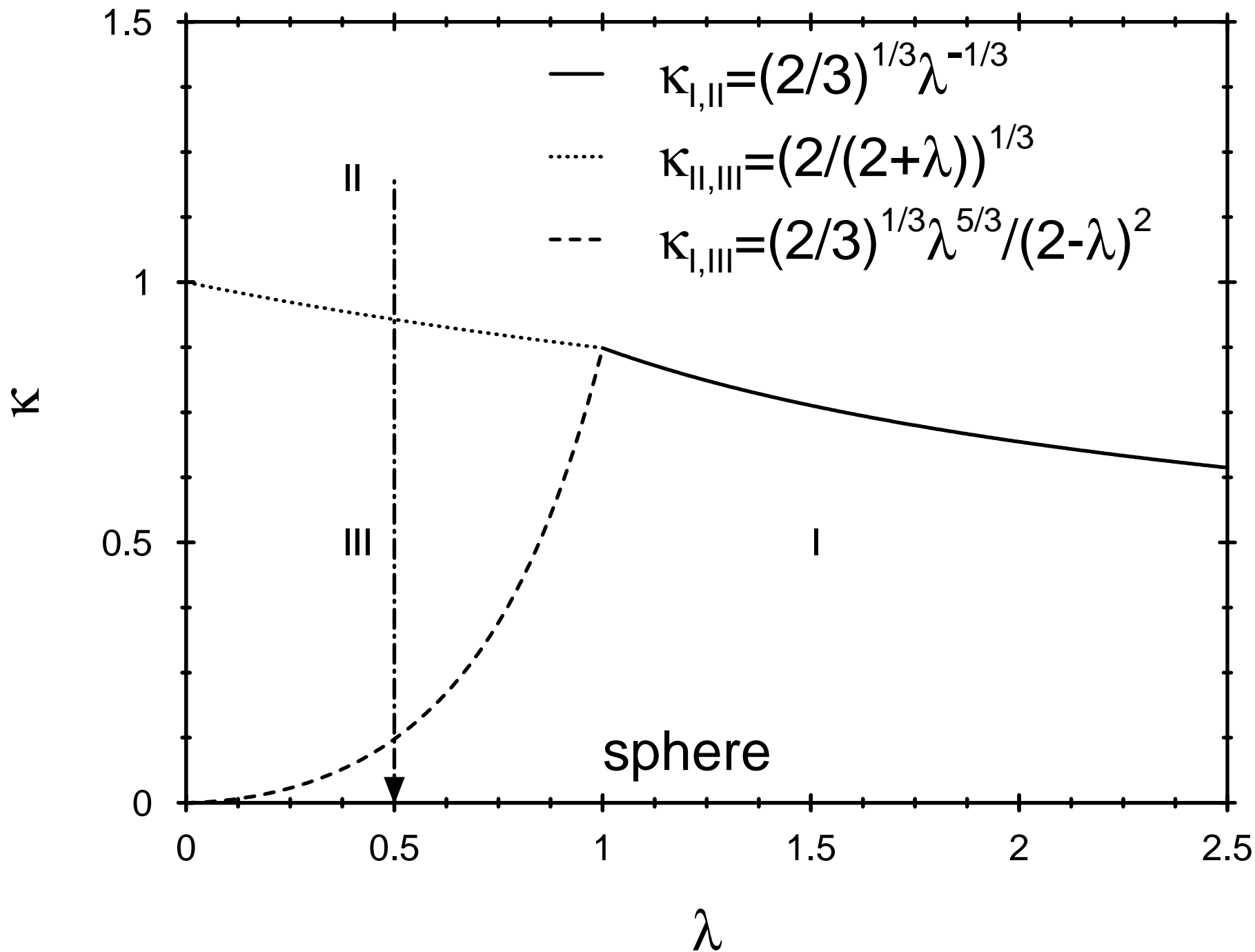


Fig. 7

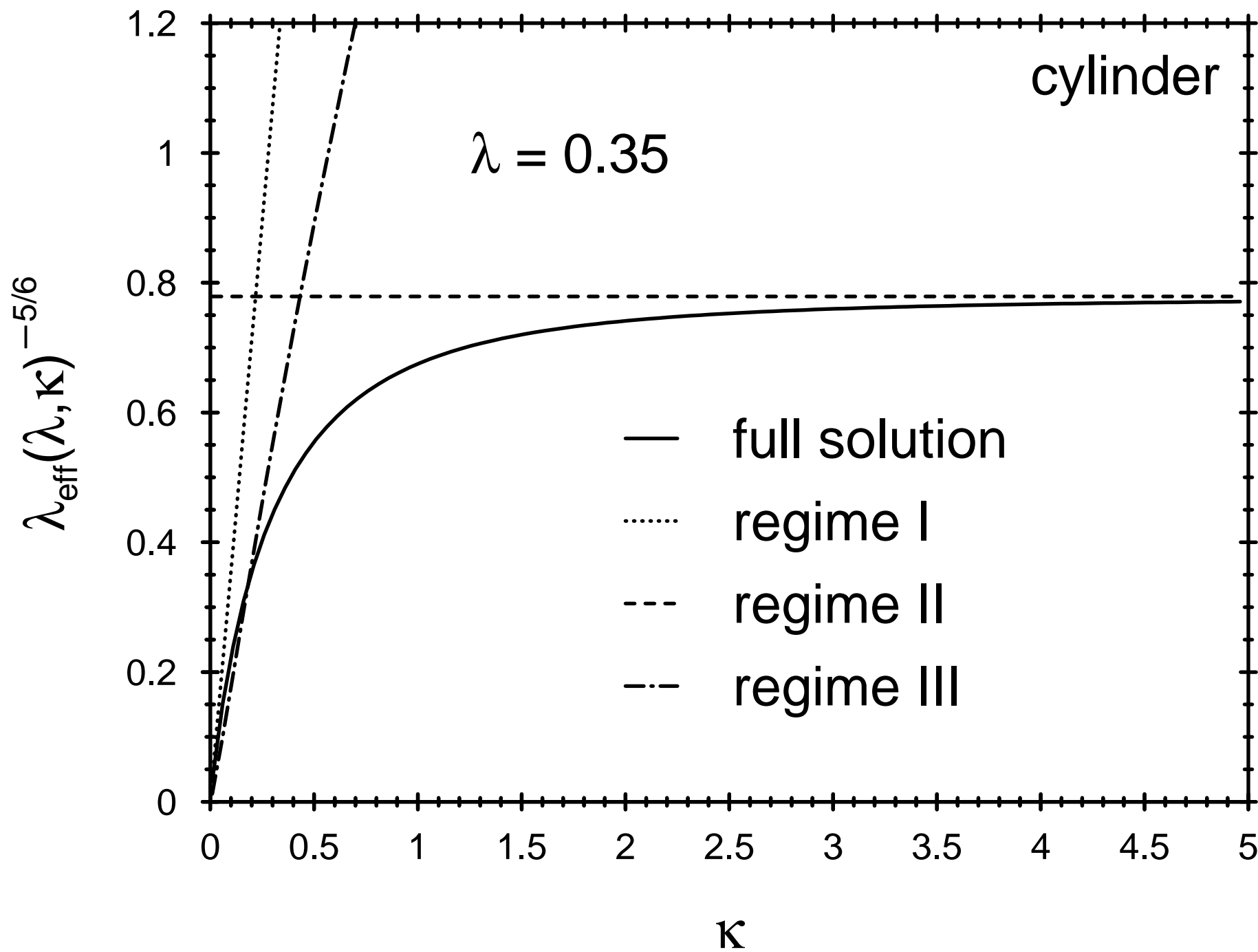


Fig. 7

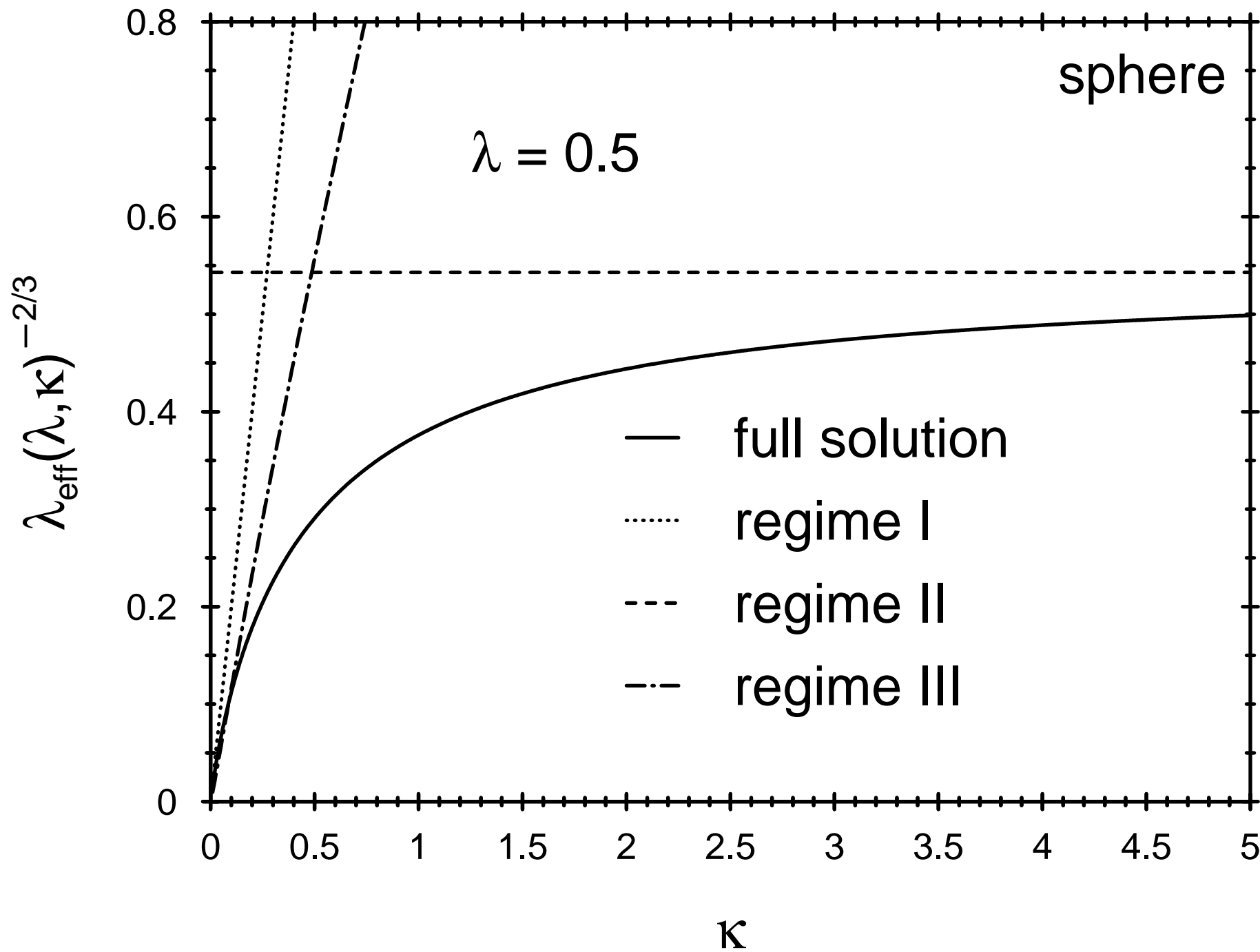


Fig. 8

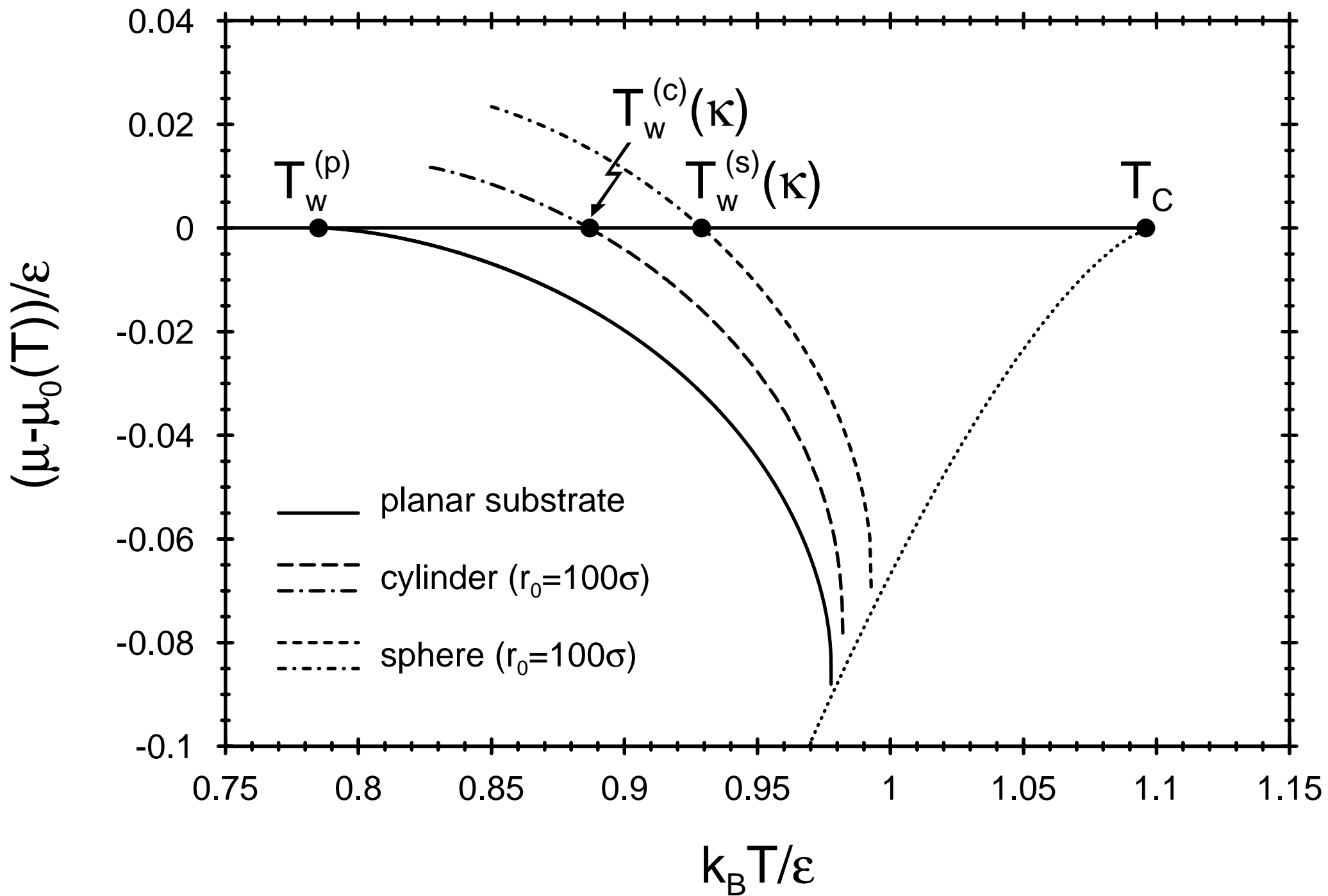
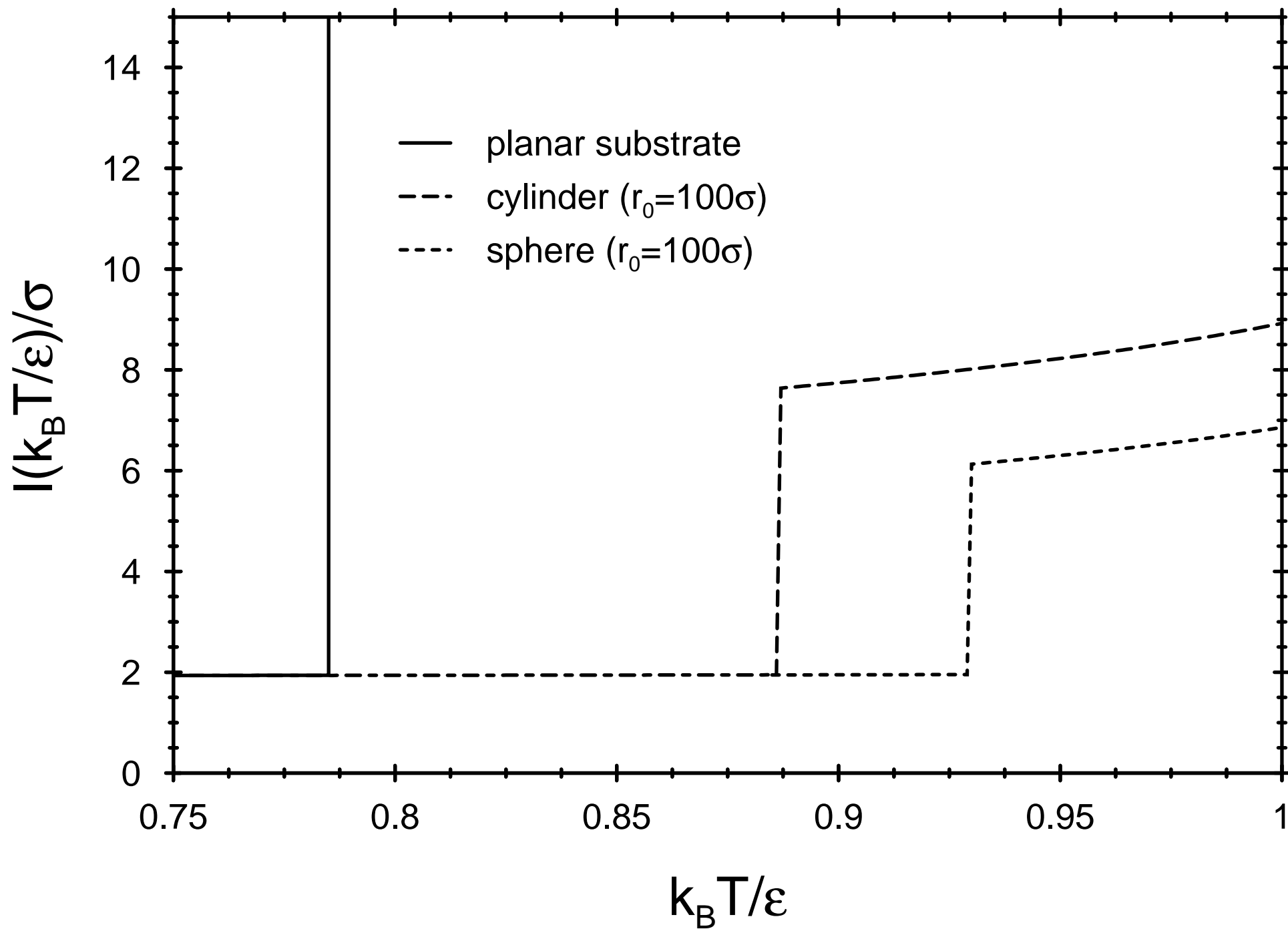


Fig. 8



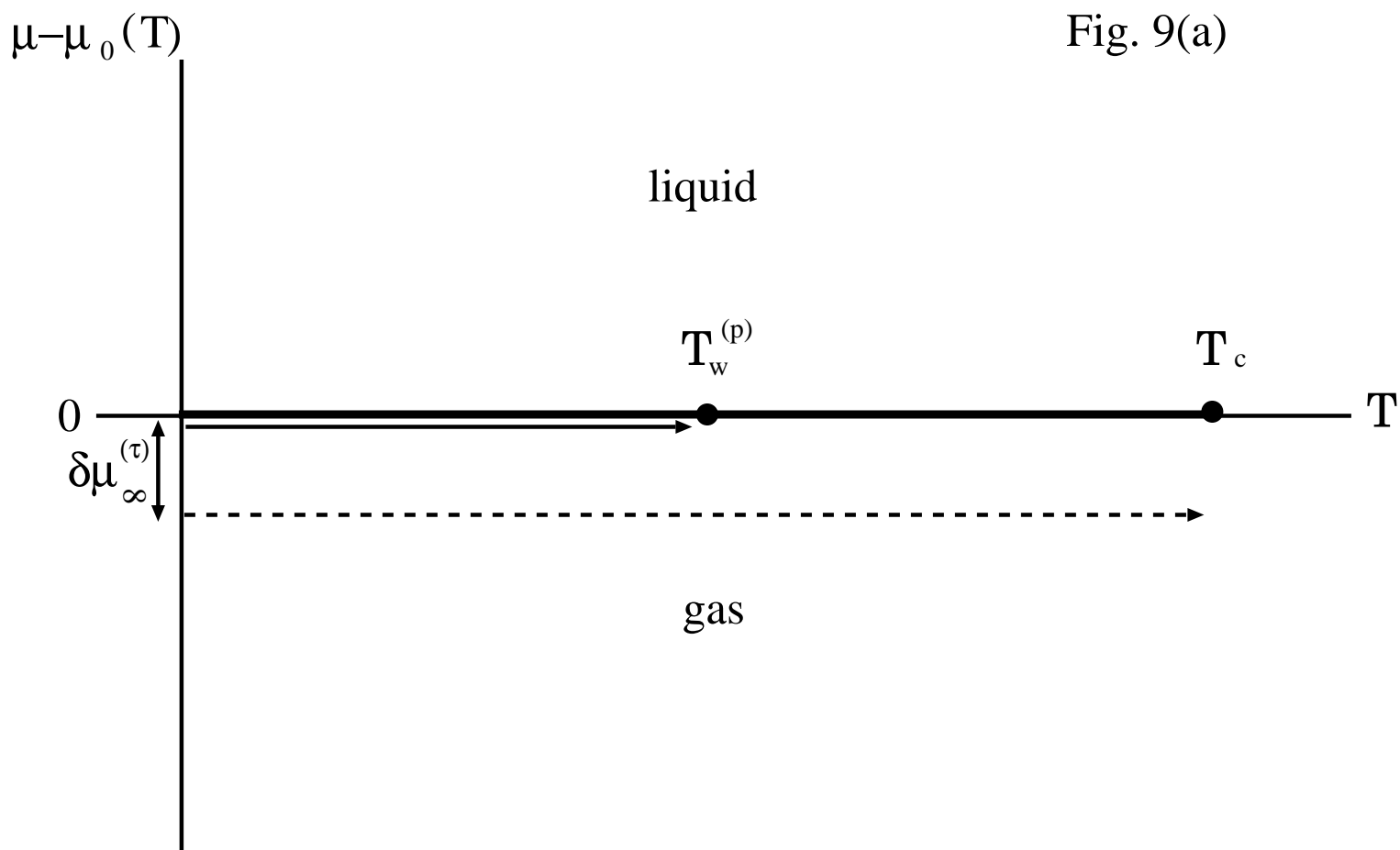


Fig. 9(a)

Fig. 9

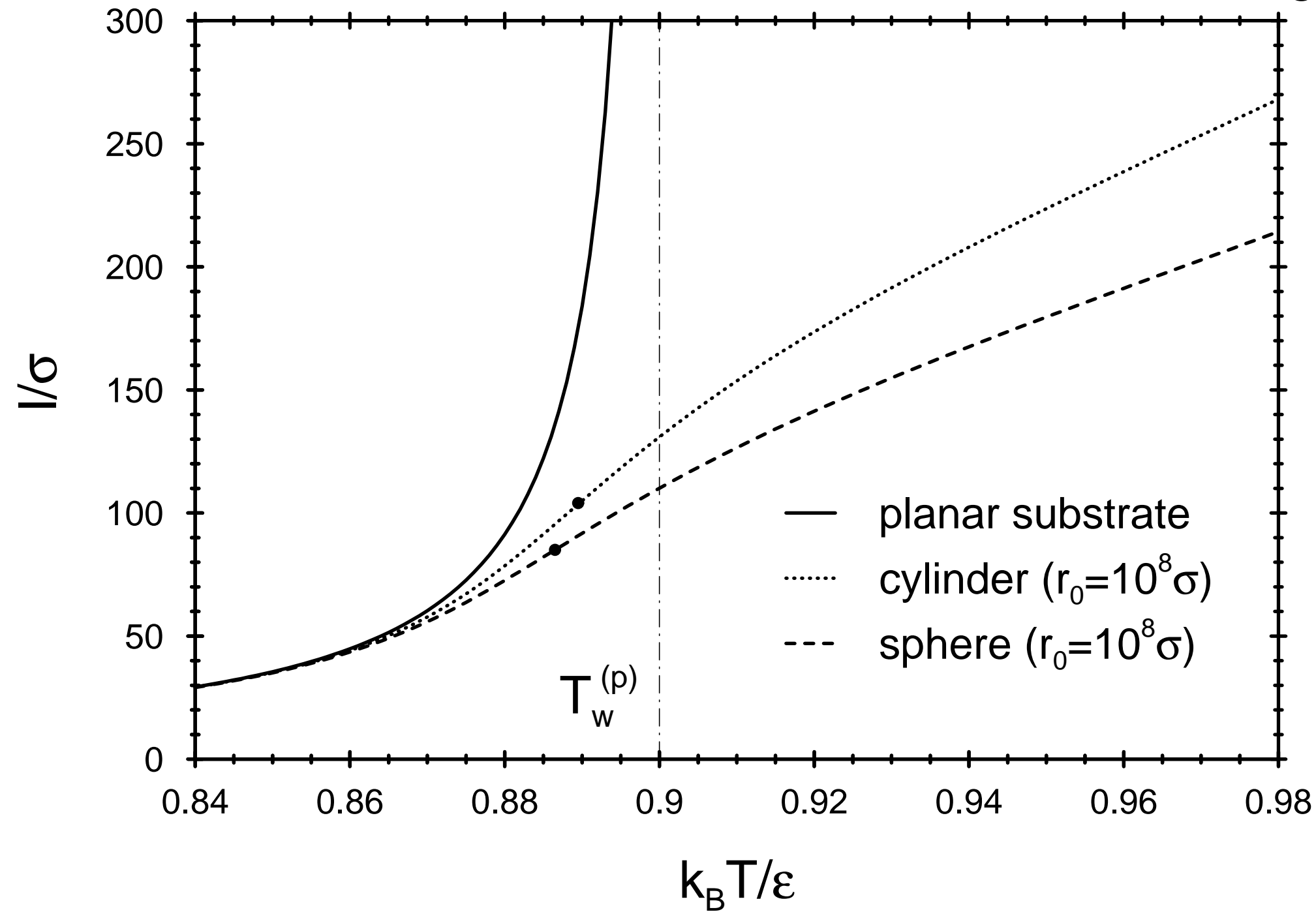


Fig. 10

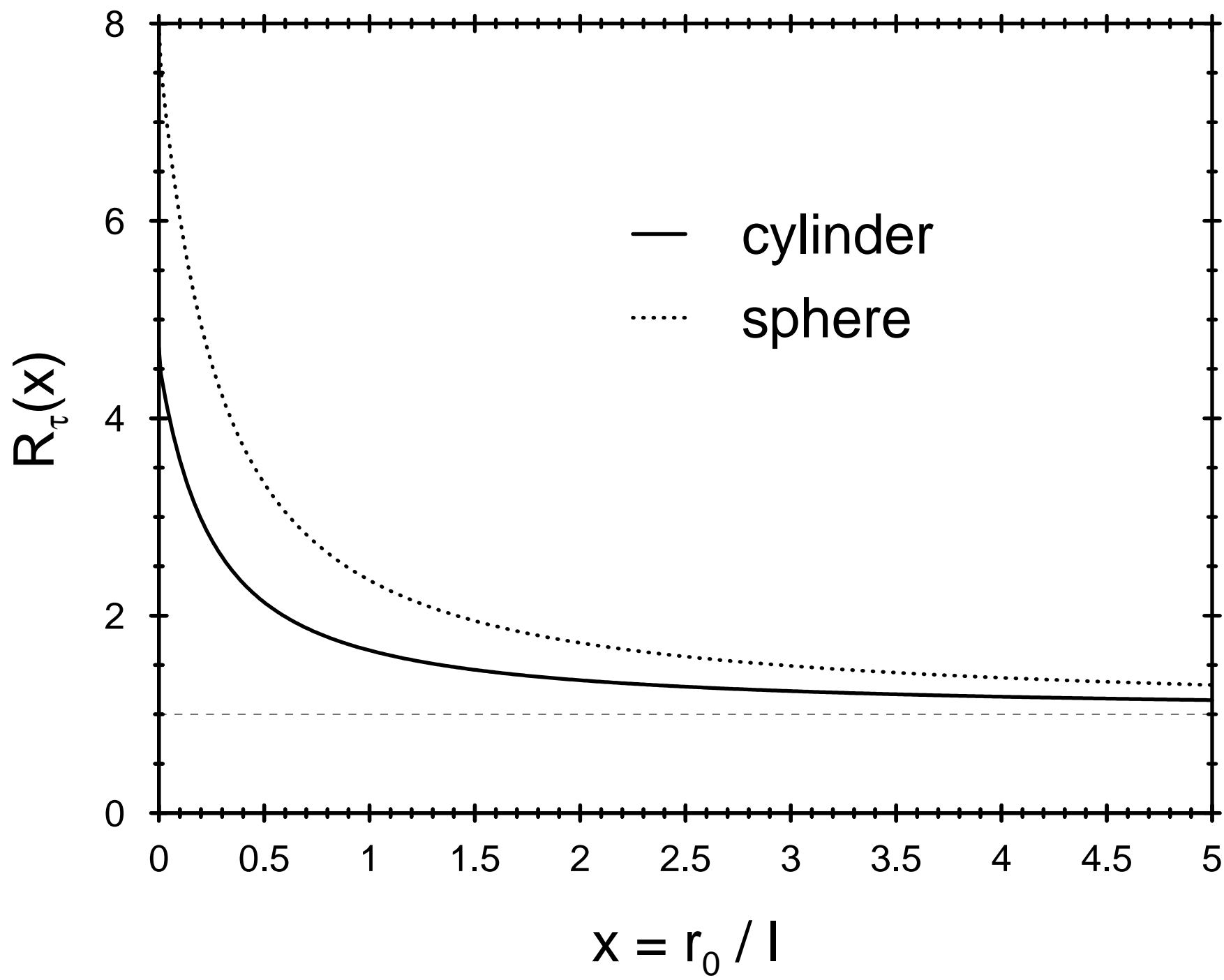


Fig. 1

